



Studies of corneal development and tissue engineering

Thomas Duncan

Structural Biophysics Research Group
Cardiff School of Optometry and Vision Sciences
Cardiff University

Supervisors:

Prof. Andrew Quantock

Prof. Keith Meek

ABSTRACT

The overall objective this work is to contribute to the understanding of how the precise structure of the corneal stroma is achieved during development, and to apply this knowledge to the latest attempts at engineering effective stromal constructs for use in transplantation.

The cornea is the major refractive element of the human eye, accounting for two-thirds of total focusing power. Representing around 85% of corneal thickness, the stroma possesses the mechanical strength needed to protect intraocular tissues, whilst still achieving the high level of transparency necessary for light transmission. This is chiefly due to the small, uniform diameter collagen fibrils arranged into a precisely ordered series of orthogonal lamellae. Proteoglycans in the stroma are thought to regulate the arrangement and diameter of the collagen fibrils, although the mechanism by which this occurs is not fully understood.

The deceptively complex organisation of the stroma may be responsible for the relatively little progress that has been made in engineering constructs that can reproduce the structural and functional characteristics of the cornea. Further study into the embryonic development of the cornea may aid attempts to recapitulate *in vivo* mechanisms for corneal construction. Of particular relevance would be the method of collagen organisation and deposition in the developing avian corneal stroma and the interactions that occur within the collagen fibril bundles as development progresses.

Initially, en face sections were used to study the organisation and arrangement of collagen fibrils in the developing stroma. It is hypothesized that in tendon, the formation of parallel arrays of collagen fibrils occurs via fibroblast surface recesses and invaginations. It was evident through transmission electron microscopy that this process also occurs in the developing corneal stroma via surface recesses on stromal keratocytes.

Analysis of the interactions between the collagen and proteoglycans within fibril bundles demonstrated that the developing cornea is less well structured than often considered and is possibly a much more fluid and dynamic system than originally thought. Proteoglycan size and orientation show a degree of variety and disorder and appear to follow no set organisation or positioning. The data suggests that proteoglycans were seen forming aggregates that were capable of bridging the gap between more distant neighbouring fibrils.

Following the study of the developing corneal stroma, collagen gel based constructs were engineered and their structural and functional characteristics were analysed to assess their potential as stromal equivalents for use in tissue engineering. Manipulating the assembly of collagen fibrils by varying the pH and cross-linker concentration had a dramatic effect on the structure and functionality of the final gel construct. A range of collagen gels were then implanted into intra-stromal pockets to determine their biocompatibility and *in vivo* properties.

ACKNOWLEDGEMENTS

I would first like to thank Professor Andrew Quantock, Professor Keith Meek and Professor Kohji Nishida for their support and encouragement during my Ph.D. Over the course of my Ph.D., I have had the privilege to work in both the UK and Japan. My placement in Tohoku University Hospital under the leadership of Professor Kohji Nishida was an unforgettable experience, that I am very grateful to have had the opportunity to be a part of.

I would also like to thank Dr. Rob Young, Dr Yuji Tanaka and Dr. Christian Pinali for their time and effort in teaching me various techniques during the course of my Ph.D.

Finally, I would like to thank all the members of the Structural Biophysics Research Group at Cardiff University, and of the Ophthalmology Department at Tohoku University Hospital.

This work was made possible by a Doctoral Training Award funded by the EPSRC.

LIST OF PUBLICATIONS

Duncan T, Tanaka Y, Shi D, Kubota A, Quantock A J, Nishida K (2010) Flow manipulated, cross-linked collagen gels for use as corneal equivalents. *Biomaterials* 31 (34) 8996-9005.

Tanaka Y, Baba K, **Duncan T J**, Kubota A, Asahi T, Quantock A J, Yamato M, Okano T and Nishida K (2011a) Transparent, tough collagen laminates prepared by oriented flow casting, multi-cyclic vitrification and chemical cross-linking. *Biomaterials* 32 (13) 3358-3366.

Tanaka Y, Kubota A, Matsusaki M, **Duncan T**, Hatakeyama Y, Fukuyama K, Quantock A J, Yamato M, Akashi M and Nishida K (2011b) Anisotropic mechanical properties of collagen hydrogels induced by uniaxial-flow for ocular applications. *J Biomater Sci Polym Ed* 22 (11) 1427-1442.

CONTENTS

1. Chapter One: INTRODUCTION.....	1
1.1. Background.....	1
1.1.1. Ocular structures.....	1
1.1.2. The cornea.....	3
1.1.2.1.Epithelium.....	3
1.1.2.2.Bowman’s layer.....	4
1.1.2.3.Stroma.....	4
1.1.2.4.Descemet’s membrane.....	5
1.1.2.5.Endothelium.....	5
1.2. Collagen.....	6
1.2.1. Collagen super family.....	6
1.2.2. Biosynthesis.....	6
1.2.3. Different classes of collagens.....	9
1.2.3.1. Fibrillar collagens.....	9
1.2.3.2.Fibrillogenesis.....	10
1.2.3.3.FACIT collagens.....	13
1.2.3.4.Other non-fibril forming collagens.....	15
1.2.4. Collagen organisation.....	16
1.3. Proteoglycans.....	17
1.3.1. Glycosaminoglycans.....	18
1.3.1.1.Chondroitin Sulphate.....	21
1.3.1.2. Dermatan sulphate.....	21
1.3.1.3. Keratan sulphate.....	22
1.3.1.3.1. Keratan sulphate biosynthesis.....	22
1.3.2. Small leucine rich proteoglycans.....	23
1.3.3. Corneal proteoglycans.....	24
1.3.3.1.Decorin.....	24
1.3.3.2.Keratocan.....	25
1.3.3.3.Mimecan.....	25
1.3.3.4.Lumican.....	26
1.3.4. The role of corneal proteoglycans.....	27
1.4. Corneal transparency.....	32
1.5. Development of the chick cornea.....	34
1.5.1. Primary stroma.....	34
1.5.2. Secondary Stroma.....	36
1.5.3. Collagen in the developing corneal stroma.....	37
1.5.4. Collagen assembly in the developing corneal stroma.....	40
1.5.5. Proteoglycans in the developing corneal stroma.....	42
1.5.6. The mature corneal stroma.....	43
1.6. Tissue engineering.....	44
1.6.1. Corneal structure and function.....	44
1.6.2. Approaches to stromal tissue engineering.....	46
1.6.3. Future engineering techniques.....	49
1.7. Transmission Electron Microscopy.....	50
1.8. Three-dimensional electron tomography.....	50
1.9. Aims and objectives of the study.....	51

2. Chapter Two: GENERAL METHODS.....	52
2.1. Transmission Electron Microscopy	52
2.1.1. <i>Fixation and staining.....</i>	52
2.1.2. <i>Dehydration and resin embedding.....</i>	53
2.1.3. <i>Sectioning and post-staining.....</i>	53
2.1.4. <i>Observation and Imaging.....</i>	54
3. Chapter Three: AVIAN CORNEAL STROMA.....	55
3.1. Introduction.....	55
3.2. Methods.....	56
3.2.1. <i>Sample collection.....</i>	56
3.2.2. <i>Sample preparation</i>	57
3.2.2.1. <i>Polyetherimide Support Films.....</i>	57
3.2.2.2. <i>Sectioning.....</i>	57
3.2.2.3. <i>Section Staining.....</i>	57
3.2.3. <i>Electron microscopy and Electron Tomography.....</i>	58
3.2.3.1. <i>Tilt Series.....</i>	58
3.2.3.2. <i>Alignment of tilt series.....</i>	59
3.2.3.3. <i>Segmentation of Three-Dimensional Reconstruction.....</i>	60
3.3. Results.....	61
3.3.1. <i>Low magnification Study.....</i>	61
3.3.2. <i>High magnification Study.....</i>	66
3.4. Discussion.....	72
3.4.1. <i>Low magnification Study.....</i>	72
3.4.2. <i>High magnification Study.....</i>	74
3.5. Conclusions.....	78
4. Chapter Four: IN VITRO SYNTHESIS OF COLLAGEN GEL STROMAL EQUIVALENTS.....	79
4.1. Introduction.....	79
4.2. Methods.....	81
4.2.1. <i>Collagen solution preparation.....</i>	81
4.2.2. <i>Cross-linking of collagen gels.....</i>	81
4.2.3. <i>Collagen fibril alignment within the gel.....</i>	82
4.2.4. <i>Collagen laminate gel preparation.....</i>	82
4.2.4.1. <i>Optical clearing and cross-linking of collagen laminate gels</i>	82
4.2.5. <i>Polarized Light Microscope imaging.....</i>	83
4.2.6. <i>Mechanical testing.....</i>	83
4.2.7. <i>Transparency testing.....</i>	83
4.2.8. <i>Transmission electron microscopy.....</i>	83
4.3. Results.....	83
4.3.1. <i>Single layer gels.....</i>	85
4.3.2. <i>Laminated gels.....</i>	91
4.4. Discussion.....	94
4.4.1. <i>Single layer gels.....</i>	94
4.4.2. <i>Laminated gels.....</i>	95
4.5. Conclusions.....	99

5. Chapter Five: <i>IN VIVO</i> CHARACTERISTICS OF COLLAGEN GEL STROMAL EQUIVALENTS.....	100
5.1. Introduction.....	100
5.2. Methods.....	102
5.2.1. <i>Collagen solution preparation.....</i>	<i>102</i>
5.2.2. <i>Cross-linking of collagen gels.....</i>	<i>102</i>
5.2.3. <i>Collagen fibril alignment within the gel.....</i>	<i>102</i>
5.2.4. <i>In vivo implantation.....</i>	<i>102</i>
5.2.5. <i>Corneal thickness measurements.....</i>	<i>103</i>
5.2.6. <i>Histology.....</i>	<i>103</i>
5.2.7. <i>Transmission electron microscopy.....</i>	<i>104</i>
5.3. Results.....	104
5.4. Discussion.....	109
5.5. Conclusions.....	111
6. Concluding Discussion.....	113
7. References.....	122
8. Appendices.....	156
8.1. Appendix 1.....	159
8.2. Appendix 2.....	162

LIST OF FIGURES

Figure 1.1: Cross section of a Mammalian eye (left) and Avian eye (right).....	1
Figure 1.2: Cross section of the human cornea.....	3
Figure 1.3: Collagen type I biosynthesis.....	7
Figure 1.4: Collagen triple helix structure.....	8
Figure 1.5: Corneal type I collagen molecule packing.....	11
Figure 1.6: Orthogonal collagen lamellae in human corneal stroma.....	17
Figure 1.7: Glycosaminoglycan chain structure.....	19
Figure 1.8: Glycosaminoglycan linkage mechanism to proteoglycan protein core.....	20
Figure 1.9: The three-dimensional organisation of a leucine rich repeat motif.....	23
Figure 1.10: Collagen fibril morphology in Decorin and Biglycan-null corneal stroma.....	30
Figure 1.11: Early development of the eye at stages 14-18 and 19-22.....	34
Figure 1.12: Development of the primary stroma at stages 24 and 25.....	35
Figure 1.13: Development of the secondary stroma from stage 27 to 30.....	36
Figure 1.14: Spin coating method of collagen deposition.....	48
Figure 3.1: JEOL 1010 Transmission electron microscope.....	58
Figure 3.2: Screenshot showing the fine alignment stage in eTOMO.....	59
Figure 3.3: Screenshot showing the segmentation and rendering stage in EM3D.....	60
Figure 3.4: En face section of fibrilpositors and collagen.....	62
Figure 3.5: En face section of small fibril bundles and keratocyte surface recesses.....	63
Figure 3.6: En face section of fibril bundles and keratocyte surface recesses.....	64
Figure 3.7: En face section of large fibril bundles and keratocyte compartments.....	65
Figure 3.8: Transmission electron micrographs of the developing chick corneal stroma.....	67
Figure 3.9: Transmission electron micrograph of collagen and proteoglycans in the developing chick corneal stroma.....	68
Figure 3.10: Stereo pairs of three-dimensional reconstructions	69
Figure 3.11: Proteoglycan size scatter graph.....	70
Figure 3.12: Models of collagen fibril and proteoglycan interactions in the chick cornea.....	70
Figure 3.13: Stereo pairs of three-dimensional reconstructions following treatment with chondroitinase ABC.....	75
Figure 4.1: Deacidification of a 10% (w/w) collagen solution through the addition of NaOH..	84
Figure 4.2: Flow-manipulation of collagen mixture to form aligned collagen gels.....	86

Figure 4.3: Cross-linked collagen gels transparency data.	87
Figure 4.4: Mechanical properties of collagen gels.....	88
Figure 4.5: Transmission electron micrographs of collagen gels at x3500 magnification.....	90
Figure 4.6: Formation of laminated gels by centrifugation.....	92
Figure 4.7: Transmission electron micrographs of multi layer collagen gels.....	93
Figure 4.8: Cross sections through parallel and orthogonal laminated gels.	96
Figure 4.9: Mechanical properties of laminated gels.	98
Figure 5.1: Six month implantation of collagen gels into rabbit intra-stromal pockets.....	104
Figure 5.2: Rabbit corneal thickness measurements following implantation of collagen gels.....	105
Figure 5.3: Rabbit corneal cross sections 1 and 6 months post-implantation of collagen gels into intra-stromal pockets.....	107
Figure 5.4: Transmission electron micrographs of rabbit corneal stroma 1 and 6 months post-implantation of collagen gels into intra-stromal pockets.....	108

1. INTRODUCTION

1.1. Background

Although there are similarities between the mammalian and avian eye, it could be argued that the avian eye is in many ways more evolved than the mammalian eye, resulting from the avian sensory world being largely visual. There are also remnants of the reptilian eye that remain present in the structures of the avian eye, such as the scleral ossicles that support the shape of the eye.

The avian eye is considerably flatter than the spherical mammalian eye (Figure 1.1). Relative to body size, the avian eye is also larger, permitting increased depth of focus and a larger retinal image. Whilst an adult human eye has a 25mm approximate diameter, a mature hen eye has an 11.86mm diameter across its equator (Gottlieb et al., 1987).

1.1.1. Ocular structures

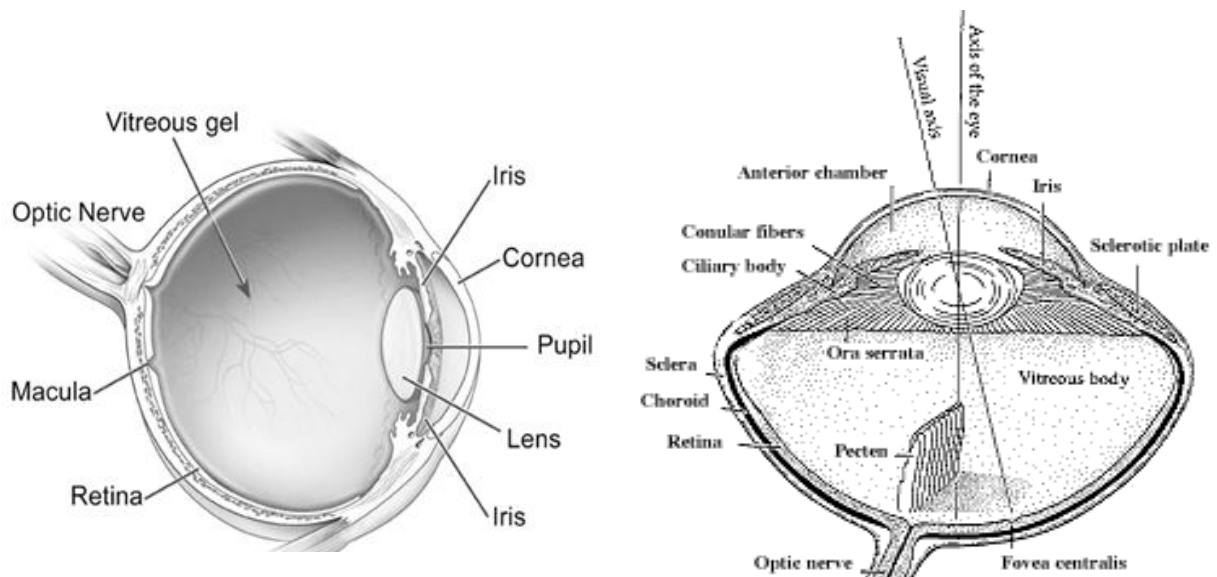


Figure 1.1: Cross section of a mammalian eye (left) and avian eye (right).

(Taken from <http://www.nei.nih.gov/diabetes/content/english/faq.asp> (left) and <http://www.birdsnways.com/wisdom/ww31eii.htm> (right)).

Chapter 1 - Introduction

The sclera is a tough fibrous layer that covers most of the eyeball. The surface of the sclera is covered by the conjunctiva - a mucous membrane consisting of cells and a basement membrane. However, anteriorly the cornea and its surface epithelial cells form the tunic of the eye. Together the sclera and cornea protect the ocular tissues from trauma and infection. Both are composed of a dense network of collagen fibrils, although scleral collagen fibrils are larger and more varied in diameter.

Six extraocular muscles insert into the sclera, to control eye movement. Focusing of avian eyes utilizes corneal and/or lenticular accommodation (Glasser and Howland, 1996). In chicks, corneal accommodation occurs as the anterior ciliary muscles to pull backwards on the inner lamella of the cornea (Glasser et al., 1994).

In avian eyes, small bones known as the scleral ossicles are arranged around the cornea within the sclera. They support the eye and provide an attachment site for the ciliary muscles (Murphy et al., 1995), which in turn help control lens tension via thin zonular fibres attached to the lens capsule. The consequence of this arrangement is that lens shape, dioptric power and focal point can be accurately controlled.

The cornea is the major refractive element of the human eye, responsible for about two-thirds of the total focusing of the human eye (von Helmholtz, 1962) equal to around 42.4 Dioptres. The lens is responsible for the remaining third of focusing power. In the mature avian eye, Schaeffel and Howland (1987) observed that in chick accommodation, up to 9 Dioptres could be accounted for by corneal curvature changes, equivalent to around 40% of the full range of artificially stimulated accommodation (Troilo and Wallman, 1987). Corneal accommodation in chicks occurs because the cornea is able to change shape. This ability is not present in the human cornea.

The tear film is formed from the continuous fluid secretions of the lachrymal gland. Spread across the eye by blinking, this fluid nourishes the front of the eye, lubricates the eyelids, keeps the corneal surface wet and free from irritating particles, and creates a smooth refracting surface. In addition, meibomian glands found at the rim of the eyelids produce an oily substance that helps prevent the evaporation of the tear film.

1.1.2. *The cornea*

The majority of the corneal tissue is composed of uniform collagen fibrils tightly packed together into an entirely avascular matrix, which gains innervation from thin nerve fibres. The highly organised lamellae structure of the collagen fibrils conveys transparency and strength to the tissue. Maintenance of corneal curvature and transparency is integral to its continued function. Any disruption to this arrangement often results in reduced visual acuity.

The cornea is composed of five layers (Hay and Revel, 1969) – epithelium, Bowman's layer, stroma, Descemet's membrane, and endothelium (Figure 1.2).

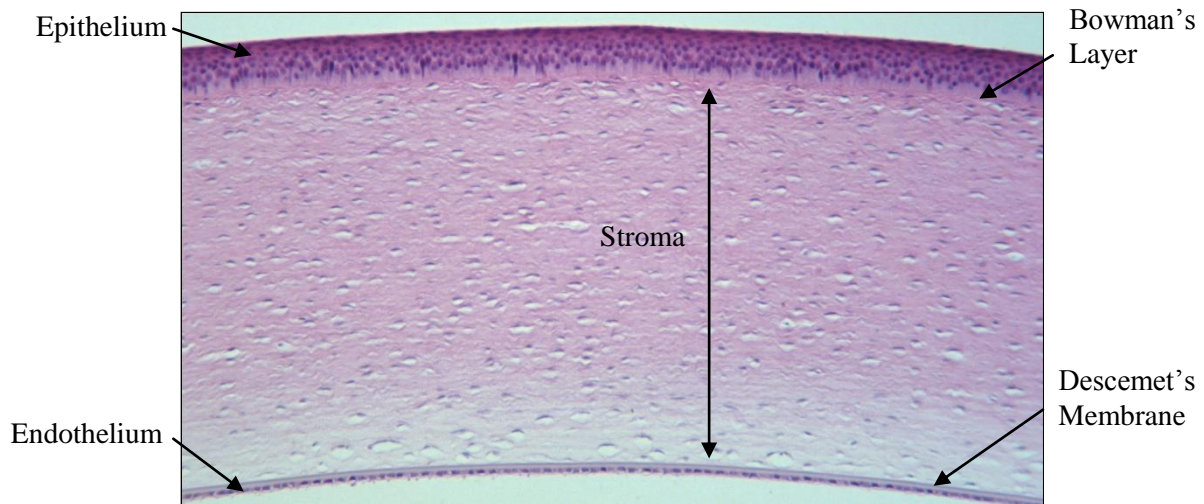


Figure 1.2: Cross section of the human cornea.

(Adapted from http://www.vetmed.ucdavis.edu/courses/vet_eyes/images/archive/s_4015_a.jpg)

1.1.2.1. *Epithelium*

The epithelium constitutes around 10% of the cornea's total thickness, and is composed of layers of three different cell types. The superficial-most layers are made up of non-keratinized, squamous cells. Tight junctions form between these cells, producing a protective barrier against chemical and bacterial damage. The middle layers of cells are polygonal daughter cells produced by a single subjacent dividing layer of cells. These daughter cells migrate superficially to replace the surface cells that degrade and are washed away by the tear

film. The deepest layer of the epithelium contains the basal cells that undergo mitotic divisions, serving as an indefinite supply of replacement cells.

Beneath these cellular layers lies the basal lamina. As the epithelium serves to protect the cornea from abrasive forces, it requires strong anchorage to the underlying stroma. The basal lamina anchors into the lamina densa of the subjacent stromal matrix (Bowman's layer) via epithelial attachment complexes. The basal surface of the deepest layer of epithelial cells possess adhesion complexes called hemidesmosomes, which along with anchoring filaments of type IV and type VII collagen form these strong epithelial attachment complexes.

1.1.2.2. Bowman's Layer

Subjacent to the corneal epithelium, this uniquely organised acellular layer of compact striated collagen fibrils is around 6-8 μ m thick in the chick cornea (Gordon et al., 1994; Marchant et al., 2002), constituting to around 2% of the cornea's total thickness. The collagen fibrils that make up this layer are deposited as a feltwork, and have a smaller diameter of 18-22nm, compared to the 24nm fibrils found within the stroma (Hay and Revel, 1969). The collagen fibrils of Bowman's layer have a functional role as the region of epithelial anchorage via attachment complexes, thus making this layer particularly resistant to mechanical strain. In man Bowman's layer is around 8-12 μ m thick (Tisdale et al., 1988; Komai and Ushiki, 1991), however in some species such as rabbits, this layer is not apparent at any developmental stage, nor in the mature tissue.

1.1.2.3. Stroma

The stroma represents around 85% of the cornea's total thickness. It is a precisely organised, multi-layered structure arising from a tightly controlled sequence of developmental events. It possesses the mechanical strength needed to protect of the intraocular structures, whilst still maintaining the high degree of transparency necessary for light transmission. This ability is the result of small uniform diameter collagen fibrils (approx. 24nm under electron microscopy) arranged into an alternating orthogonal array of separate and distinct layers. The human cornea contains approximately 240 lamellae through the central region (Maurice, 1957; Bergmanson et al., 2005). These lamellae are synthesised by the resident keratocytes, and are orientated parallel to the corneal surface.

In addition to collagen fibrils, the stroma also contains a large amount of water, as well as various glycoproteins and proteoglycans that serve to aid collagen spacing and organisation, and contribute to stromal hydration via their hydrostatic glycosaminoglycan side chains.

1.1.2.4. Descemet's Membrane

Descemet's membrane occupies around 1% of the cornea's total thickness, and acts as a specialized basement membrane-like structure for the corneal endothelium, serving as a barrier to substances in the anterior chamber of the eye. As with all basement membranes, it contains fibronectin and laminin glycoproteins, as well as various collagen types that may be involved in stromal attachment.

However its similarities to a basement membrane have previously been questioned. Fitch (1990) showed that the nodal matrix of Descemet's membrane contained no type IV collagen, a feature inherent to mature basement membranes. This collagen type was however seen penetrating the membrane, forming irregular plaques in the boundary between Descemet's membrane and the stroma, enhancing endothelial adhesion.

1.1.2.5. Endothelium

The endothelial cell layers constitute around 1% of the cornea's total thickness. A mosaic pattern of hexagonal cells, this single cellular layer has a role in maintaining corneal transparency by regulating corneal hydration via a complex pump-leak mechanism (Hodson and Miller, 1976): bicarbonate ions leak across the endothelium into the stroma of the cornea, the ion-pump then transports the ions back into the aqueous humour via a continuous pump. It keeps stromal hydration at an equilibrial state, preventing stromal swelling that would then lead to a loss in transparency. Cell population density in this layer decreases naturally with age; as a result cell shape and size adjust to retain the integrity of the layer. When the endothelial cell density decreases to a critical point of around 800 cells/mm², stromal swelling results in the disruption of the organized collagen arrays (Forrester et al., 2002; Edelhauser, 2006), which leads to corneal opacity.

1.2. Collagen

1.2.1. Collagen superfamily

The collagen super-family represent around 25% of the total body protein in mammals (Horton et al., 2002). Present in most connective tissues (bone, blood vessels, cornea, cartilage and skin), there are currently 29 genetically unique collagen subtypes in the vertebrate system (Soderhall et al., 2007). However, all collagen molecules are still structurally connected on some level. For example, they all contain a characteristic triple helix domain, and are composed of three polypeptide subunit α -chains. These chains have particular amino acid sequences and individual gene loci. There are a total of forty different α -chains from which collagen molecules can be composed; collagen type I for example contains two α -1 chains and one α -2 chain.

Dependant on their particular function and anatomical location, the collagen molecules can then either assemble into fibrils, or into non-fibrillar formations. Whereas fibril forming collagens will possess a triple-helix domain often around 95% of their length, non-fibrillar collagen molecules possess only short triple-helix segments. These molecules may then form globular structures that interact with other matrix components.

1.2.2. Biosynthesis

The collagen biosynthesis pathway is a complex series of biochemical processes that varies between collagen subtypes. Often the precise structural engineering of these molecules depends on their particular functions. For example collagen type XII is frequently spliced into long and short forms; consequently these different forms have different spatial and temporal locations, presumably reflecting different functional roles (Wessel et al., 1997; Young et al., 2002).

The three α -chains are synthesised on the rough endoplasmic reticulum within stromal keratocytes, they are then assembled into an immature collagen fibril form, known as procollagen (Comper, 1996). Post-translational modification of the procollagen molecules determine the structure (and thus function) of the collagen fibrils. This initially occurs intracellularly, where proline residues are hydroxylated to enable hydrogen bonding between

hydroxyproline residues, this then enhances the stability of the triple helix (Hay, 1991). In addition, in some collagen types lysine residues also undergo enzymatic hydroxylation. Hydroxylysine then has a role in the formation of cross-links within and between collagen molecules (Comper, 1996).

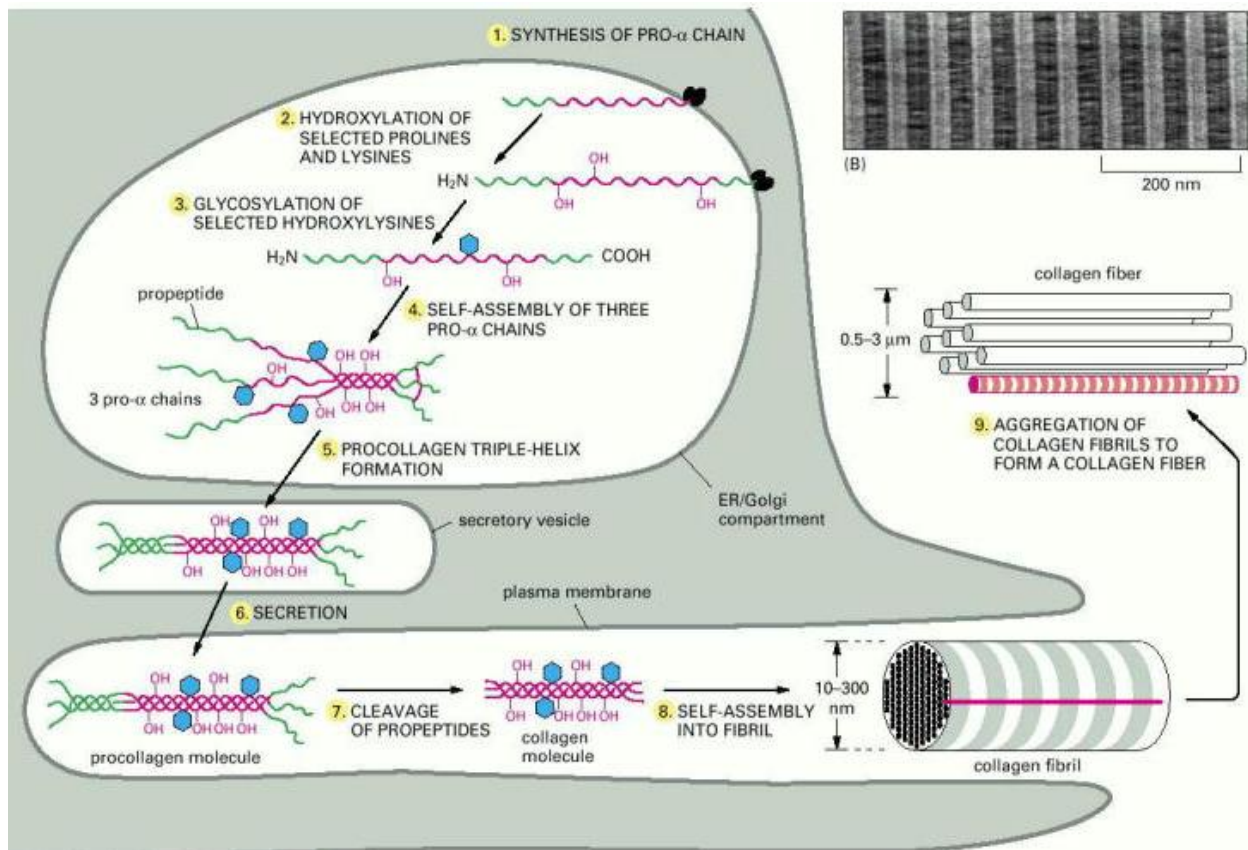


Figure 1.3: Collagen type I biosynthesis.

Steps 1-5 occur within the cytoplasmic endoplasmic reticulum/Golgi compartment. Transportation in a secretory vesicle to the cell surface membrane is then followed by the extracellular assembly of the procollagen molecules into mature fibrils (Steps 7-8). Step 9 shows one example of how collagen fibrils are arranged into a three-dimensional array – these collagen fibres are found within the extracellular matrix of tendon and muscle tissue. In the cornea, collagen fibrils do not form fibres, instead they assemble into orthogonally orientated lamallae (Taken from Alberts et al., 2002).

Extracellular modifications process the procollagen molecule into a mature state (Figure 1.3). Propeptidase enzymes cleave the terminal sequences from the ends of the molecule, allowing the molecules to associate into parallel arrays of fibrils. These may then in turn assemble with

other fibrils into a collagen fibre, or in the case of the corneal stroma, into orthogonal lamellae.

The collagen molecule is composed of three α -chains that form a triple helical structure. The α -chains are left handed polypeptide molecules contain a repeating Gly-X-Y amino acid motif, where X and Y are frequently proline and hydroxyproline. This repeating amino-acid motif is essential for the formation of the helical rope-like structure. X-ray diffraction has confirmed the triple helical structure of collagen molecules (Ramachandran, 1967). The three left handed α -chains associate to form the right handed triple helix structure (Figure 1.4), which is then stabilized by hydrogen bonding between the proline carbonyl groups and glycine amino groups of adjacent α -chains, as well as inter and intramolecular cross-links.

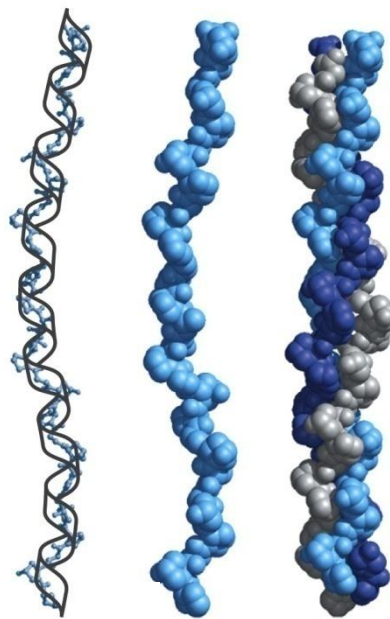


Figure 1.4: Collagen triple helix structure.

A single left handed α -chain composed of a Gly-X-Y amino acid motif (left). Three α -chains associate to form a right handed triple helix structure (right) which is stabilized by hydrogen bonding, intermolecular and intramolecular cross-links (Adapted from Lehninger et al., 2005).

The precise primary structure of the α -chains varies between collagen types. Similarly, the collagen molecule can be heterotypic or homotypic, depending on whether they are composed of different or identical α -chains. Collagen type I is a heterotypic molecule,

containing two identical, and one different α -chain [$\alpha 1(I)_2 \alpha 2(I)$]. Collagen type II however, is homotypic. Containing three identical α -chains [$\alpha 1(II)$]₃. The molecular components of these collagen molecules affect the overall structure and thus the functional role that the collagen fibril will have in the tissue.

1.2.3. Different classes of Collagens

Within each family of collagen molecules there is a shared genomic ancestry, having derived from a common parental gene (Buttice et al., 1990). The classification of collagen molecules into these different families is dependent on the particular molecule structure, organisation, and size.

1.2.3.1 Fibrillar Collagens

There is now considerable evidence that suggests that the fibrillar collagens of the avian cornea (type I, II, V) frequently form heterotypic structures, containing multiple collagen types (Linsenmayer et al., 1983, 1984; Fitch et al., 1984, 1988; Birk et al., 1988; Mendler et al., 1989). Antibody masking (Linsenmayer et al., 1983; Birk et al., 1988), and enzymatic digestion of selective components of the heterotypic fibrils (Fitch et al., 1984, 1988) revealed that collagen type V and type I are assembled together into heterotypic fibrils in the stroma of the mature avian cornea. The triple helix domain of type I collagen can be seen within and at the surface of the heterotypic fibrils. Conversely, numerous type V collagen molecules run strictly within the fibril, only the large NH₂ terminal domain of the molecules can be seen protruding through gap zones to the fibril's surface. It is hypothesized that this formation would then serve to inhibit the addition of further collagen molecules to the fibril's surface – thus mediating fibril diameter (Linsenmayer et al., 1998).

Type I collagen is primarily responsible for the tensile mechanical strength of the cornea. It is the predominant collagen type in Bowman's layer and the stroma. It is integral to the development of stromal organisation. In the Mov13 mutant mouse model, where no type I collagen forms, the corneal stroma contained thin collagen fibrils with no structural orthogonality (Bard and Kratochwil, 1987). Synthesised by keratocytes in the corneal stroma, type I collagen forms heterotypic fibrils with collagen type II in the developing avian corneal stroma, and with type V in the mature avian stroma (Hendrix et al., 1982; Birk et al., 1988).

Type II collagen is present only in the primary stromal stage of avian corneal development, reaching undetectable levels by the stage of corneal condensation (Cai et al., 1994). It has been observed in the primary stroma forming heterotypic fibrils with type I collagen, and forming covalent links to type IX collagen (Fitch et al., 1994).

Type V collagen is prolific throughout the avian corneal stroma (Hay, 1991). Its appearance coincides with mesenchymal cell invasion (Linsenmayer et al., 1984), as it is synthesised by the differentiated stromal keratocytes (Ruggiero et al., 1996). Forming heterotypic fibrils with type I collagen (Linsenmayer et al., 1983; Birk et al., 1988), it may serve to regulate fibril diameter within the stroma and play a role in anchoring of basement membranes to the subjacent stromal matrix (Birk et al., 1990). Around 20% of collagen in the mature cornea is type V, resulting in the synthesis of thin heterotypic fibrils with a uniform diameter (Linsenmayer et al., 1983). *In vitro* fibrillogenesis studies (Birk et al., 1990) have demonstrated that by altering the relative proportions of type I and type V fibrillogenesis, fibril diameter can be controlled – the greater the proportion of type V fibrillogenesis, the thinner the diameter of the resultant heterotypic fibril. This heterotypic collagen arrangement is also found in the human cornea (Ruggiero et al., 1996; White et al., 1997). In addition, in humans, naturally occurring mutations that affect the relative levels of these collagen types produce a similar effect on collagen fibril diameter (Bonaventure et al., 1989; Wenstrup et al., 1996).

1.2.3.1.1. Fibrillogenesis

Collagen fibrillogenesis is the process of assembling and packing the collagen molecules into fibrillar structures. It has been hypothesized, from studies on chick and murine tendon that initiation of procollagen processing and collagen fibrillogenesis occurs within intracellular membrane bound vesicles. Transported from the Golgi apparatus to the plasma membrane, the collagen fibrils are then excreted into the extracellular matrix by plasma membrane protrusions (fibripositors) and the adjacent extracellular channels they form aligned along the cell's axis (Canty et al., 2004) (see Figure 1.3). The nucleation stage of fibrillogenesis occurs at the base of these channels (several microns within the cell); whilst towards the end of these processes the fibrils are then deposition into the extracellular matrix. This suggests that the parallel arrangement of collagen fibres in tendon is established by the late secretory pathway

and interactions of adjacent fibrilpositors and the extracellular channels they form (Canty et al., 2004). However the fibrilpositor theory has yet to be proved conclusively. Furthermore, whilst this theory is conceptually easy to visualize for simple uniaxial tissues such as tendon, whether it can also relate to the production of a complex three-dimensional matrix such as the corneal stroma remains largely unknown.

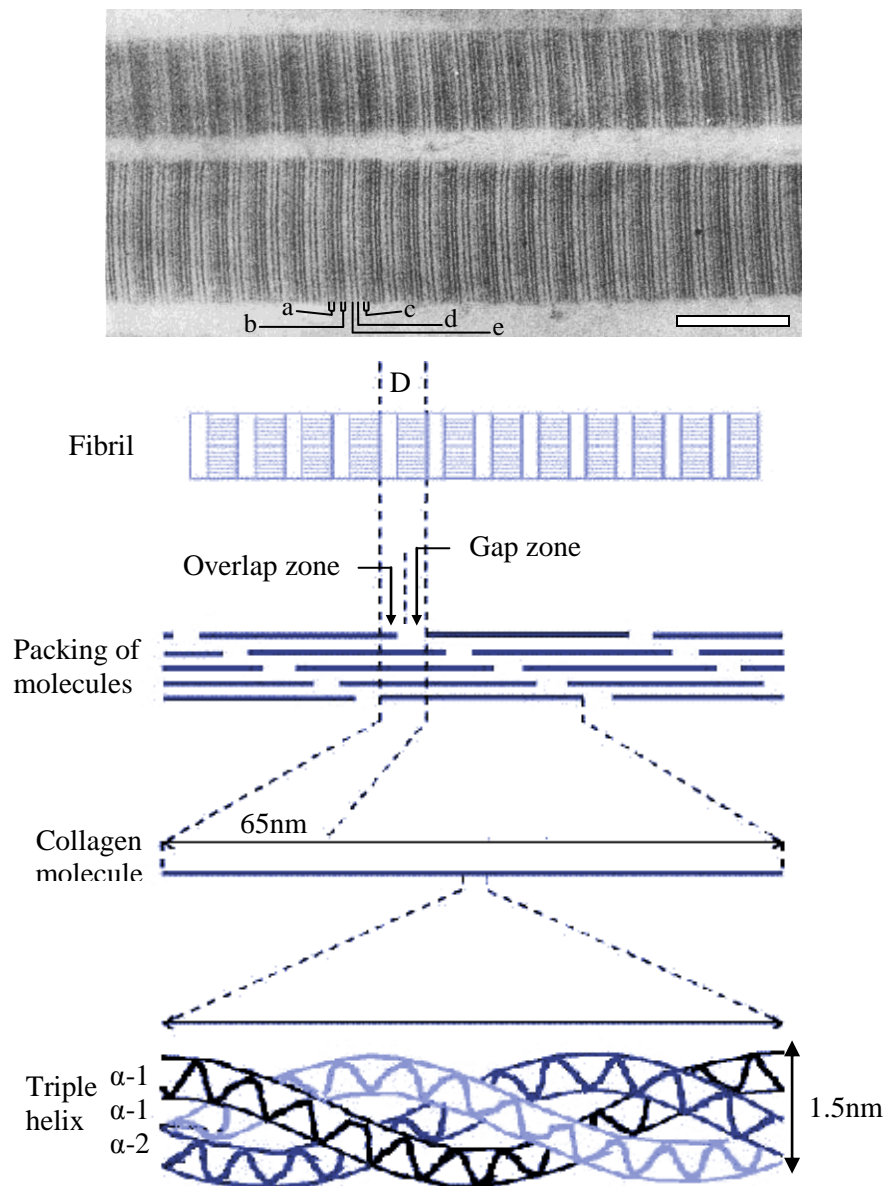


Figure 1.5: Corneal type I collagen molecule packing.

Collagen molecules pack together to form a collagen fibril. The staggered arrangement of collagen molecules creates overlap and gap zones that produce the characteristic 'a', 'b', 'c', 'd' and 'e' banding pattern of collagen fibrils seen under electron microscopy. Scale bar = 250nm. (Diagram adapted from Ross et al., 1989; micrograph adapted from Young, 1985).

The collagen molecules within tendon fibrils are arranged with a longitudinal staggering equal to 67nm or 234 amino acids (Meek et al., 1979), occurring through a process of axial translation called the D-periodicity (Hodge and Petruska, 1963). Consequently there is a 0.6D gap between the amino end terminal of one collagen molecule and the start of the next molecule (Figure 1.5). This creates overlap zones and gap zones within each D-period that correspond respectively to the 'a' and 'c' bands, and the 'd' and 'e' bands of the collagen fibril. These zones appear under transmission electron microscopy as alternating dark and light bands. In skin and corneal collagen fibrils, the axial periodicity is closer to 65nm (Marchini et al., 1986). The different banding patterns observed in these tissues are the result of corneal (C-type) collagen molecules possessing an angular orientation of 15° (with respect to the fibril axis) as they run helicoidally throughout the length of the collagen fibril (Holmes et al., 2001). Conversely in tendon (T-type) fibrils, the highly tensile nature of the tissue results in only a 5° angular displacement of the collagen molecules from the fibril axis (Marchini et al., 1986).

There are several models that describe the three-dimensional assembly of collagen molecules into mature fibrils, often dependant on the technique in use (such as transmission electron microscopy or X-ray diffraction). Smith's microfibrillar theory (1968) was the first accepted model based on the lateral aggregation of five tropocollagen molecules to form a microfibrillar collagen filament. Hulmes and Miller (1979) suggested a model of quasi-hexagonal collagen molecule packing that occurs without the need for microfibrillar substructures, where the molecules within the fibril create sheet structures that have a molecular para-crystalline formation. This model also indicated that the collagen molecules were angularly displaced from the fibril axis, either by tilting of the straight molecules, or by super coiling of the molecule as first suggested by Miller and Wray (1971). Orgel et al (2006) demonstrated a similar organisation within type I collagen microfibrils. They purposed that adjacent collagen molecules twist into a super-coiled right-handed microfibril. In this arrangement, quasi-hexagonally molecular packing creates the para-crystalline lattice structure.

Holmes et al (2001) reported that in bovine cornea, each collagen fibril may in fact be composed of smaller 4nm diameter microfibrils. The microfibril lateral packing also demonstrated structural regions of both order and disorder, commonly at the N terminal and C terminal telopeptides, as well as the d-band of the gap zone. The regions of ordered

structure also coincided with binding regions for extracellular macromolecules such as proteoglycans. Fibril stability is enhanced by interfibrillar and intermolecular cross-links that grant a tensile strength to the structure. It is also hypothesized that these cross-links aid in the transmission of force across the entire structural array, dissipating stress and enhancing structural integrity (Orgel et al., 2006).

In the cornea, collagen fibrils then assemble into flat lamellae, where fibril diameter and interfibrillar spacing may be mediated in part through proteoglycan interactions (Scott 1985; 1988). Electron microscopy techniques have reported that the collagen fibril diameter within these lamellae appears to be a relatively constant 24nm throughout a large proportion of the vertebrate kingdom (Craig and Parry 1981). However, X-ray diffraction studies have shown that this measurement may in fact vary dependant on the technique used to study the tissue, as it affects the hydration levels of the stroma (Sayers et al., 1982; Meek et al., 1991). Standard electron microscopy, that shows fibril diameter to be around 24nm, requires the chemical dehydration of the tissue being processed. However, Sayers et al (1982) demonstrated using X-ray diffraction that air dried bovine corneal samples show a markedly increased fibril diameter of 40nm. Further X-ray diffraction studies undertaken by Meek and Leonard (1993) using an alternative method, gave a reading of 38.2nm in bovine cornea at physiological hydration. Similarly Worthington and Inouye (1985), also using X-ray diffraction on untreated (hydrated) bovine cornea, showed a fibril diameter of 39nm. Low temperature electron microscopy studies indicate fibril diameter to be around 38nm (Craig et al., 1986). This figure correlates closely with the results from X-ray diffraction studies (Sayers et al., 1982; Worthington and Inouye, 1985; Meek and Leonard 1993), demonstrating that the conventional dehydration and embedding used in standard electron microscopy dramatically affects the fibril diameter observed.

1.2.3.2. FACIT collagens

Characterised as ‘Fibril associated collagens with interrupted triple helices’, there are seven members in the FACIT family including collagen types IX, XII, XIV, XVI, XIX, ,XX, and XXI (Gordon et al., 1989; Comper et al., 1996; Fitzgerald et al., 2001). They universally possess several triple helical domains that alternate with non-triple helical domains. Functionally, they interact with other matrix components and the surface of fibrillar collagen molecules. Consequently, FACIT molecules have several structural domains. Some lie along

Chapter 1 - Introduction

the fibril surface and often anchor the molecule to the underlying fibrillar collagen by covalent cross-links (Vaughan et al., 1988). Other domains extend outwards from the fibril, interacting with adjacent fibrils and other matrix components (Comper, 1996). However, the exact supramolecular organisation of these molecules is currently unknown.

Type IX is the major FACIT collagen involved in avian corneal development (Svoboda et al., 1988). This collagen molecule associates with the surface of type II collagen fibrils in the primary corneal stroma. Absent during the period of stromal swelling, it is implicated as a stabilizing factor, whose presence maintains the primary stroma as a compact matrix (Cai et al., 1994). In the developing avian corneal stroma, two different isoforms have been detected. One of which possesses non-collagenous domains that may function as a bridge between fibrils or to other matrix components (Fitch et al., 1995).

Types XII and XIV are structurally similar molecules, and are also present during development of the avian corneal stroma. Generally associated with the surface of type I collagen fibrils (Keene et al., 1991), these FACIT collagens may have a role in stabilizing the fibrillar architecture within the stroma through interactions with adjacent cells and extracellular matrix components (Gordon et al., 1996).

The mRNA for both molecules can be differentially spliced, forming 'long' or 'short' form polypeptides. Both forms of type XII collagen are expressed in several tissues during avian embryogenesis, localised in the developing primary and secondary corneal stroma at variable temporal and spatial locations (Young et al., 2002).

Type XIV collagen has been observed progressing posteriorly from the subepithelial region during mesenchymal cell invasion. Consequently, it is distributed throughout the stroma just before stromal compaction (Gordon et al., 1996). Synthesis of type XIV collagen across the secondary stroma then increases as compaction begins, peaking between days 10 to 14, at which point production declines (Young et al., 2002). It is therefore possible that interactions between this collagen type and the surface of fibrillar collagens may stabilize the movement of fibrils and stromal compaction.

Type XII collagen is synthesized by the corneal epithelium, and is present in the primary stroma by developmental day 5. During synthesis of the secondary stroma, type XII collagen

is localised in the subepithelial and subendothelial regions (Akimoto et al., 2002) – such as the interface between the anterior stroma and Bowman’s layer, and the interface between the posterior stroma and Descemet’s membrane. This suggests it may serve to stabilize these regions (Gordon et al., 1996).

As type XII and type XIV collagen molecules are expressed at different developmental stages, they may interact with different matrix components, and hence may have slightly different roles. Type XII is implicated in fibril organisation and matrix stability (Gordon et al., 1996), whilst type XIV may assist in fibrillogenesis (Young et al., 2002).

In the mature avian corneal stroma the long form of type XII collagen is no longer present. Whilst in the mature human cornea it can be seen in the stroma, epithelial basement membrane and Bowman’s layer (Wessel et al., 1997).

Type XX FACIT collagen was discovered in the embryonic chick relatively recently. Found only in minor quantities, it is weakly expressed in several connective tissues including tendon, skin, and to a greater extent in corneal epithelium (Koch et al., 2001). Here it is expressed at a constant level between days 7 and 13 in a similar pattern to type XII collagen.

1.2.3.3. Other non-fibril forming collagens

Type IV collagen is a ubiquitous component of basement membranes. Along with other matrix components it forms mesh-like networks that are situated beneath all epithelial and endothelial cell layers. In the developing avian cornea type IV collagen is also found in the interface region between Descemet’s membrane and the posterior stroma. Observed extending into both structures, it promotes endothelial adhesion by forming contacts with endothelial cell processes (Linsenmayer et al., 1998). Type IV collagen is also found in unique structures within the developing avian corneal stroma, such as stromal strings and plaques of basement membrane-like material (Fitch et al., 1991).

Type VI collagen molecules are organised into beaded filaments that become detectable at the time of mesenchymal cell invasion (Linsenmayer et al., 1986). Synthesised by mesenchymal cells in the developing cornea, type VI collagen associates with striated fibrils in the loose stroma to form an interlocking matrix (Linsenmayer et al., 1986). In the mature

cornea, synthesised by fibroblasts, these beaded filaments run between lamellae and fibril bundles.

Type VII collagen is present at the epithelial-stromal interface. It forms anchoring fibrils that help stabilize the attachment of the basement membrane to the underlying stromal matrix (Keene et al., 1987), through interactions with collagen type IV anchoring plaques.

Type VIII collagen is a component of Descemet's membrane in the avian cornea. Belonging to a class of small collagens half the size of fibrillar collagens (Yamaguchi et al., 1991), type VIII collagen molecules likely form a hexagonal lattice arrangement (Jakus, 1956).

Type XVII collagen is thought to have a role in epithelial attachment complexes and is a component of transmembrane hemidesmosomes in the avian cornea. The intracellular globular domains of the collagen molecules form the hemidesmosome, whilst the extracellular collagenous domains provide basement membrane attachments (Gordon et al., 1997; Linsenmayer et al., 1998).

Type XXIII is a member of MACIT (membrane associated collagens with interrupted triple helices) collagen types. Collagen type XXIII is related to types VIII and XV, and is associated with the epithelium and endothelium of the developing avian cornea (Koch et al., 2006). It is thought to have a stabilizing role in regions of matrix-matrix interface such as Bowman's layer and Descemet's membrane.

1.2.4. Collagen organisation

The collagen lamellae of the avian stroma are stacked so that adjacent layers are orientated orthogonally (Figure 1.6). Transparency is brought about by this highly organised collagen structure, combined with the avascular nature of the cornea.

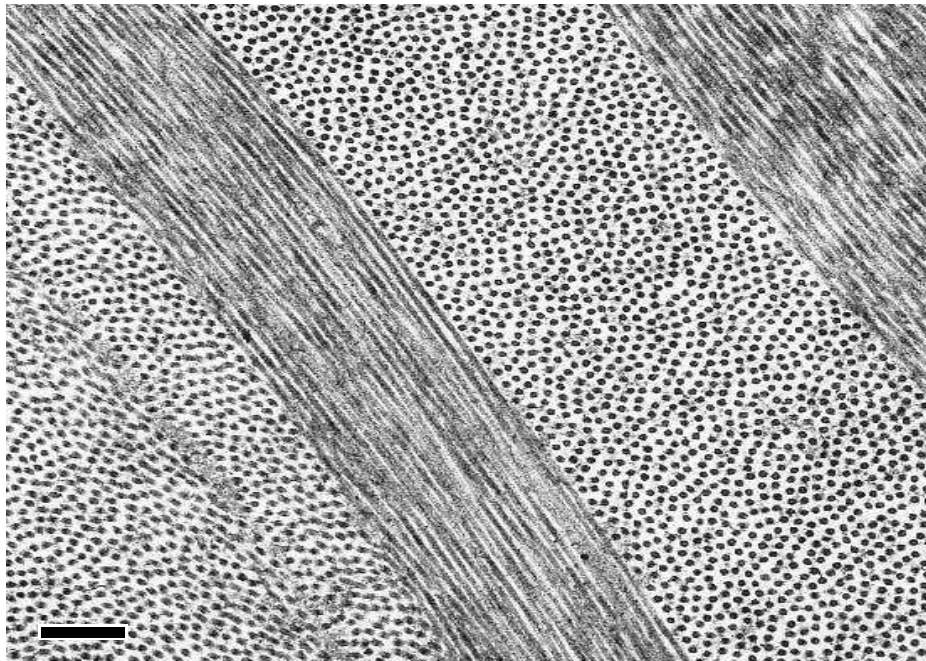


Figure 1.6: Orthogonal collagen lamellae in human corneal stroma.

Scale bar = 500nm (Courtesy of Dr Rob Young, unpublished data).

Although striated collagen fibrils within the cornea appear uniform, increased fibril stability in certain areas of the cornea suggest possible structural and functional differences. Similarly, organisation of the lamellae varies depending on location within the stroma. The collagen lamellae cross the apex of the corneal dome as they run from limbus to limbus. In the anterior of the stroma, collagen lamellae appear as thin, narrow bundles densely interwoven. Consequently, the tighter packing and denser interweaving causes the layers run at an oblique angle to the corneal surface (Radner et al., 1998). Conversely in the posterior stroma, lamellae are thicker and wider and run parallel to the corneal surface, with a lesser degree of interlacing (McTigue, 1967). Throughout the stroma, interconnections between lamellae are formed by interweaving of adjacent layers, disulphide cross-links between fibrils, and interlacing of the divided sublayers of adjacent lamellae (Radner and Malingier, 2002).

1.3. Proteoglycans

Proteoglycans are found throughout most tissues, either within intracellular vesicles, on a cell surface, or in the extracellular matrix. They are water-soluble molecules composed of a protein core around which is covalently bound one or more polysaccharide carbohydrate chains called glycosaminoglycans. Proteoglycans are distinguishable from glycoproteins by

the structure of their protein core. They are more acidic in nature due to the high negative charge generated by the long, unbranching, highly sulphated sugar chains attached to their protein cores.

Proteoglycans can be categorized according to function, for example basement membrane proteoglycans, large extra-cellular proteoglycans, and cell-associated proteoglycans. However due to their prolific nature and diverse structures, some proteoglycans belong to more than one group, having multiple biological functions. When categorized by glycosaminoglycan structure, the two predominant proteoglycan families within the corneal stroma are those with keratan sulphate side chains, and those with chondroitin sulphate/dermatan sulphate side chains.

1.3.1. Glycosaminoglycans

Glycosaminoglycans are sulphated carbohydrate polymers containing 40-100 repeating disaccharide units. These units contain an N-acetylated hexosamine (such as D-glucosamine or D-galactosamine) and a second sugar residue of either L-uronic acid or D-galactose (Figure 1.7). Consequently, one of the two sugars in the repeating disaccharide is always an amino sugar (where the nitrogen of the amino group has an acetyl group attached) – either N-acetylglucosamine or N-acetylgalactosamine – hence the name glycosaminoglycan. The specific glycosaminoglycan type is determined by their linkages, the various sugar residues present in the disaccharide units, and the location and number of sulphation sites. The two major glycosaminoglycan types in the cornea are keratan sulphate and a chondroitin sulphate/dermatan sulphate hybrid. Other types include hyaluronic acid and heparan sulphate.

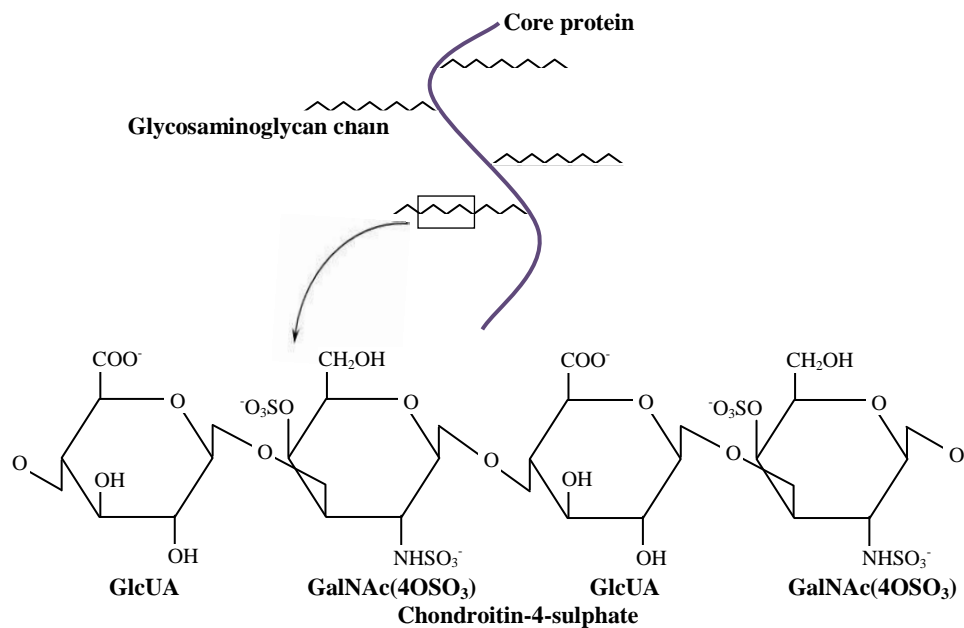


Figure 1.7: Glycosaminoglycan chain structure.

Glycosaminoglycans are composed of repeating disaccharide units composed of an N-acetylated hexosamine and a second sugar residue of either L-uronic acid or D-galactose (Adapted from Bomsel and Alfsen 2003).

The region of sulphation on the N-acetylgalactosamine unit often shows a high degree of variability. This may reflect the diverse biological functions of these molecules. For example, more immature articular cartilage shows a greater degree of sulphation is seen at position four relative to that seen at position six (Saamanen et al., 1989). It is hypothesized that sulphation at position six results in a more spatially free orientation. This then supports a greater degree of interaction with other components in the extracellular matrix (Saamanen et al., 1989).

Glycosaminoglycans are covalently linked to the proteoglycan protein core by specific oligosaccharide structures (with the exception of hyaluronic acid which exists as a free chain) (Figure 1.8). Keratan sulphate is either N-linked to Asn residues, or O-linked to Ser or Thr residues in mature skeletal tissues (Barry et al., 1995). Chondroitin sulphate, dermatan sulphate and heparan sulphate are O-linked to the protein core by Ser residues (Comper, 1996).

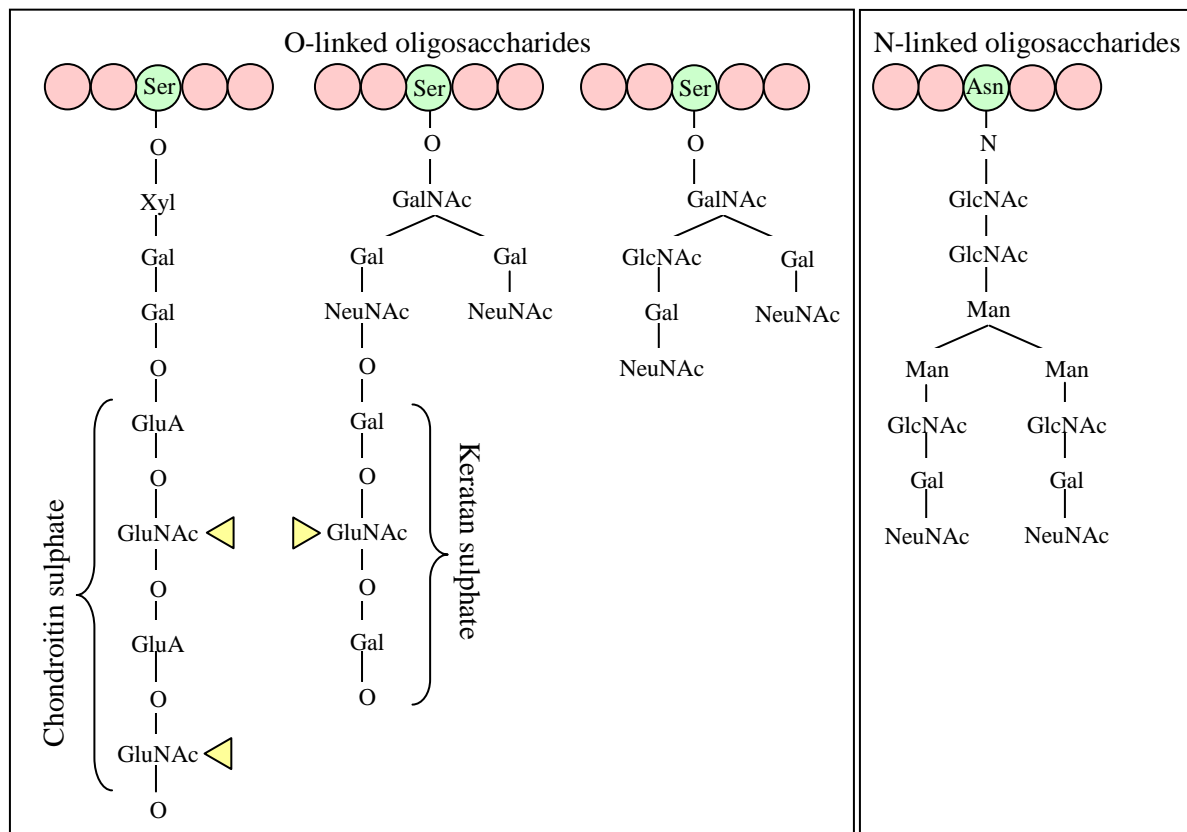


Figure 1.8: Glycosaminoglycan linkage mechanism to proteoglycan protein core.

Covalent linkage to the proteoglycan protein core occurs through specific oligosaccharide structures. Ser-Serine; Asp-Asparagine; Xyl-Xylose; GalNAc-N-acetylgalactosamine; GlcNAc-N-acetylglucosamine; Gal-Galactose; NeuNAc-N-acetyl-D-neuraminic acid; Man-Mannose; GluA- β -D-glucuronic acid. Yellow arrowheads indicate sulphate groups (Adapted from Garrett and Grisham 2005).

Under physiological conditions, the charged anionic groups on the glycosaminoglycan molecules are fully ionized. They therefore show a high negative charge, often varying between disaccharide units dependant on the particular sulphate content (Comper and Laurent, 1978). The resulting electrostatic interactions allow proteoglycans to interact with other macromolecules. This negative charge also results in an osmotic draw, causing matrix swelling and the formation of a compression resistant structure (Comper and Laurent, 1978). In addition, the glycosaminoglycan charge is also thought to contribute to corneal transparency through the maintenance of fibril spacing, with the electrostatic forces exerting a repulsive force on adjacent fibrils (Hedblom, 1961; Scott, 1988).

Recent studies in reconstruction three-dimensional corneal proteoglycans have observed large proteoglycan complexes spanning across the width of several collagen fibrils. It is thought that these larger proteoglycans are the result of self-assembly or aggregation of glycosaminoglycan chains from individual proteoglycans to form anti-parallel multimers. Whilst it is possible to determine the structure of the bond from these reconstructions, several models have been suggested as to how these aggregations may be organised (Knupp et al., 2009; Lewis et al., 2010; Parfitt et al., 2010). The mechanism by which these lateral associations form is also not clear. The ionic balance of the stroma is known to be important for proteoglycan interactions. It is possible that the negative charge of the glycosaminoglycan chains is cancelled out by positively charged ions within the stroma (K^+ , Na^+), allowing them to associate through hydrophobic attraction and hydrogen bonding (Scott, 2001).

1.3.1.1. Chondroitin sulphate

The precise structure of chondroitin sulphate varies depending on its anatomical location, with both chain length and sulphation patterns fluctuating between individual molecules (Roughley and Lee, 1994). However the standard structure of this glycosaminoglycan is a repeating disaccharide unit is composed of N-acetylgalactosamine and glucuronic acid (Cheng et al., 1992; Roughley and Lee, 1994). In the cornea, chondroitin sulphate is present in both sulphated forms chondroitin-4-sulphate and chondroitin-6-sulphate (Handley and Phelps, 1972). Initially synthesised by the epithelial cells of the developing cornea, this glycosaminoglycan may have a morphogenetic role in conjunction with other matrix molecules (Trelstad et al., 1974).

1.3.1.2. Dermatan sulphate

The repeating disaccharide units of dermatan sulphate's glycosaminoglycan chains are composed of N-acetylgalactosamine and iduronic acid (Rosenberg et al., 1985). Dermatan sulphate could be considered a modified form of chondroitin sulphate, as the iduronic acid residues are formed simply from the action of an epimerase enzyme on a glucuronic acid residue (Malmstrom and Aberg, 1982). Sulphation of the iduronic acid residues occurs at the second position, whilst sulphation at position 4 of the N-acetylgalactosamine residues is also common in the cornea (Roughley and Lee, 1994). The resulting dermatan-4-sulphate form

constitutes around a fifth of the glycosaminoglycan content in the adult mammalian corneal stroma (Scott Bosworth, 1990).

1.3.1.3. Keratan sulphate

Unlike chondroitin sulphate and dermatan sulphate glycosaminoglycan chains, keratan sulphate does not contain uronic acid residues. Rather the repeating disaccharide units are composed of N-acetylglucosamine and galactose (Roughley and Lee, 1994). In addition it also possesses two forms of linkage to a protein core. The type I isoform, present in the cornea, links via the amino group of an Asn amino acid in small proteoglycan protein core (Greiling and Scott, 1989). This isoform is the predominate glycosaminoglycan found in mammalian and avian corneal stroma, constituting to around half of the total glycosaminoglycan content of the mature tissue (Scott Bosworth, 1990). The type II isoform is found in skeletal tissues, and links via the hydroxyl group of Ser or Thr residues of large proteoglycan protein cores (Nilsson et al., 1983). Sulphation of these isoforms can occur at position 6 of both the hexosamine and the galactose residues (Roughley and Lee, 1994).

1.3.1.3.1. Keratan sulphate biosynthesis

The keratan sulphate polymer is elongated by the alternating addition of galactose and N-acetylglucosamine by a glycosyltransferase enzyme (Funderburgh et al., 2000). Cai et al (1996) observed that during avian development, increased keratan sulphate biosynthesis in the corneal stroma coincides with increased glycosyltransferase activity. The enzyme activity is then also sustained within adult cells (Cai et al., 1996).

After assembly of the polymer, keratan sulphate undergoes sulphation by multiple sulphotransferase enzymes (Kusche-Gullberg and Kjellén, 2003). In corneal keratan sulphate, most N-acetylglucosamine residues are sulphated, as are around half of the galactose residues. However unlike galactose sulphation, N-acetylglucosamine sulphation is coupled with chain elongation (Funderburgh, 2002). Mutations in the CHST6 gene that encodes the N-acetylglucosamine-6-sulphotransferase enzyme are thought to lead to the inactivation or loss of this enzyme, and are responsible for type I and type II macular corneal dystrophy (Akama et al., 2000). A second enzyme is involved in the sulphation of galactose, and has been observed preferentially targeting internal galactose residues if they lie adjacent to sulphated

N-acetylglucosamine residues (Torii et al., 2000). In addition, sulphation of terminal galactose residues appears to inhibit polymer elongation (Akama et al., 2002).

1.3.2. Small leucine-rich proteoglycans

Stromal proteoglycans belong to a twelve member superfamily of small leucine-rich proteoglycans (SLRP). The predominate SLRPs of the cornea are decorin (Bianco et al., 1990; Li et al., 1992), biglycan (Bianco et al., 1990; Funderburgh et al., 1998), lumican (Blochberger et al., 1992), mimecan (Funderburgh et al., 1997) and keratocan (Corpuz et al., 1996).

This superfamily is characterised by a terminal ‘leucine-rich repeat’ consensus sequence motif that runs through the COOH- terminal cysteine cluster, as well as throughout the protein core sequence (Hocking et al., 1998). Amongst the different members of this superfamily, this consensus sequence is repeated between 6 and 11 times between the cysteine clusters and varies in length between 20-29 amino acid residues, the most common being 24 (Hocking, 1998). Although the leucine-rich repeat sequences are often highly conserved between SLRPs, there is no common amino-acid sequence amongst every protein core. Whilst considerable similarities have been observed in the C-terminal domain sequences, there are several regions along the molecules that show a high level of variability (Iozzo, 1998).

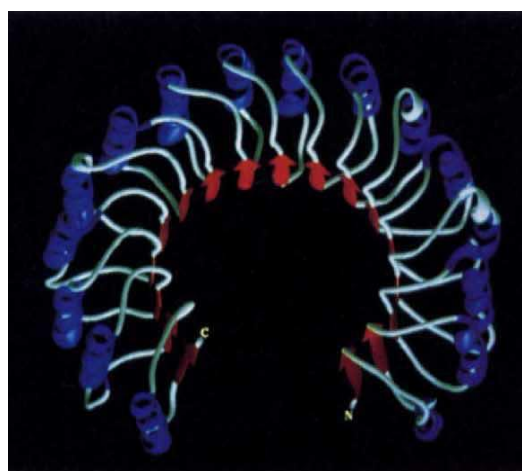


Figure 1.9: The three-dimensional organisation of a leucine rich repeat motif.

Red arrows represent β -strands; blue ribbons represent α -helices (Taken from Kobe and Deisenhofer 1993).

The three-dimensional organisation within these proteoglycans has been likened to that of the intracellular ribonuclease inhibitor protein (Kobe and Deisenhofer, 1993). The leucine rich regions form a horse-shoe shaped coil of parallel alternating α -helices and β -sheets stabilized by H-bonding between the concave surfaces of parallel chains (Scott, 1996) (Figure 1.9). Consequently the horseshoe shape is able to accommodate a single collagen triple helix (Dunlevy et al., 1998).

1.3.3. Corneal proteoglycans

In the corneal stroma, decorin is the predominant proteoglycan possessing chondroitin sulphate/dermatan sulphate side chains (Bianco et al., 1990; Li et al., 1992), whilst keratocan (Corpuz et al., 1996), lumican (Blochberger et al., 1992) and mimecan (Funderburgh et al., 1997) all possess keratan sulphate glycosaminoglycan side chains. These proteoglycans interact with the cellular and extracellular matrix components of the corneal stroma via particular binding sites. In the corneal stroma, different proteoglycan binding sites have been observed along the collagen fibrils corresponding to the 'a' and 'c' bands of the overlap zone, and the 'd' and 'e' band of the gap zone (Scott and Haigh, 1985; Meek et al., 1986). It has also been identified that particular proteoglycans will associate with different binding sites on the collagen fibril. Of the two different classes of proteoglycans, keratan sulphate proteoglycans bind to the 'a' and 'c' bands of the fibril, whilst chondroitin sulphate/dermatan sulphate proteoglycans bind to the 'd/e' bands (Scott and Haigh, 1985; Young, 1985; Meek et al., 1986; Scott and Bosworth, 1990).

1.3.3.1. Decorin

Decorin is a member of the SLRP family, and may have a role in interacting with collagen fibrils, helping to stabilize and orientate them during fibrillogenesis (Scott, 1996). First discovered in bone and cartilage (Rosenburg et al., 1985; Fisher et al., 1989), decorin is named after its appearance under electron microscopy, 'decorating' the collagen fibril surface, specifically at the 'd' and 'e' bands (Scott et al., 1981).

During decorin biosynthesis the core protein is glycosylated by a single glycosaminoglycan chain at the N-terminal Ser-Gly site. The chain is constructed from repeating disaccharide

units of N-acetylgalactosamine and either iduronic acid or glucuronic acid. Consequently, decorin can have either a chondroitin sulphate or dermatan sulphate side chain. In the cornea (as in articular cartilage) decorin is present with either of these glycosaminoglycans attached. In addition, studies by Midura et al (1989) have also identified the presence of several oligosaccharides N- and O-linked to the protein core of decorin in the embryonic chick cornea. Conversely, in the mature avian cornea decorin may exist as one of two isoforms – either possessing the standard chondroitin sulphate/dermatan sulphate side chain, or as a hybrid isoform that contains both a chondroitin sulphate/dermatan sulphate side chain and a keratan sulphate side chain (Blochberger et al., 1992).

Decorin is also able to undergo dimerisation (Scott et al., 2004). This molecular self-recognition allows decorin core protein molecules to bind together into dimers. In the corneal stroma long multimer glycosaminoglycan aggregations have also been observed (Knupp et al., 2009; Lewis et al., 2010; Parfitt et al., 2010). Previous studies have identified these longer aggregations to be chondroitin sulphate/dermatan sulphate proteoglycans (Scott, 1992; Liles et al., 2010).

1.3.3.2. Keratocan

Keratocan is abundant throughout the cornea. Synthesised by keratocytes, it is named due to the keratan sulphate glycosaminoglycan chains bound to its protein core. It is also present to a lesser extent in skin, ligament, cartilage, artery, and striated muscles as a glycoprotein containing short non-sulphated keratan sulphate chains (Corpuz et al., 1996). Only in the cornea is the 38kDa core protein linked to highly sulphated keratan sulphate chains (Corpuz et al., 1996), indeed three keratan sulphate-linkage sites have been observed on the protein core (Funderburgh et al., 1991).

1.3.3.3. Mimecan

Mimecan is another member of the SLRP family that has recently been shown to be present in the developing chick cornea (Dunlevy et al., 2000), having first been discovered in bovine bone (Madisen et al., 1990). As with keratocan, mimecan is also present to a lesser extent in other tissues as a non-sulphated glycoprotein. The 25kDa sulphated form of mimecan found in the cornea contains keratan sulphate glycosaminoglycan side chains and is synthesised by

stromal keratocytes (Funderburgh et al., 1997). It is expressed in much lower quantities than either keratocan or lumican; consequently in the mature chick cornea its levels fall to the extent that it is virtually undetectable (Dunlevy et al., 2000).

Mimecan does not show the high degree of amino acid sequence identity shared between the other two cornea keratan sulphate proteoglycans – lumican and keratocan. Nonetheless there is evidence that suggests certain molecular characteristics remain conserved within the particular structural domains of all the members of the keratan sulphate proteoglycan family. For example in the N-terminal region, a minimum of one tyrosine amino acid is universally located adjacent to any acidic amino acids such as glutamate or aspartate, forming then the consensus site for tyrosine sulphation (Funderburgh et al., 1997)

1.3.3.4. Lumican

Lumican is a keratan sulphate proteoglycan found in several connective tissues, including cornea, skin, and cartilage (Comper, 1996). Its name is derived from its role in corneal transparency. In the cornea, the keratan sulphate glycosaminoglycan chains are highly sulphated, whereas in other tissues such as skin or cartilage, it exists in either poorly sulphated or non-sulphated forms. It is suggested that the sulphation of corneal lumican, is directly involved in the development of corneal transparency (Blochberger et al., 1992). Indeed, the onset of corneal transparency in developing chick coincides with the production of the sulphated form of lumican (Cornuet et al., 1994).

Lumican in the cornea is usually expressed by stromal keratocytes; but is also expressed transiently by corneal epithelial cells during the initial stages of the wound healing process (Saika et al., 2000). The 37kDa protein core of the molecule is highly sulphated. In the bovine cornea one keratan sulphate chain is bound to the protein core (Funderburgh et al., 1991). Whilst in the chick cornea, five potential keratan sulphate binding sites have been identified – four N-linked glycosylation sites within the leucine rich region, and one site outside of it (Blochberger et al., 1992). However in the mature chick, only two to three of the five potential binding sites are thought to be associated with keratan sulphate chains (Dunlevy et al., 1998; Midura et al., 1989).

Lumican and keratocan are thought to be structurally alike and possess many of the three-dimensional characteristics of the intracellular ribonuclease inhibitor protein (Kobe and Deisenhofer, 1993). The leucine rich regions of the protein cores of these molecules coil into a spiral, this then forms a horse-shoe shape that is thought to accommodate a single collagen triple helix. The leucine residues are thought to be involved in interacting and binding the collagen fibril (Scott, 1996). The glycosaminoglycan chains of these proteoglycans then protrude from the convex surface of the horse-shoe shape, to play a role in collagen fibril spacing (Weber et al., 1996).

1.3.4. The role of corneal proteoglycans

The interactions between proteoglycans and collagens are both wide-ranging and complex. It is thought that through these interactions, the organisation of the corneal structure is controlled. Cellular and extracellular components of the stromal matrix interact extensively with proteoglycans. For example spatial and temporal variations in proteoglycans may, along with other extracellular matrix components, mediate cell migration, proliferation, differentiation and adhesion (Doane et al., 1996; Davies et al., 1999; Ameye and Young, 2000).

It is also thought that interactions between proteoglycans and fibrillar collagens of the extracellular matrix may mediate collagen fibril size, spacing and organization in the stroma (Scott, 1985; Scott, 1988). The core protein domain of the proteoglycan interacts with collagen fibrils whilst the glycosaminoglycan side chains occupy the interfibrillar space, assisting in the spatial organisation of collagen fibrils (Dunlevy et al., 1998), and causing an osmotic pressure that serves to expand the stromal matrix (Hedblom, 1961). As such, proteoglycans and their associated glycosaminoglycan side chains contribute to the cornea's compressive and swelling changes (Comper and Laurent, 1978).

Previously studies have suggested a symmetrical six-fold arrangement of proteoglycans around a central collagen fibril (Müller et al., 2004). However, recent studies of mature bovine and mouse corneas that utilized three-dimensional reconstructions of stromal extracellular matrix (Knupp et al., 2009; Lewis et al., 2010; Parfitt et al., 2010) suggest that the proteoglycans have no symmetrical organisation or set azimuthal positioning. With no regular proteoglycan organisation evident, alternative theories have emerged as to how

proteoglycans are able to modulate interfibrillar spacing. One current theory is that two equal but opposing forces are exerted simultaneously on the fibrils due to the presence of proteoglycans. Thermal motion of the glycosaminoglycan chains, arising from the constant molecular collisions of the proteoglycans and other extracellular matrix molecules, creates an attractive force that pulls the two terminal ends of the chain, and subsequently the attached collagen fibrils together. Simultaneously, the negatively charged glycosaminoglycan chains attract positively charged ions within the stroma resulting in an osmotic pull. This creates a repulsive force as the influx of water molecules into the interfibrillar spaces increases the pressure between the collagen fibrils (Knupp et al., 2009; Lewis et al., 2010). This force counteracts the attractive force caused by thermal motion of the glycosaminoglycan chains, resulting in a balanced system. Together these forces, resulting from the presence of proteoglycans, stabilize fibril architecture and regulate interfibrillar distances.

Studies have confirmed the regulatory role of lumican in collagen fibrillogenesis and the development of corneal transparency (Rada et al., 1993; Chakravarti et al., 1998). Associating with newly synthesized collagen fibrils at the keratocyte surface, lumican was found to regulate fibril diameter by mediating lateral fibril associations. Lumican-null mice have increased stromal light scattering and corneal opacification (Chakravarti et al., 1998; 2000). This supports the theory of keratan sulphate having role in development of transparency. In addition, lumican-null mice show increased collagen fibril diameter as a result of fibril fusion. There is abnormal fibril architecture in the posterior stroma that contains the mature collagens, an area where lumican has been shown to have a greater concentration in normal mice. Conversely the anterior stroma, containing newly synthesized collagen fibrils, maintained normal collagen architecture (Chakravarti et al., 2000). In addition, lumican null mice show decreased keratan sulphate content throughout the whole eye, demonstrating significantly lower sulphation levels to those in other mammalian species (Young et al., 2005).

In contrast, keratocan-null mice demonstrate normal corneal transparency, although stromal collagen fibril organisation is still disrupted to an extent. They have a thinner stroma in cross section, and a narrower corneal–iris angle of the anterior segment, as well as increased collagen fibril diameter and less organized fibril packing (Meek et al., 2003). Whilst these changes are not seen in mimecan-null mice, a slight reduction in collagen fibril diameter has been observed in the cornea and skin (Tasheva et al., 2002). However, similar studies

undertaken by Beecher et al (2005) have shown no significant changes in corneal fibril diameter or local order within mimecan-null mice.

Lumican- and keratocan-null mice both show decreased stromal thickness (Chakravarti et al., 2000; Meek et al., 2003). This thinning may be due to stromal dehydration resulting from reduced keratan sulphate proteoglycan levels. The strong negative charge on stromal proteoglycans causes an osmotic flow into the tissue, as water molecules are attracted to the sulphated glycosaminoglycan side chains. Keratan sulphate has a greater ability to attract water than chondroitin sulphate/dermatan sulphate glycosaminoglycans, therefore causing a dehydrating effect once removed (Bettelheim and Plessy, 1975).

Chondroitin sulphate/dermatan sulphate proteoglycans, in particular decorin, may aid collagen fibril movement during developmental deformation of the stroma (Bard et al., 1988; Pins et al., 1997). Dermatan sulphate proteoglycans may have a morphogenetic role in the developing chick (Hart, 1976; Hahn, 1992), as specific disruption of dermatan sulphate proteoglycan synthesis leads to abnormalities in lamellar organization and packing of the collagen fibrils (Hahn, 1992). Fibril diameter remains unaffected. Therefore dermatan sulphate proteoglycans may control fibril-fibril spacing and lamellar organization, but not the regulation of fibril diameter (Hahn, 1992; Danielson et al., 1997).

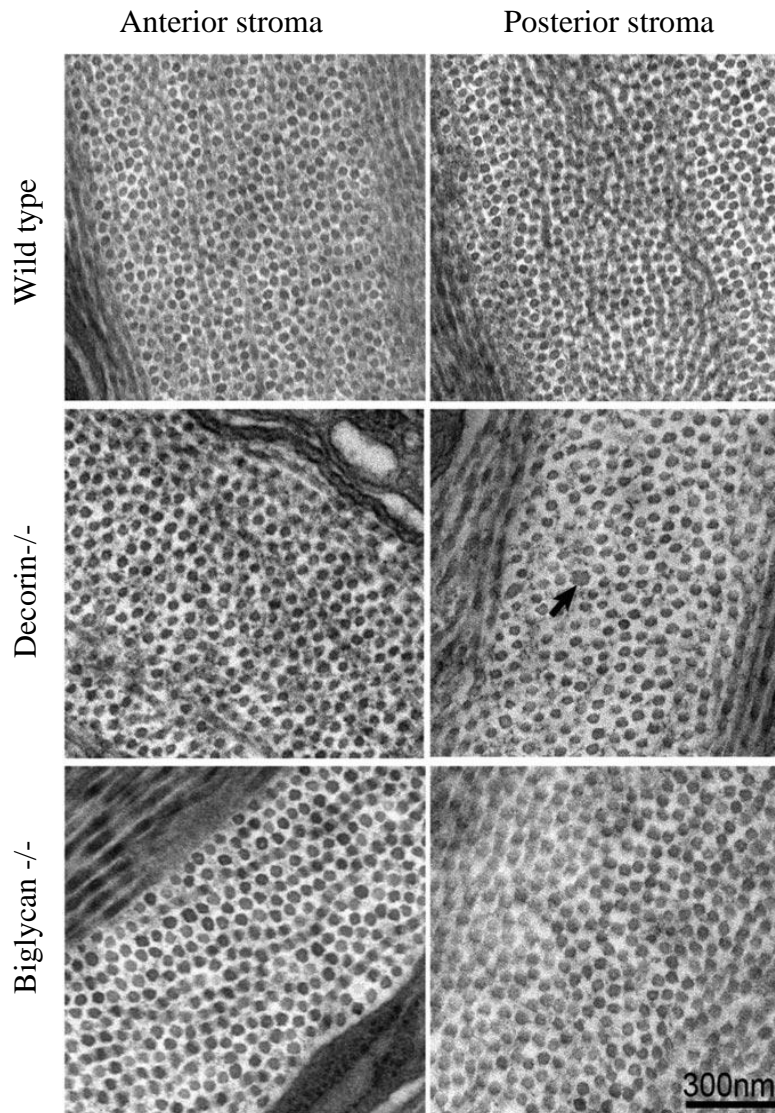


Figure 1.10: Collagen fibril morphology in Decorin and Biglycan-null corneal stroma.

Altered collagen fibril diameters can be seen in the corneal stroma of P60 decorin and biglycan knockout mice. Black arrow indicates an abnormal collagen fibril. (Adapted from Zhang et al., 2009).

Whilst decorin-null mice do show skin and tendon abnormalities, no corneal phenotype is present (Danielson et al., 1997). *In vitro* studies have demonstrated the effect of decorin and lumican on fibrillogenesis of type I collagen. They can delay fibril formation by inhibiting the rate of collagen fibrillogenesis. They also prevent fibril diameter growth, resulting in the formation of thinner collagen fibrils. This inhibitory role is thought to be a function of the core proteins of these proteoglycans, rather than the glycosaminoglycan side chains (Rada et al., 1993). These findings were contradicted in another study, which showed decorin has no role in mediating collagen fibril diameter (Li et al., 1992). Alternatively, decorin may have a

role in preventing lateral association of procollagen molecules (Figure 1.10). Decorin was seen to be secreted along procollagen molecules within vesicles, supporting the proposed role in fibril formation (Birk et al., 1995).

Mice deficient in both decorin and biglycan show significantly disrupted stromal organization and fibril packing, with larger and more abnormal fibril structure present particularly in the posterior stroma. These double deficient mice demonstrate that decorin does have a role in stromal fibril assembly; its importance is however masked in decorin-null mice by the compensatory up regulation of biglycan that consequently prevents any fibrillogenesis disruption (Zhang et al., 2006).

Current research suggests that only lumican-null mice produce a clinical corneal phenotype, whilst corneal transparency remains unaffected with keratocan, decorin and mimecan deficiencies (Chakravarti et al., 2000). This suggests that keratan sulphate has the defining role in corneal transparency. Whilst mimecan carries keratan sulphate in bovine and human corneas, in the murine cornea it does not. However, keratocan and lumican in the murine cornea does possess highly sulphated keratan sulphate chains. Whilst decreased keratan sulphate levels are noted in keratocan-null mice, corneal transparency remains unaffected, suggesting that lumican and keratocan may bind to different regions on collagen fibrils, altering their function.

Keratan sulphate biosynthesis, if disrupted, can have a dramatic impact on corneal clarity. Macular corneal dystrophy type I (MCD-I) is a rare inherited disorder resulting in the production of immature keratan sulphate molecules (Klintworth and Smith, 1977; Hassell et al., 1980). Consequently there is disruption to the organisation of the extracellular matrix, including collagen interfibrillar spacing and reduced corneal thickness. This then causes clouding and reduced corneal transparency (Hassell et al., 1980). However, whilst this phenotype is attributed to disruption of keratan sulphate biosynthesis, other glycosaminoglycan irregularities occur that may contribute to the disease characteristics. For example in MCD-I, larger over sulphated chondroitin sulphate proteoglycans and increased levels of chondroitin-6-sulphate are found in the stroma (Klintworth and Smith, 1977; Meek et al., 1989; Plaas et al., 2001). In addition hyaluronic acid, usually absent in normal cornea, is present in MCD-I corneas and may affect hydration levels in the stroma (Plaas et al., 2001).

Corneal scars also show similarly abnormal proteoglycan composition and distribution (Funderburgh et al., 1990). In corneal scar tissue there is a reduction in keratan sulphate levels, increased quantities of highly sulphated chondroitin sulphate/dermatan sulphate proteoglycans (Wollensak and Buddecke, 1990), and initiation of hyaluronic acid synthesis (Hassell et al., 1983; Fitzsimmons et al., 1992). The altered expression profile of the keratocytes is also consistent with the observed transdifferentiation of these cells into fibroblasts and myofibroblasts (Funderburgh et al., 2003). These changes then contribute to the formation of scar tissue that is structurally disorganised and opaque. Furthermore, in Alzheimer's disease afflicted cerebral tissue, reduced keratan sulphate synthesis is associated with inflammation (Lindahl et al., 1996). Down regulation of corneal keratan sulphate proteoglycan biosynthesis may then also be initiated by the influx of proinflammatory cytokines associated with inflammation.

1.4. Corneal Transparency

The transparency of the cornea is dependent on the minimal absorption and deflection of the light passing through the tissue (Goldman et al., 1968; Cox et al., 1970). Several theories have arisen that attempt to explain how the structure of the cornea is tailored to this function.

One theory suggests that transparency in the stroma is the result of the organised lattice arrangement of the collagen fibrils. Transparency occurs when fibrils are parallel and organised into a precise lattice, resulting in individual scattered waves destructively interfering in all directions except in the incident direction (Maurice, 1957). This theory suggests that it is the regular long range organisation of the fibril lattice that confers transparency to the tissue. However, other studies have since disproved this theory, demonstrating theoretically and experimentally that short range collagen order is more essential for corneal transparency (Hart and Farrell, 1969; Goodfellow et al., 1978)

Smith (1970) proposed another theory, claiming that transparency depended on regular fibril spacing and a uniform refractive index across a homogenous stromal matrix. Here, the refractive index of the collagen fibrils was considered similar to that of the other matrix components, thus resulting in light passing through the tissue with minimal light scattering. However, studies using X-ray diffraction techniques have since revealed that collagen fibrils

in the stroma show a higher refractive index than the other components of the surrounding matrix (Leonard and Meek, 1997).

The X-ray diffraction results concur with the most widely accepted model of corneal transparency, proposed by Farrell (1994). This theory states that the fraction of undeviated light transmitted through the cornea (F) is a function of the scattering cross-section per unit length (σ), the density of fibril packing (ρ), and the thickness of the tissue in the direction of the light path (t). The formula can be expressed as $F = e^{-\sigma\rho t}$ (Farrell, 1994). The scattering of light is a function of the wavelength of light, the collagen fibril mode of packing, fibril diameter, and the ratio of the refractive index of the hydrated fibrils to the refractive index of the interfibrillar matrix.

Keratan sulphate proteoglycans may also have a role in corneal transparency. They have a critical role in the maintenance and development of the unique collagen organisation that is integral to corneal transparency, for example maintaining interfibrillar spacing (Hassell et al., 1980). It has also been noted that keratan sulphate proteoglycan levels are lower and the molecular sulphation patterns are structurally altered, in opaque sclera and new corneal scar tissue, when compared to transparent cornea tissue (Funderburgh et al., 1988). In addition, older scar tissues show increasing keratan sulphate proteoglycan levels that accompanied the return of transparency (Hassell et al., 1983; Cintron et al., 1990).

In addition, it is also thought that tissue hydration has a profound effect on corneal transparency. Until day 14 of avian corneal development, collagen fibril bundles are separated by large collagen-free lakes (Hay and Revel, 1969; Hirsch et al., 1999). Compaction of the corneal stroma occurs due to progressive dehydration, occurring most prominently between days 13 and 14. This first stage of dehydration occurs largely through the absorption of these collagen free lakes within the stroma. At this stage, collagen interfibrillar spacing remains fairly constant. Not until the second major phase of stromal dehydration between days 16 and 18 does collagen interfibrillar spacing reduce (Siegler and Quantock, 2002). It is suggested that if these collagen free spaces remained, and exceeded half the incident light's wavelength in size, scattering of light would occur and corneal transparency would then be affected (Goldman et al., 1968). However transparency of the developing avian cornea does not improve until day 15 (Coulombre and Coulombre, 1958),

suggesting that the reducing size of these lakes between days 13 and 14 has little impact on the development of corneal transparency.

1.5. Development of the chick cornea

The developmental stages that the avian cornea undergoes are tightly controlled. Both proteoglycans and uniform collagen fibrils are implicated in the formation of a transparent and structurally organised tissue matrix. The expression and organisation of both these components alters during development, consequently affecting both the ultra structure and optical properties of the cornea as development progresses.

1.5.1. The Primary Stroma

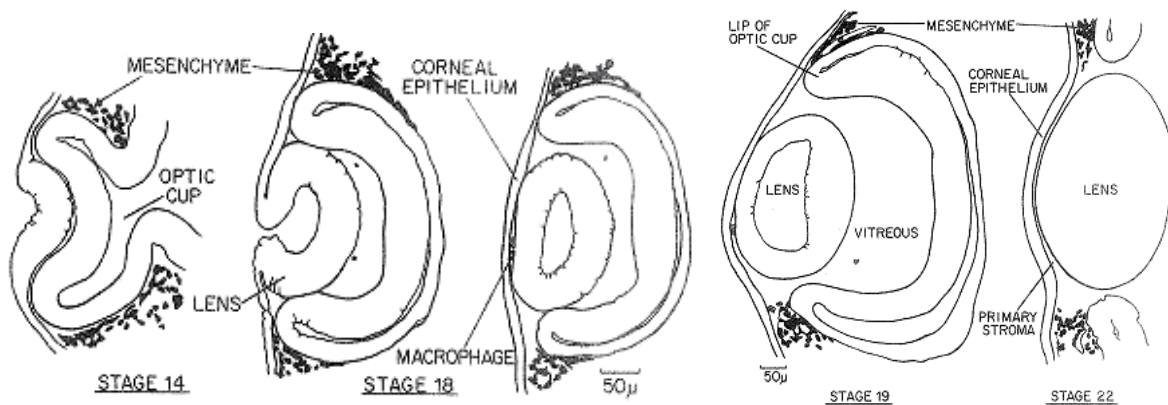


Figure 1.11: Early development of the eye at stages 14-18 and 19-22.

(Taken from Hay and Revel, 1969)

Development begins with the formation of a cup-shaped structure in the optic vesicle (Figure 1.11). This then induces the development of the lens placode from the overlying ectoderm. Following detachment of the primitive lens, the overlying ectoderm differentiates into corneal epithelium. At around developmental day 3 the epithelium is a two cell layer that begins to synthesise an underlying precursor to the secondary stroma known as the primary stroma. Similar in structure to the secondary stroma, this acellular matrix begins as a thin collagenous layer (Hay and Revel, 1969).

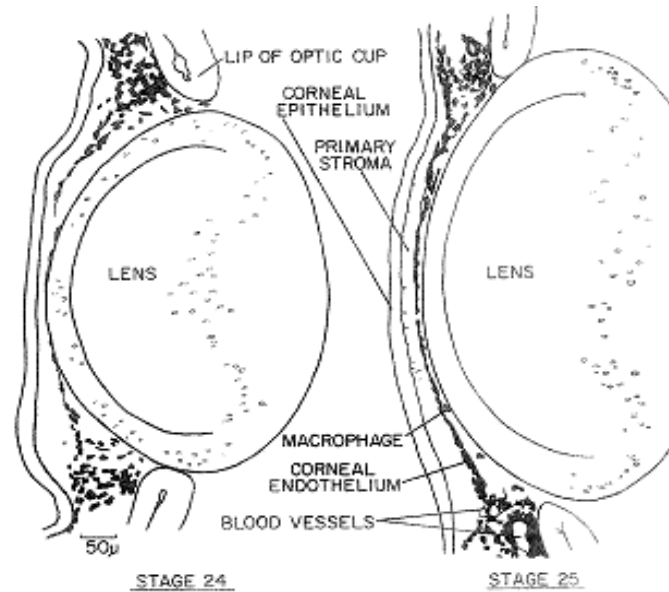


Figure 1.12: Development of the primary stroma at stages 24 and 25.

(Taken from Hay and Revel, 1969)

From early to mid day 5 the stroma increases in thickness from around $10\mu\text{m}$ to approximately $60\mu\text{m}$. The primary stroma at this stage consists of heterotypic collagen fibrils with uniform diameters. Structurally they do not form continuous sheets of thin, regularly spaced collagen fibrils; rather they are present as collections of laterally associated fibril bundles (Trelstad and Coulombre, 1971). The corneal endothelium forms from cells that have migrated between the primary stroma and the lens at around day 4, having originated in the vascular mesenchyme at the edge of the optic cup (Figure 1.12).

This primary stroma is considered to act as a template for the arrangement of the secondary stroma, which is synthesized by differentiated mesenchymal cells. Characteristic swelling of the primary stroma is closely followed by an influx of undifferentiated mesenchymal cells from the surrounding area. These cells begin invading the primary stroma (initially posteriorly) at day 5 (Hay and Revel, 1969; Linsenmayer et al., 1998). This population of cells resemble ciliated fibroblasts at the time of invasion at day 6. At this point the primary stroma is around $110\mu\text{m}$ thick; however the anterior $10\mu\text{m}$ region adjacent to the epithelium remains cell free.

It is thought that the invading mesenchymal cells use the primary stroma as a scaffold to guide migration (Bard and Hay, 1975). However, the precise mechanism for this guidance is unknown. The primary stroma may act as a template for alignment of the invading cells, or it may act as a scaffold for collagen assembly (irrespective of cell alignment). Alternatively, the invading keratocytes may possess spatial knowledge independent of any guidance structure (Doane and Birk, 1991).

1.5.2. The Secondary Stroma

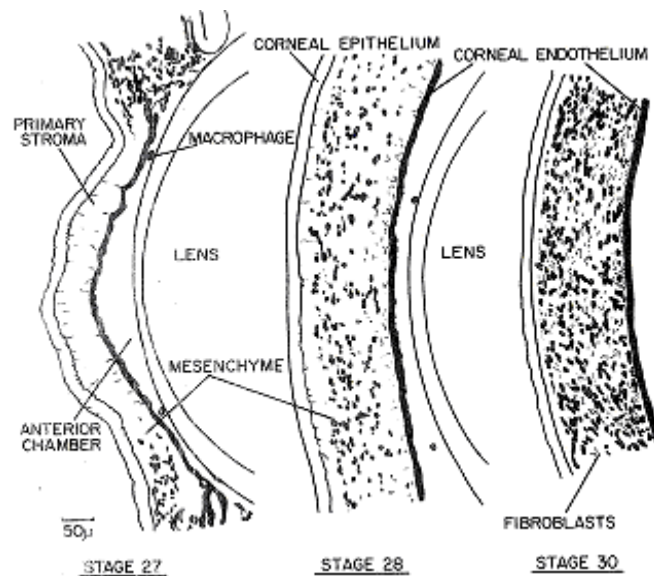


Figure 1.13: Development of the secondary stroma from stage 27 to 30.

(Taken from Hay and Revel, 1969)

Synthesis of the secondary stroma's matrix components occurs over the collagenous scaffold of the primary stroma, following the differentiation of the precursor cell populations into stromal fibroblasts around day 7 (Trelstad and Coulombre, 1971; Linsenmayer et al., 1998) (Figure 1.13). Descemet's membrane is synthesised by the endothelium between days 8 ½ and 9, at which point stromal swelling is at its greatest. Furthermore, at the same developmental time point, corneal curvature develops as a result of increased intraocular pressure, altered stromal composition, and interactions between the cornea and the sclera (Coulombre and Coulombre, 1958).

At day 9, the stroma is at its thickest, between 190 μm (Trelstad and Coulombre, 1971) and 220 μm (Hay and Revel, 1969). Between days 12 to 14, Bowman's layer forms from an anterior 1 μm region of the stroma that remained free from the migrating mesenchymal cells. Progressive dehydration of the developing stroma then occurs, accompanied by structural reorganisation and compaction. Consequently the stroma thins to around 150 μm by day 14 (Hay and Revel, 1969). The secondary stroma compresses to 50% its thickness as the collagenous layers compact, reducing the collagen free 'lakes' between the fibril bundles (Hay and Revel, 1969; Cannon et al., 2003). In addition, the resident cells take on a more rounded morphology typical of mature stromal keratocytes. As a consequence of this matrix dehydration and compaction, tissue transparency increases resulting in light transmission improving from 40% to 95% by day 19 (Coulombre and Coulombre, 1958; Hay and Revel, 1969).

Cannon et al (2004) report an increase in fibril number density between days 14 and 18. This supports studies that observed from day 14 onwards, the dry weight of the stroma continued to increase whilst the wet-weight of the tissue did not (Coulombre and Coulombre, 1958).

1.5.3. Collagen in the developing corneal stroma

Type I and type II collagen are present in the developing stroma from embryonic day 3, expressed by epithelial cells (Trelstad and Coulombre, 1971; Linsenmayer et al., 1977). However studies by Hayashi et al (1988) also suggest endothelial cells may also have a role in collagen synthesis from day 5 onwards. In the developing stroma, these two collagen types associate to form uniform diameter heterotypic fibrils that then assemble into orthogonal lamellae. Following stromal swelling, type V collagen can also be seen forming heterotypic fibrils with type I collagen (Linsenmayer et al., 1983; Fitch et al., 1984, 1988; Birk et al., 1988). Type II collagen in the primary stroma may function in a similar way to type V collagen in the mature stroma. Structurally similar, the amino-terminal domain of collagen type II may, like type V collagen, protrude out from within the heterotypic fibril, serving to regulate lateral associations and thus control collagen fibril diameter (Fitch et al., 1995). As development progresses, type II collagen is localised to increasingly anterior regions of the stroma. Its synthesis decreases progressively until it is no longer expressed in the secondary stroma by day 8, mature molecules do however remain present until stromal condensation (Fitch et al., 1995).

The primary stroma may also contain type IX FACIT collagen fibrils (Fitch et al., 1988, 1995). Studies using monoclonal antibodies localised immature type II and type IX collagen molecules to the subepithelial region of the primary stroma (Fitch et al., 1994). Two isoforms of collagen type IX have been identified in the developing stroma. One isoform observed on the surface of type II fibrils possesses a non-collagenous domain that forms covalent links with the underlying fibrillar collagen (Fitch et al., 1994, 1995). It was therefore suggested that type IX collagen may stabilize the stromal matrix by cross-linking adjacent collagen fibrils to other fibrillar and non-fibrillar matrix components such as hyaluronic acid.

In addition, collagen type IX could also be classified as part of a functional class of collagen molecules (Fitch et al., 1995; Linsenmayer et al., 1990) that assist and stabilize the morphogenetic changes that occur in the matrix, namely stromal swelling and compaction. It was initially thought that the high concentration of hyaluronic acid present in the primary stroma caused an osmotic draw (as a result of the negatively charged glycosaminoglycan side chains) that would then produce the characteristic swollen, hydrated primary stroma (Toole and Trelstad, 1971). However, as hyaluronic acid synthesis occurs several developmental stages prior to stromal swelling, another regulatory mechanism must also be involved in addition to hyaluronic acid. Namely, collagen type IX and the cross-links it forms between adjacent collagen fibrils and with hyaluronic acid (consequently binding this proteoglycan in a compact state) (Fitch et al., 1995; Linsenmayer et al., 1998). Cleavage of this collagen molecule would release both adjacent collagen fibrils and the hyaluronic acid molecules. The resulting osmotic draw from the released proteoglycans would then force adjacent collagen fibrils apart, expanding the stroma and allowing the invasion of mesenchymal cells. Several studies have confirmed the proposed transitory existence of this collagen molecule: detected a few days after type II collagen, its expression falls dramatically just prior to stromal swelling, and by day 11 it is undetectable (Svoboda et al., 1988; Fitch et al., 1988; Cai et al., 1994). In addition, inhibiting the cleavage of type IX collagen from the surface of the fibrils produced a compact and acellular matrix (Cai et al., 1994), confirming its role in assisting matrix swelling and the subsequent cellular invasion. This work demonstrates that mesenchymal cell influx is triggered not by a molecular cue, but rather by developmentally controlled cleavage of collagen cross-links.

Fitch et al (1991) observed another mechanism that may be involved in stabilization of swelling in the secondary stroma – elongated, radiating ‘stromal strings’ containing collagen type IV, fibronectin and collagen type VI. Following initiation of stromal swelling and cellular invasion, these strings can be seen spanning radially across the corneal stroma. In addition, they were commonly observed inserting into the epithelial basement membrane and exerting a tensile force, suggesting a role in resisting and stabilizing matrix swelling. They were also observed running between keratocytes, connecting adjacent cell surfaces. It is hypothesized that these structures may assist in preserving cellular spacing and subsequently the width of the stromal lamellae, as well as stabilizing the expansion of the stroma, as they disappear at around day 15 following matrix compaction (Fitch et al., 1991).

Types XII and XIV FACIT collagens are structurally similar, but show different expression profiles. They may also function differently, interacting with different matrix components. However both collagen types are thought to have wider roles in matrix condensation, and the development of stromal transparency. Specifically, type XIV may be involved in fibrillogenesis (Young et al., 2002) whilst type XII may aid fibril organisation and matrix stability (Gordon et al., 1996).

Type XII collagen is initially synthesized by the epithelial cells, and is detectable throughout the primary stroma prior to the influx of mesenchymal cells. However by day 7, following stromal swelling, it is located solely in the subepithelial and subendothelial regions of matrix-matrix interface (Akimoto et al., 2002). It is thought that type XII collagen may assist in stabilizing these regions as it has been observed localizing with the surface of fibrillar collagens (Linsenmayer et al., 1986; Keene et al., 1991; Gordon et al., 1996). This collagen type is present in either a long or short form, with each form showing different temporal and spatial localisation in the developing stroma (Akimoto et al., 2002; Young et al., 2002). For example, the mRNA of the long form, localised to the matrix-matrix interface regions, maintains a constant level from day 10 until hatch, at which point its level declines. The mRNA of the short form however peaks at day 12, and then also declines (Young et al., 2002).

Type XIV collagen is initially expressed by epithelial cells and is consequently primarily located in the subepithelial region at the early stages of development (around day 7). Epithelial expression increase up to day 9 at which point it can be detected throughout the

stroma. By day 11, epithelial synthesis of this collagen begins to decline. However, type XIV continues to be present throughout the stroma from day 9 as expression by stromal fibroblasts increases. Levels in the secondary stroma continue to rise particularly as compaction begins, peaking between days 10 to 14 (Gordon et al., 1996). After this stage production begins to decline. Collagen type XIV is then undetectable by hatch (Young et al., 2002). It is suggested that interactions between this collagen type and the surface of fibrillar collagens may stabilize the movement of fibrils and may have a role in stromal compaction.

1.5.4. Collagen assembly in the developing corneal stroma

From studies using embryonic tendon, it has been hypothesized that fibrillogenesis occurs in recesses and invaginations on the surface of stromal keratocytes. Collagen fibrils are transferred to the extracellular matrix by plasma membrane protrusions called fibripositors and the adjacent extracellular channels that form between these processes (Canty et al., 2004; Canty and Kadler, 2005). In tendon, studies have shown that deposition into the matrix occurs at the tip of the fibripositor, whilst it is at the base of the fibripositor lumen (several microns within the cell) where the nucleation stage of fibrillogenesis occurs (Canty et al., 2004). Similarly, in the developing corneal stroma small bundles of between 5 and 12 collagen fibrils have been seen protruding from small recesses on the keratocyte surface. These small bundles then coalesce on the cell surface into larger bundles which then form the lamellae (Birk and Trelstad, 1984). In addition, this study also observed that these processes and cellular recesses aligned along the two major axes of the cell, thus conferring the orthogonality of the collagenous lamellae (Birk and Trelstad, 1984). However, these cell-associated lamellae have also been seen in developing chick cornea, running in multiple directions, particularly around day 14 when the stroma is loose (Young et al., 2007).

Collagen deposition may occur during migration of the stromal cells, with the fibrillar extrusion occurring in a direction determined by the migratory path. However, the simultaneous production of collagen fibrils in many different orientations (as seen in Young et al., 2007) suggests there may be some cellular control over the formation of basic lamellae. Coordinating the production of fibrils for several lamellae of different orientations, would be a complex process requiring tight cellular control and the use of fibripositors on the surface of migrating stromal cells.

To assess whether the migrating cell populations possess inherent spatial information, Doane and Birk et al (1991) cultured fibroblasts in a three-dimensional collagen gel. Collagen fibrils expressed by the tendon fibroblasts grew in parallel bundles along a primary axis. Dermal fibroblasts produced collagen fibrils with no particular orientation. After three days, corneal fibroblasts produced collagen fibrils orientated perpendicular to each other, eventually forming orthogonal sheets by day seven (Doane and Birk 1991). This work suggests that the cells may possess pre-programmed, tissue specific spatial information that may assist in the formation of correctly orientated collagen fibrils.

Adjacent lamellae are arranged orthogonally in both the primary and secondary stroma. In the primary stroma the orthogonal axes of fibril orientation are fixed, one parallel and one perpendicular to the choroid fissure axis (Trelstad and Coulombre, 1971). In the secondary stroma however, the orthogonal orientation of the stromal lamellae is accompanied by an additional small degree of angular displacement clockwise, 2.5-5° per micron of corneal thickness (Trelstad and Coulombre, 1971). The direction of this rotational displacement is the same in both the left and the right eye, suggesting that corneal development may be a self assembly process where the tissue dictates its own architecture. Interestingly, the posterior of the stroma shows no rotational displacement, and it is in this region that compaction of the collagenous matrix is believed to occur first (Trelstad and Coulombre, 1971).

Until developmental day 14 in the avian corneal stroma, collagen fibrils are arranged into groups separated by large collagen-free lakes (Hay and Revel, 1969; Hirsch et al., 1999). It is hypothesized that if these collagen free 'lakes' exceed half the wavelength of the incident light, corneal transparency would be affected (Goldman et al., 1968). Studies using X-ray diffraction have revealed after day 12, collagen fibrils pack closer together, even as collagen fibril synthesis continues (Quantock et al., 1998). From day 14 onwards, lamellar organisation increases as the matrix compacts and collagen fibrils within the groups become better orientated and structured (Hay and Revel, 1969). More recent studies have recorded the change in interfibrillar spacing across development by measuring collagen fibril Bragg spacing (Liles et al., 2010). Interfibrillar spacing was recorded at day 12 as 60.8nm (± 0.6), at day 14 as 63.9nm (± 0.99), and at day 16 as 59.8nm (± 0.87). Further readings confirm that compaction is initiated after day 14, within the bundles of collagen fibrils (Liles et al., 2010). From electron microscopic study of this developmental period, it is clear that the compaction of fibrils within these bundles occurs simultaneously with the progressive coalescing of the

bundles eventually forming lamellae. Collagen synthesis is believed to continue within the lamellae even after hatch (Hay and Revel, 1969). Interestingly, whilst fibrillar and lamellar organisation increases as development progresses, it has been suggested that the mean diameter of the collagen fibrils remains constant throughout development, between 30.3nm and 31.2nm as measured by quick-freeze, deep-etch electron microscopy (Hirsh et al., 1999).

1.5.5. Proteoglycans in the developing corneal stroma

Keratan sulphate and chondroitin sulphate/dermatan sulphate proteoglycans are known to have important functions in corneal development; their exact roles however still remain unclear. With respect to these proteoglycans, it has been suggested that two critical stages exist within corneal development – matrix dehydration and compaction between days 9 and 14, and the onset on corneal transparency between days 15 and 18 (Dunlevy, 2000). Prior to day 9 however, the primary glycosaminoglycan synthesised in the developing stroma is an unsulphated form of hyaluronic acid (Toole and Trelstad, 1971). Thought to be expressed by epithelial and endothelial cells in the primary stroma (Toole and Trelstad, 1971), and by keratocytes in the secondary stroma (Conrad, 1970), it is believed to have a role in corneal swelling and mesenchymal cell influx (Toole and Trelstad, 1971; Fitch et al., 1995; Linsenmayer et al., 1998)

It has been well established that the distribution of glycosaminoglycans during corneal development is not uniform (Coulombre and Coulombre, 1958). Keratan sulphate synthesis begins around day 6 (Hart, 1976; Funderburgh et al., 1986), expressed by the invading mesenchymal cells in an under-sulphated form until day 14, at which point it become more highly sulphated (Hart, 1976). However the quantities produced do begin to decline from days 9 to 18. Using antibodies selective for minimally sulphated keratan sulphate glycosaminoglycans, Young et al (2007) demonstrated that prior to day 14 keratan sulphate is located primarily in anterior stromal regions, later spreading posteriorly throughout the stroma as corneal transparency increases.

Keratocan, lumican, and mimecan are the major keratan sulphate containing proteoglycans in the developing cornea. Expression of keratocan mRNA begins around day 6, as it is synthesised by the invading and differentiating cell populations (Conrad and Conrad, 2003). Expression of keratocan declines from day 9 to 18, during which time it is located in the

anterior stroma. However, its distribution here is not homogeneous. From day 10 to 14 it moves from being mainly cell-associated, to largely extracellular in nature (Gealy et al., 2007). During the final week of development, the nature of keratan sulphate antigenicity changes. Synthesis of a more highly sulphated form of keratan sulphate takes precedence over the lesser sulphated form. Accumulation of this more sulphated form first occurs at around day 15, after the initialisation of stromal compaction (Liles et al., 2010).

Lumican follows a similar expression pattern to that of keratocan, present in equal quantities until day 9. At which point lumican expression although also in decline, remains several fold higher than either keratocan or mimecan (Dunlevy et al., 2000). Similarly Funderburgh et al (1991) demonstrated that throughout development the relative levels of lumican, keratocan and mimecan in the cornea can be expressed in the ratio of 6:3:2.

Chondroitin sulphate/dermatan sulphate glycosaminoglycans are also present in the developing stroma during mesenchymal cell invasion (Doane et al., 1996). Decorin, the predominant chondroitin sulphate/dermatan sulphate proteoglycan in the avian cornea, is increasingly expressed from days 9 to 18 (Dunlevy et al., 2000).

Tenascin is an extracellular glycoprotein that has been found in the primary and secondary stroma, the endothelium, and Descemet's membrane (Tucker, 1991). It is thought to have a role in cell adhesion, and migration. Fibronectin also has a similar function; whether it is also expressed in the primary stroma is not currently clear (Kurkinen et al., 1979; Doane et al., 1996).

1.5.6. The mature corneal stroma

The mature avian corneal stroma consists of orthogonally arranged collagenous lamellae around 25 fibrils thick, running parallel to the corneal surface (Linsenmayer et al., 1998). Each collagen fibril is a heterotypic association of type V collagen with the predominant type I collagen molecules. Type V collagen therefore constitutes around 5-20% of total stromal collagen (Linsenmayer, 1988). Type VI collagen is also prevalent, and may associate with the various proteoglycans (Takahashi et al., 1993) present with it between the collagen fibrils and the lamellae (Linsenmayer et al., 1986).

Numerous proteoglycans have been observed in the mature corneal stroma, including keratocan, lumican, mimecan, and decorin (Dunlevy et al., 2000). Whilst mimecan is thought only to have a minor role in mature corneal tissue, lumican is considered the predominate keratan sulphate proteoglycan, present at 38 times the level of mimecan, and five times the level of keratocan (Dunlevy et al., 2000). The chondroitin sulphate/dermatan sulphate proteoglycan decorin may undergo post-translational modifications as corneal development progresses, as two different isoforms have been observed in the mature stroma. One containing the standard chondroitin sulphate/dermatan sulphate side chains, and a second hybrid form containing a keratan sulphate side chain substituted onto its core protein (Blochberger et al., 1992).

1.6. Tissue engineering

Whilst the cornea may appear to be a reasonably simple avascular tissue, its matrix organization is deceptively complex and highly ordered at a molecular level. In addition, the cornea possesses three phenotypically different cell types – epithelial, keratocyte, and endothelial. For these reasons, no clinically viable examples of tissue engineered corneal constructs are currently available. However, the importance of developing a successful treatment for corneal defects cannot be understated.

Firstly, corneal disease and injury continues to affect over 10 million people worldwide, and is currently the second largest cause of vision loss (Whitcher et al., 2001). Secondly, the increasing use of LASIK techniques for treatment of sight defects currently disqualifies the corneal tissue for use in donor transplantations. Lastly, graft failure occurs in approximately 10% of corneal graft surgeries after a five year period (Thompson et al., 2003).

1.6.1. Corneal structure and function

Engineering corneal constructs requires the consideration of three principle design requirements that reflect the function and matrix organization of the cornea. Firstly, it ensures the protection of the intraocular structures. This is achieved through the formation of a barrier by the epithelial cells and the tight junctions that link them, and through the mechanical strength of the stroma brought about by the ordered collagenous lamellae that allow it to withstand trauma and intraocular pressures without rupturing. Secondly, the highly organized,

Chapter 1 - Introduction

avascular nature of the corneal matrix allows it to be transparent to visible light. In addition, both the relative hydration of the stroma (Goldman et al., 1968), and the phenotype of the cells within it (Jester et al., 1999) also play a role in corneal transparency. For example, dedifferentiation of keratocytes to a fibroblastic phenotype during wound healing induces corneal opacity (Jester et al., 1999). Thirdly, in conjunction with the tear film, the cornea forms a near perfect optical interface that serves to focus and refracts light onto the retina.

Considerable advances have been made culturing and expanding both epithelial and endothelial cells sheets often for use on stromal scaffolds or as grafts (Pellegrini et al., 1997; Griffith et al., 1999; Li et al., 2003; Ide et al., 2006; Koizumi et al., 2007).

Nishida et al (2004) developed an alternative strategy for the replacement of damaged corneal epithelium, using tissue-engineered multi-layered epithelial cell sheets cultured from autologous oral mucosal epithelial cells. Cultured on amniotic membrane, the cell-cell junctions and extracellular matrix on the basal side of the cell sheets remained structurally and functionally intact. Furthermore, transplantation into rabbit showed successful integration and re-epithelialisation of the damaged corneal surface (Nakamura et al., 2003).

Comparatively, there has been little progress in producing effective stromal constructs that accurately reproduce the structural and functional characteristics of the corneal stroma (Orwin et al., 2003; Hu et al., 2005; Torbet et al., 2007). Consequently, the difficulties associated with stromal engineering have held back the production of effective whole corneal constructs.

The formation of hydrated gels from monomeric type I collagen solution was first reported over 30 years ago (Bell et al., 1979). Following this discovery, skin equivalents (Bell et al., 1981) and corneal equivalents (Griffith et al., 1999) were also proposed. However, current research efforts aiming at engineering functionally suitable and clinically useable cornea are in their infancy, and research worldwide into the establishment of a mechanically robust and optically transparent corneal matrix is active.

1.6.2. Approaches to stromal tissue engineering

Classically, stromal constructs are often created by seeding corneal stromal cells into degradable collagen-based scaffolds which can then be remodelled either *in vitro* or *in vivo* (Griffith et al., 1999; Orwin et al., 2000; Li et al., 2003; Oh et al., 2003). Collagen gel scaffolds constructed from long collagen type I fibrils have also been used to create stromal constructs (Minami et al., 1993; Schneider et al., 1999; Germain et al., 1999; Tegtmeier et al., 2001; Tanaka et al., 2011b). However, though highly biocompatible, collagen-gel constructs occasionally show contractions, mechanical instability and reduced transparency.

Introducing glycosaminoglycans and other additives into the collagen constructs has also been studied (Matsuda et al., 1990; Chen et al., 1995; Zhong et al., 2005). We are however, still a long way off being able to produce fibrillar arrangements using proteoglycan additions. In 2003, Li et al developed an optically clear collagen-copolymer hydrogel matrix, containing cell adhesion factors such as the laminin pentapeptide motif YIGSR to promote cellular invasion and epithelialisation of the construct surface. After implantation into pigs, the matrices integrated effectively with the host tissue, and demonstrated successful growth of stratified epithelium and stromal fibroblasts.

Collagen gels are often improved by inducing cross-linking systems between the collagen fibrils. Cross-linkers such as 1-ethyl-3-(3 dimethyl aminopropyl) carbodiimide (EDC) and poly (ethylene glycol) dibutylaldehyde (PEG-DBA) used in collagen hydrogel constructs have resulted in good host-graft integration, enhanced mechanical strength and elasticity, high optical transparency (Rafat et al., 2008), as well as extensive repopulation with corneal epithelial and stromal cells 12 months post-implantation (Liu et al., 2009). These cross-linking agents exhibit less toxicity and better biocompatibility than other cross-linkers such as glutaraldehyde.

Similarly, Griffith et al (1999) demonstrated that by exposing a collagen-chondroitin sulphate substrate to 0.03-0.04% glutaraldehyde, the stromal scaffold could be sufficiently stabilized and consequently seeded with fibroblasts. In addition this study constructed epithelial and endothelial cell layers for attachment onto the stromal construct. Consequently they reported

the production of a three layered, morphologically and physiologically accurate corneal equivalent (Griffiths et al., 1999).

Fibrillar alignments from a solution of monomeric collagen molecules has also been engineered through the application of flow manipulations (Koster et al., 2007; Lanfer et al., 2008), electron spinning (Zhong et al., 2006; Chew et al., 2007), strong magnetic fields (Guo et al., 2007; Torbet et al., 2007), and dip pen nanolithography (Wilson et al., 2001). It may be possible through these methods to produce a biomimetic corneal construct that demonstrates structural and mechanical properties similar to that of native corneal tissue. However, currently this still remains a challenge.

The most common method of flow manipulation uses a shearing flow to align the collagen onto a substrate in an organised, uniform manner (Figure 1.14). However fibrillar loops are frequently formed, resulting from collagen fibrils attempting to grow upstream only to be swept back downstream. Consequently, producing uniform collagen alignment using shear force alone has been shown to be problematic. Furthermore, the collagen fibrils produced did not exhibit classic D-band morphology (Ruberti and Zieske, 2008). A similar method known as spin-coating, utilizes a cover slip to confine the collagen fibrils. Consequently, this not only improved the fibrillar alignment, but also permitted multiple collagenous layers to be produced at varying orientations by rotating the cover disk through a particular angle between coating runs (Ruberti and Zieske, 2008). Processing these alternating collagen layers into three-dimensional stromal-like structures remains a challenge that has yet to yield results. In addition, fibrillar loops although lower in number, still remained an issue with regards to the production of a uniformly aligned layer of collagen fibrils. Nevertheless, the collagen structures produced so far may be aligned well enough for use as a contact guide for the migration and orientation of introduced fibroblasts populations.



Figure 1.14: Spin coating method of collagen deposition.

(Left) An aligned collagen layer on a glass substrate produced by spin coating. The black arrows indicate the direction of flow, whilst the white arrow demonstrates an example of unwanted upstream fibril growth. (Right) The effect of utilizing an offset glass substrate, producing a radial spread of collagen flow over the substrate surface. The 3D alternating arrays of collagen fibrils are produced by rotating the glass substrate between coating runs. (Adapted from Ruberti and Zieske 2008)

Alternatively, *de novo* methods utilize a biomimetic approach to collagen organization. The theory of collagen fibril deposition occurring through a fibripositor mechanism (Canty et al., 2004; Canty and Kadler, 2005) has resulted in the development of techniques designed to imitate this process. The nanoloom is a device currently under US patent that attempts to recreate the environmental conditions favourable for the fibripositor mechanism of collagen fibril deposition (Ruberti et al., 2007). By controlling temperature, pH, pressure, and collagen concentrations, this device is structured to recreate the proposed cell membrane extrusions of the fibripositor theory. However so far, only limited results have been obtained using this method (Ruberti and Zieske, 2008).

An alternative method involves seeding collagen sponges with primary corneal cell populations *in vitro*. Keratocytes within these scaffolds have been observed aligning along the axes of the fibrils, and synthesising collagen and proteoglycans (Orwin et al., 2000). Additional inducing of cross-linking within these sponges and the introduction of chondroitin sulphate glycosaminoglycans and hyaluronic acid produced a construct that was better both

optically and mechanically than the collagen-gel based stromal constructs (Orwin et al., 2000; Orwin et al., 2003). However, these collagen sponges still lacked the mechanical stability and transparency of natural corneal tissue.

Some of the cell-based developmental methods of tissue engineering attempt to recapitulate the developmental conditions of the stroma *in vitro*, stimulating the production of a functioning stromal matrix from fibroblast cell populations, prior to implanting the construct.

Whilst accurately reproducing every developmental stage would present a considerable challenge, particular processes have been observed and duplicated *in vitro*. For example, human corneal stem cells cultured in large numbers will subsequently orientate themselves into multilayered structures. The long axis of the cells would also alternate in an orthogonal pattern between the adjacent layers (Newsome et al., 1974). Similarly, addition of ascorbic acid into human corneal stem cell cultures induces collagen production of the correct type, and in the quantities found naturally in the corneal stroma (Stoesser et al., 1978). The mutability of the keratocyte phenotype also provides a potential avenue of interest. The ability in culture, to direct the dedifferentiation and re-differentiation of these cell populations may also provide a method of reproducing the developmental stromal environment (Jester et al., 1999; Berryhill et al., 2002).

1.6.3. Future engineering techniques

De novo techniques are attractive in that they permit total control over the formation and morphology of the construct. However, current *de novo* techniques fall short of producing the desired corneal constructs and significant advances need to be made. Consequently in the near future, tissue engineering stromal constructs will remain largely dependent on cellular support. However, further study is required to accurately control the phenotype of the cell populations and the organization of the matrix components they produce. Indeed the ability of primary corneal stromal cells to synthesise stroma-like constructs given the correct environment, does suggest that by establishing the optimum environment of chemical, mechanical, spatial and structural stimuli it will be possible to induce the synthesis of a functioning stromal matrix. Alternatively, further study into the embryonic development of the cornea may aid attempts to recapitulate *in vivo* mechanisms for corneal construction. Of

particular relevance would be the methods of collagen fibrillogenesis and organisation within the corneal stroma during development.

1.7. Transmission electron microscopy

The first transmission electron microscope prototype was built by Ernst Ruska and Max Knoll in 1931. However, the first practical transmission electron microscope was not built until 1938 by Eli Franklin Burton, Cecil Hall, James Hillier, and Albert Prebus at the University of Toronto.

Historically, transmission electron microscopy was developed to overcome the limited image resolution available in light microscopy. The resolution of an image directly relates to the wavelength of the electron or photon beam used. Consequently as the wavelengths of visible light, at around 400-700nm, are often larger than many of the objects under investigation, light microscopy resolution is limited to approximately 300nm. First hypothesized by Louis de Broglie in 1925, electrons have wave-like characteristics and a wavelength considerably less than visible light. De Broglie also established that the particular wavelength of the electron beam directly relates to the electron energy, which in electron microscopy can be adjusted through the accelerating fields. Additional staining with heavy metals such as lead or uranium is often carried out prior to the samples being introduced into the electron microscope. This additional step improves the structural detail and contrast of the final image, as the dense electron clouds of the heavy metal atoms interact with the electron beam.

Transmission electron microscopy has become a widespread technique applied to a broad range of disciplines such as anatomy, biochemistry, and tissue engineering. This study will use transmission electron microscopy to study the method of collagen deposition in the chick cornea at around day 14 of embryonic development. It will also be used to study the structure of novel tissue engineered corneal constructs.

1.8. Three-dimensional electron tomography

In 1968 De Rosier and Klug published details on the principles of using electron tomography to construct high resolution three-dimensional reconstructions from two-dimensional transmission electron micrographs (De Rosier and Klug, 1968). At present, electron

tomography is able to analyse the structure of macromolecules to a resolution of 2nm (Baumeister et al., 1999). Imaging at such high resolutions allows extracellular matrix components, such as collagen fibrils and proteoglycan complexes to be accurately analysed and reconstructed in three dimensions. To reconstruct an object an electron beam is passed through the sample whilst the specimen holder is tilted through 120° around a single or a double axis. Digital images are obtained at degree increments, and this 'tilt series' is then processed and used to reconstruct the desired object (Frank, 2006). Continued technological advancement will result in unprecedented insight into the structural organisation of biological systems, revealing molecular structures and interactions with increasing accuracy and clarity.

1.9. Aims and objectives of the study

The aim of this project is to investigate how the fibril bundles of the developing avian corneal stroma are laid down into precisely organised orthogonal lamellae, and to investigate the interactions that occur within these fibril bundles - specifically, the relationship between the collagen fibrils and proteoglycans. This project is also aimed at using natural materials to engineering effective corneal stromal constructs for use in grafts and transplantation. The goal is to construct a stromal equivalent that has structural and functional characteristics that make it applicable for clinical use.

2. GENERAL METHODS

2.1 Transmission Electron microscopy

2.1.1. Fixation and staining

Corneal samples (approximately 2 x 1mm in size) that were to undergo routine processing were immediately placed in a primary fixative that utilized both glutaraldehyde and paraformaldehyde to ensure rapid and complete penetration of the fixative into the tissue. For 3 hours, these samples were immersed in a room temperature solution of 2.5% glutaraldehyde and 2% paraformaldehyde in a 0.1M sodium cacodylate buffer (pH 7.2). Further cross-linking was then halted by washing twice in sodium cacodylate buffer for 10 minutes each. The samples were then stained in 1% osmium tetroxide solution for 1 hour, followed by three rinses in distilled water, for 5 minutes each time. 0.5% aqueous uranyl acetate was then used as a further contrasting agent; the samples were immersed in this solution for 30 minutes.

Alternatively, some samples underwent processing for specific proteoglycan staining. Cuproinic blue is a cationic stain that binds to the negatively charged glycosaminoglycan side chains of proteoglycans (Scott and Haigh, 1988). The presence of copper atoms in the stain creates a favourable electron density that is then further enhanced through the addition of tungstate ions. Magnesium chloride is a negatively charged salt that results in greater amounts of the Cuproinic dye molecules attaching to the glycosaminoglycan chains, due to competitive binding.

Immediately after dissection, the corneal samples undergoing processing for Cuproinic blue staining were fixed overnight in a solution of 2.5% glutaraldehyde, 0.05% Cuproinic blue, 0.1M magnesium chloride, and 25mM sodium acetate buffer (pH 5.7). The samples were then rinsed three times in 25mM sodium acetate buffer (pH 5.7) to halt the fixation process. This was followed by three stages of washing for 5 minutes in aqueous 0.5% sodium tungstate, and 15 minutes in a 50% ethanolic 0.5% sodium tungstate solution, which serves to increase the electron density of the stain.

2.1.2. Dehydration and resin embedding

All samples then underwent the same dehydration process in a series of graded ethanol changes which consisted of 15 minutes in 70%, 90%, and twice in 100% ethanol. This was followed by two 15 minute stages in propylene oxide, then 1 hour in a 1:1 propylene oxide:araldite resin mixture. The Araldite resin is made by mixing the Araldite monomer CY212, DDSA hardener, and BDMA accelerator in a ratio of 23.3:26.6:1. The Araldite monomer and hardener were pre-warmed to reduce their viscosity and facilitate their measurement and pouring. Following six changes of Araldite resin infiltration over 24 hours, the samples were then inserted into moulds with further resin. Resin infiltration and hardening then occurred over a 48 hour period in a 60°C oven.

2.1.3. Sectioning and post-staining

Glass knives were made on a Leica EMKMR2 glass cutter (Leica, Austria). Tape, placed around the top sides of the knife and sealed with wax, creates a small well that can be used as a water bath. De-ionised water was pipetted into the bath, and the knife was set at an angle of 6°. Semi-thin sections approximately 500nm thick were cut either on a Reichart-Jung Ultracut Microtome or a Leica EM UC6 Microtome. These sections were transferred to a microscope slide, and after staining with toluidine blue the sections were observed under light microscopy. Desirable regions were polished by reducing the thickness of the sections cut by glass knife, then a diamond knife was used to obtain the ultrathin sections. Initially, the diamond knife water bath was filled with de-ionised water then sections approximately 90nm thick with gold interference colours were sectioned, stretched using chloroform vapour, and lifted onto copper grids.

Post-staining of the sections was carried out in order to enhance the contrast and detail in the final electron microscope images. The solutions used in post-staining were all centrifuged and filtered through Millipore syringes before use, in order to minimize the occurrence of stain precipitate remaining on the samples.

Routinely prepared samples were post-stained at room temperature in 2% aqueous uranyl acetate for 12 minutes, and then Reynolds lead citrate for 5 minutes. Reynolds lead citrate was made following the standard published protocol (Reynolds 1963). The grids were

positioned face down onto the surface of 25 μ m drops of the stain, which were placed on parafilm over moistened filter paper. A cover was then placed over this area to prevent any light from reacting with the stains, and NaOH pellets were placed around the drops to ensure minimal CO₂ reacted with the lead citrate. The corneal samples were washed between stains by floating on a series of four 100 μ m drops of Millipore-filtered distilled water, for 2 minutes at a time. After lead citrate staining the grids were washed using the same method, with the addition of dip washing and jet washing with Millipore filtered distilled water. The grids were then blotted dry on lint-free filter paper, and allowed to air dry.

The Cuprolinic blue stained samples were post-stained at room temperature in 1% aqueous phosphotungstic acid for 2 minutes and then 2% aqueous uranyl acetate for 12 minutes. As with the routine samples, these grids were also positioned face down onto the surface of 25 μ m drops of the stain, which were placed on parafilm over moistened filter paper. The samples were washed between stains by floating on a series of four 100 μ m drops of Millipore-filtered distilled water, for 2 minutes at a time. After uranyl acetate staining the grids were washed using the same method, with the addition of dip washing and jet washing with Millipore-filtered distilled water. The grids were then blotted dry on lint-free filter paper, and allowed to air dry.

2.1.4. Observation and Imaging

Electron microscopy was carried out at 80kV on a Hitachi H7600 and a JEOL 1010 transmission electron microscope. Images were taken on a Gatan ORIUS SC1000 CCD camera.

3. AVIAN CORNEAL STROMA

3.1. Introduction

The corneal stroma is composed predominantly of heterotypic type I/V collagen fibrils organised into orthogonally orientated lamellae. Within these lamellae, the collagen fibrils demonstrate highly ordered packing, with regular fibril diameters and interfibrillar spacing. This organisation is key to the cornea's ability to be optically transparent and still remain mechanically strong (Maurice, 1957; Farrell and Hart, 1969; Benedek, 1971).

Proteoglycans in the corneal stroma interact with these collagen fibrils, and are thought to regulate their diameter and pseudo-hexagonal array (Borcherding et al., 1975; Chakravarti et al., 2000; Quantock et al., 2001; Meek et al., 2003). As discussed previously, corneal proteoglycans are composed of one or more glycosaminoglycan side chains covalently linked to a small leucine rich repeat protein core. These glycosaminoglycan side chains are linear polymers of negatively charged disaccharides. In the corneal stroma, the two predominant side chains are keratan sulphate or a hybrid of chondroitin sulphate and dermatan sulphate. In the chick corneal stroma, the former binds to the protein core of keratocan, lumican and mimecan proteoglycans, whilst the latter binds to decorin and biglycan proteoglycans (Iozzo, 1997). The core protein of the proteoglycan binds with collagen fibrils at distinct banded regions along the fibril axis - 'a' and 'c' for keratan sulphate proteoglycans and 'd' and 'e' for chondroitin sulphate/dermatan sulphate proteoglycans (Scott and Haigh, 1985; Young, 1985; Meek et al., 1986; Scott and Haigh, 1988). The glycosaminoglycan side chains then project into the interfibrillar gap and, via their negative charge resulting from sulphated amino sugars, interact with other collagen fibrils or extracellular matrix components (Iozzo, 1997).

Several models have been put forward to explain how collagen-proteoglycan interactions regulate interfibrillar spacing (Maurice, 1962; Farrell and Hart, 1969; Müller et al., 2004). The predominant theory is based on a six-fold arrangement of glycosaminoglycan side chains radiating from a collagen fibril to connect to six adjacent fibrils. More recent studies have modified this theory to account for the length of some proteoglycans as being longer than the interfibrillar gap. It is now suggested that rather than associating with adjacent fibrils, the

glycosaminoglycan side chains formed bridges to the next nearest fibril (Müller et al., 2004). However, electron tomography studies have suggested a new theory of collagen-proteoglycan interaction (Knupp et al., 2009; Lewis et al., 2010; Parfitt et al., 2010). Three-dimensional reconstruction of murine and bovine corneal stroma have shown that rather than being bound to a six-fold arrangement, the organisation of proteoglycans is a more fluid and dynamic system, with no set azimuthal positioning. The side chains are able to form complexes with the side chains of adjacent proteoglycans, and thus may influence fibril architecture by self associating to form multimer bridges that span across several fibrils, and through the presence of equal but opposing forces created by their charged glycosaminoglycan side chains (Knupp et al., 2009; Lewis et al., 2010; Parfitt et al., 2010), allow a lattice-like organisation of the collagen fibrils.

This study uses three-dimensional electron tomography to study the developing chick cornea across developmental days 12, 14 and 16. Specifically, I investigated the relationship and interactions between type I collagen fibrils and proteoglycans in the chick corneal stroma. These reconstructions gave a view of the spatial orientation of proteoglycan side chains in three dimensions revealing the complex collagen-proteoglycan interactions that regulate the architecture of the developing stroma.

3.2. Methods

3.2.1. Sample collection

Fertilized white leghorn chicken eggs were obtained from the Henry Stuart & Co. Hatchery (Lincolnshire, UK).

For the low magnification study, fertile chicken eggs were collected at early day 14 (at 9:00am), mid day 14 (at 1:00pm), and late day 14 (at 5:00pm). The corneas were then dissected immediately from the decapitated chick embryos and placed in fixative solutions ready for routine processing.

For the high magnification study, fertile chicken eggs were collected at day 12, day 14, and day 16. One series was cut into quarters and fixed overnight in 2.5% glutaraldehyde in 25mM sodium acetate buffer with 0.05% Cuproinic blue (pH 5.7, 0.1M MgCl₂).

The use of animals in this work was carried out in accordance with ARVO (the Association for Research in Vision and Ophthalmology, Bethesda, MD, USA) statement for the use of animals for ophthalmological and vision research and local ethical rules.

All samples for the low magnification study underwent routine processing as described in Chapter 2 'General Methods' and were observed with transmission electron microscopy. Sample sections were collected on copper 300 mesh grids.

All samples for the high magnification study underwent Cuprolinic blue processing as described in Chapter 2 'General Methods'

3.2.2. Sample preparation

3.2.2.1. Polyetherimide Support films

0.76g of polyetherimide granules were dissolved in 200ml of ethylene dichloride for approximately 72 hours. Coated microscope slides were dipped into this 0.38% polyetherimide/ethylene dichloride solution for 20 seconds and then left to dry. These coated slides were then scored along each edge with a razor blade, and dipped slowly into a water bath. The polyetherimide film lifted off, and floated on the surface of the water. Slot grids were placed onto the floating film, which was then attached to another polyetherimide coated slide. This was then left to dry, before the grids were carefully lifted off the slide using a razor blade and forceps.

3.2.2.2. Sectioning

As described in Chapter 2 'General Methods'. Corneal sample sections were collected on the Polyetherimide coated slot grids.

3.2.2.3. Section staining

As described in Chapter 2 'General Methods'. Following phosphotungstic acid and uranyl acetate staining, the sections were also coated with 10nm diameter gold fiducial markers.

Gold fiducials function as points of reference to enable tracking of the desired region whilst the tilt series is being acquired. In addition, they allow the computer software to correctly align the series of micrographs with each other during computer analysis of the tilt series.

The gold fiducial solution was pipetted into 10 μ L droplets on a parafilm sheet. Both sides of the coated slot grids containing sample sections were placed onto the droplets for 20 seconds each side, then removed and left to dry.

3.2.3. Electron Microscopy and Electron tomography

3.2.3.1. Tilt Series



Figure 3.1: JEOL 1010 Transmission electron microscope.

Electron microscopy was carried out at 80kV on a Hitachi H7600 and a JEOL 1010 transmission electron microscope (Figure 3.1). The sample was tilted using the goniometer on the JEOL microscope from -60° to $+60^{\circ}$. Due to obstruction by the sample holder, images cannot be taken over a full 360° . The axis of the sample was centred and aligned before the tilt series was obtained. The image was returned to the same co-ordinates at each degree increment, to ensure that each image was aligned with the previous one. This was achieved

Chapter 3 - Avian corneal stroma

by selecting one centrally located fiducial marker and tracking its position to the same point in each micrograph. Images were taken on a Gatan ORIUS SC1000 CCD camera.

3.2.3.2. Alignment of Tilt Series

IMOD is an open source computer software package used for analyzing, modelling and displaying 3-D image data. It was developed by the Boulder Laboratory for 3D electron microscopy of cells at Colorado University (Kremer et al., 1996). Using the `tif2mrc` and `newstack` programs within the IMOD software package, the tiff images that make up the tilt series are then converted into a `.mrc` file and a `.st` image stack respectively. This `.st` file is then used by the `eTOMO` alignment software, also a sub-program of IMOD (Figure 3.2).

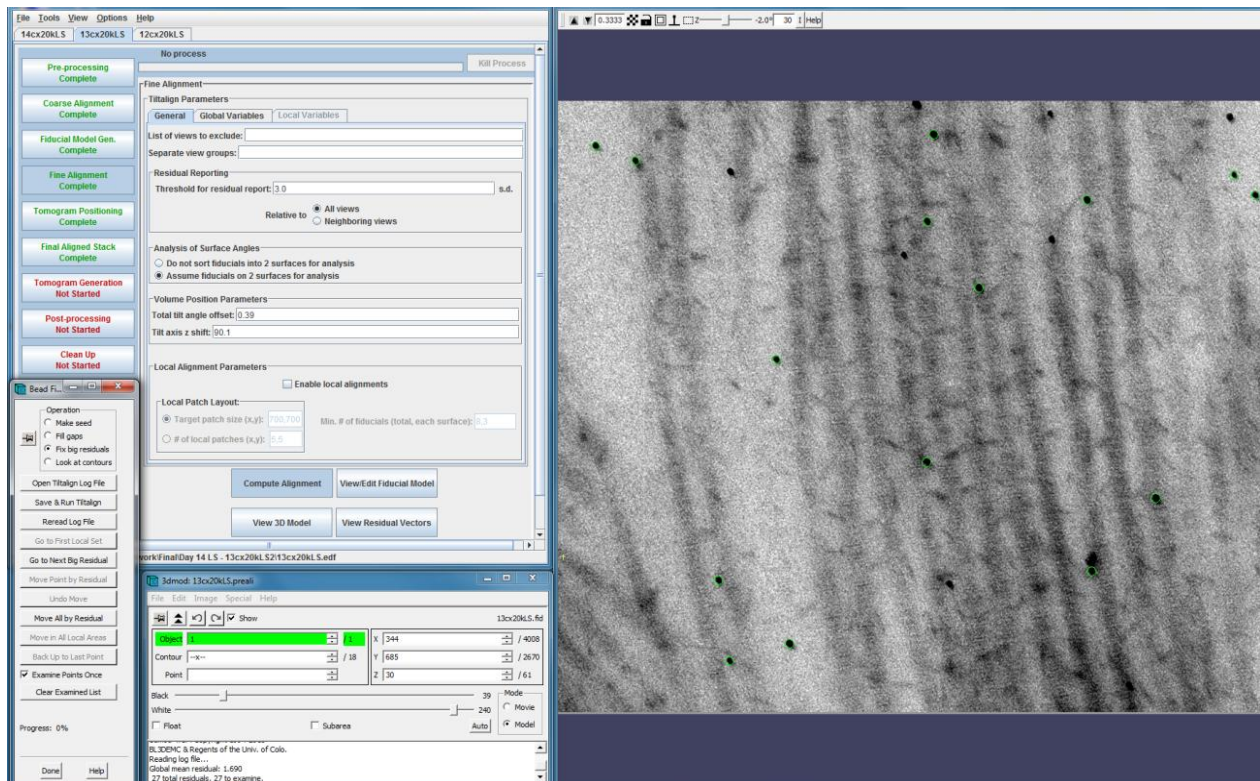


Figure 3.2: Screenshot showing the fine alignment stage in `eTOMO`.

Using the 0° micrograph from the tilt series, contours (green circles) are drawn around multiple fiducial markers for computer aided tracking.

In `eTOMO` the stack of images is then taken through a series of coarse and fine alignment stages, to generate a final tomograph. This alignment is achieved through an iterative process

of tracking of gold fiducial markers that were previously coated onto both sides of the sample. After alignment, eTOMO uses back-projection to generate a three-dimensional reconstruction of the initial two-dimensional micrographs. This final tomograph is created by the smearing of the aligned images to create an image that possesses depth, allowing the user to now pass through the thickness of the image stack.

3.2.3.3. Segmentation of Three-Dimensional Reconstruction

Using EM3D software, developed at Stanford University, USA (Ress et al., 2004), the final tomogram undergoes segmentation to make the image easier to interpret and analyse (Figure 3.3). Contours are manually drawn round each object of interest, and segmented in each individual image in the image stack. The image is then rendered, and a three-dimensional model of each segmented object of interest is produced. This model can be manipulated and rotated, giving a much clearer and more meaningful image than is possible from a two-dimensional greyscale micrograph (Figure 3.3).

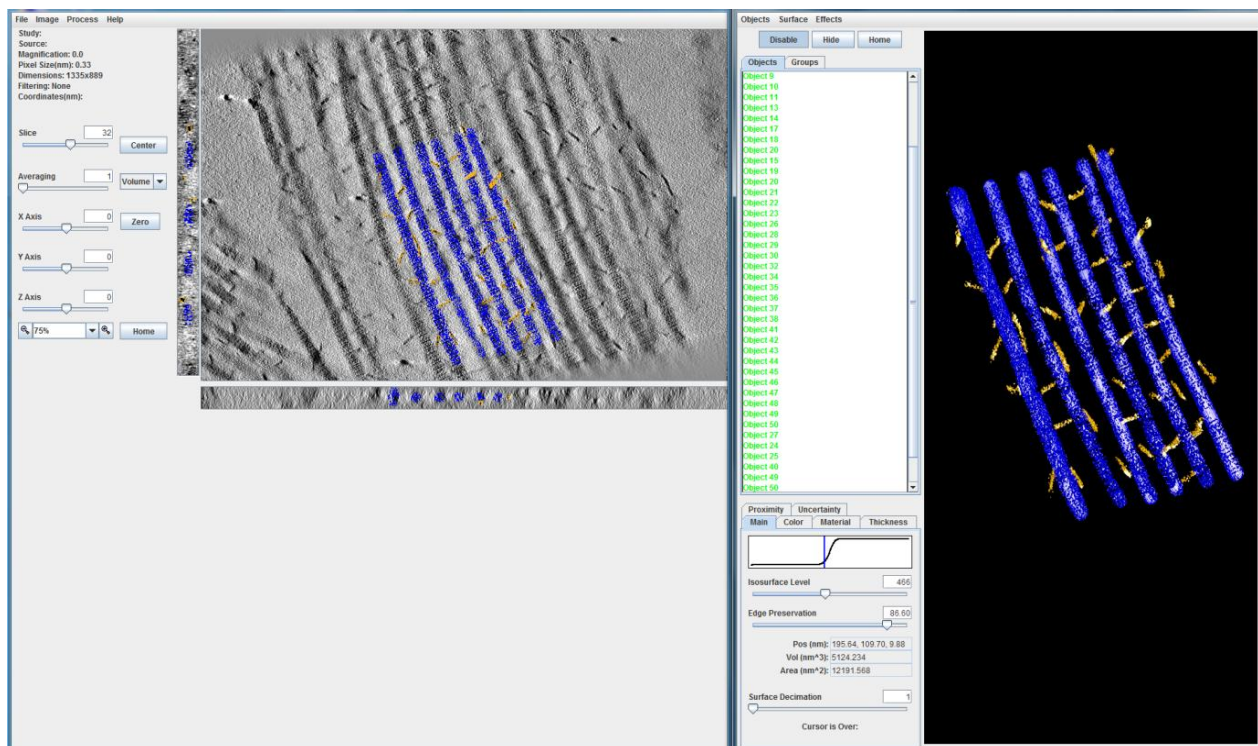


Figure 3.3: Screenshot showing the segmentation and rendering stage in EM3D.

Segmentation of the aligned tilt series (left) is then followed by rendering to produce the final three-dimensional reconstruction (right).

3.3. Results

3.3.1. *Low magnification study*

It can be hypothesised that there are several different categories of membrane compartments formed by stromal keratocytes. This membrane compartmentalisation was discovered to be the predominant method of collagen production in embryonic tendon. Plasma membrane protrusions called fibripositors, and the adjacent extracellular channels that form between these processes, transfer collagen fibrils into the extracellular matrix. These narrow membrane bound tunnels were found emerging from deep within keratocytes (shown in Figure 3.4), throughout developmental day 14. These fibripositors contained approximately 9-12 fine filamentous structures, thought to be collagen in the process of condensing into fibrils. In Figure 3.4B this collagen can be seen running in a uniform direction out of the fibripositors. The morphology of these tunnels may then facilitate fibrillogenesis and impart a degree of orientation to the newly synthesised collagen.

Small cell surface recesses were observed, containing approximately 7-15 collagen fibrils. Figure 3.5 shows that within these recesses, the fibrils were observed closely associating with the keratocyte cell surface. The small fibril bundles, and the recesses from which they emerge, were found to a greater extent during early day 14 of development (Figure 3.5A).

Larger cell surface recesses were also observed, containing fibril bundles of a greater size, approximately 20-40 fibrils. As Figures 3.6A and 3.6B show, these fibril bundles and larger recesses were present throughout day 14. However by late day 14, in addition to these large recesses, the thicker fibril bundles were also commonly orientated between thin cell processes that formed wide membrane bound channels (Figure 3.6C).

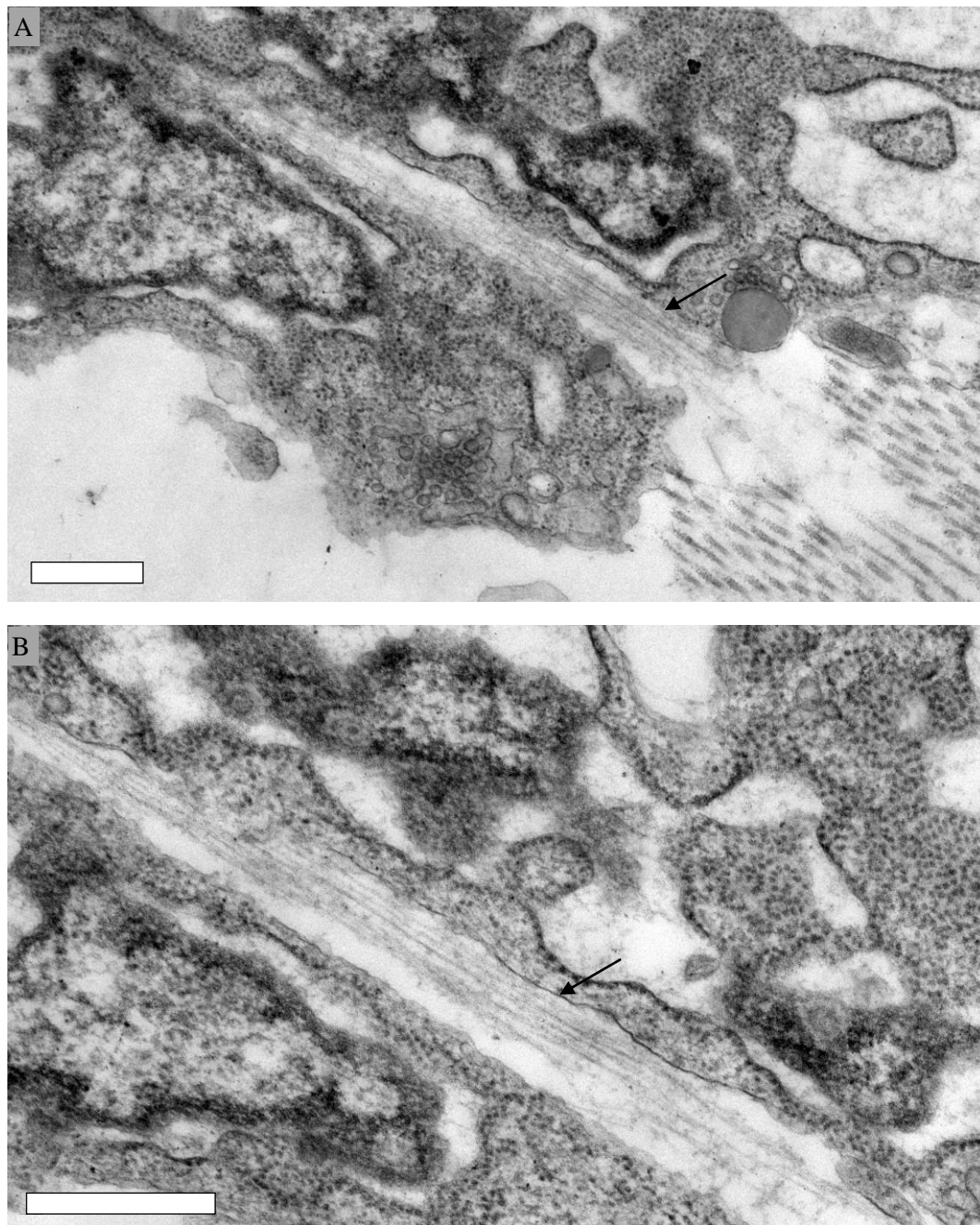


Figure 3.4: En face section of fibripositors and collagen.

(A) Mid day 14 corneal stroma at x6000 magnification. (B) Mid day 14 corneal stroma at x10000 magnification. Arrows indicates fibripositor with emerging collagen. Scale bar = 0.5 μ m.

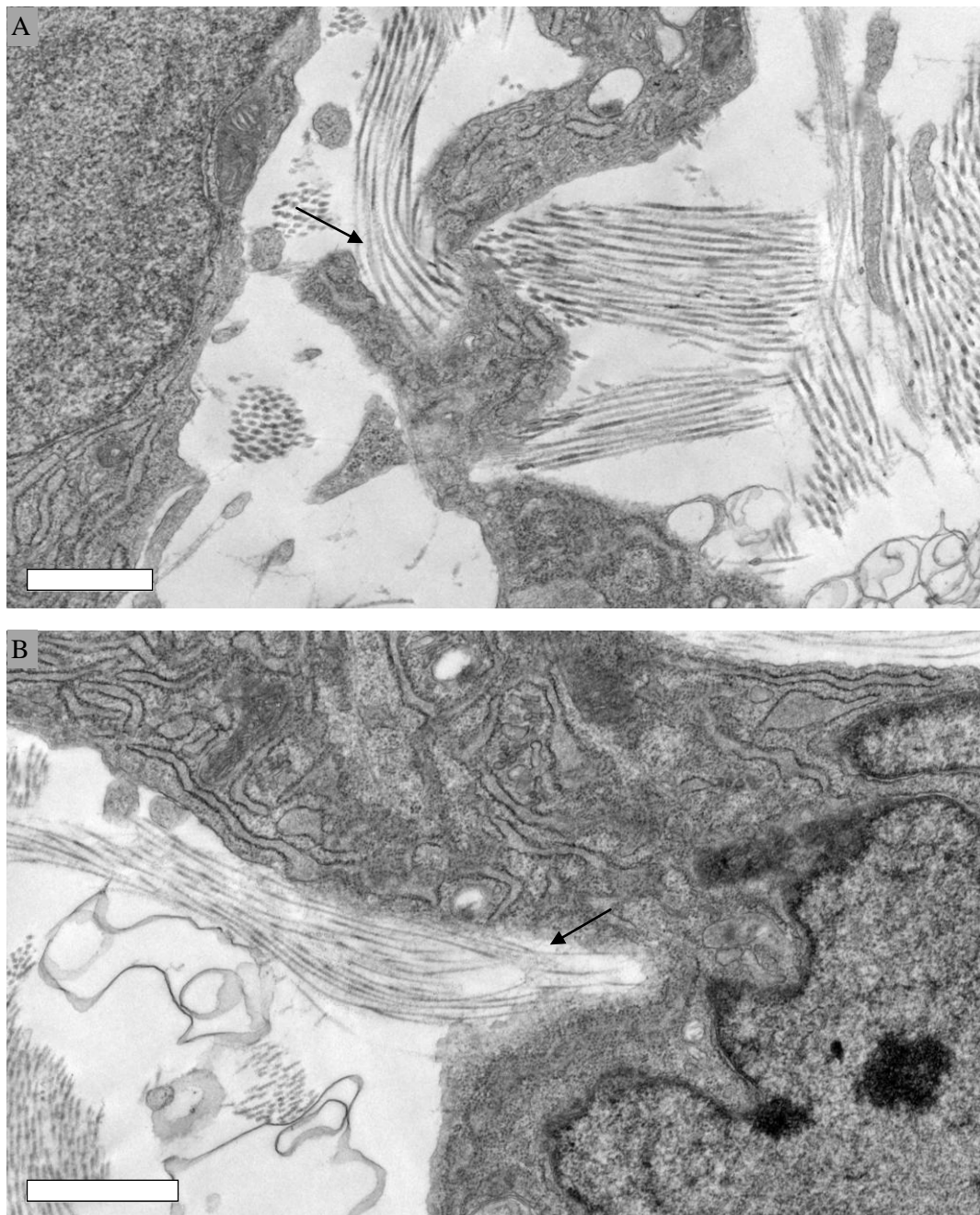


Figure 3.5: En face section of small fibril bundles and keratocyte surface recesses.

(A) Early day 14 corneal stroma at x3000 magnification. (B) Mid day 14 corneal stroma at x4000 magnification. Arrows indicates keratocyte surface recess and fibril bundle. Scale bar = 1 μ m.

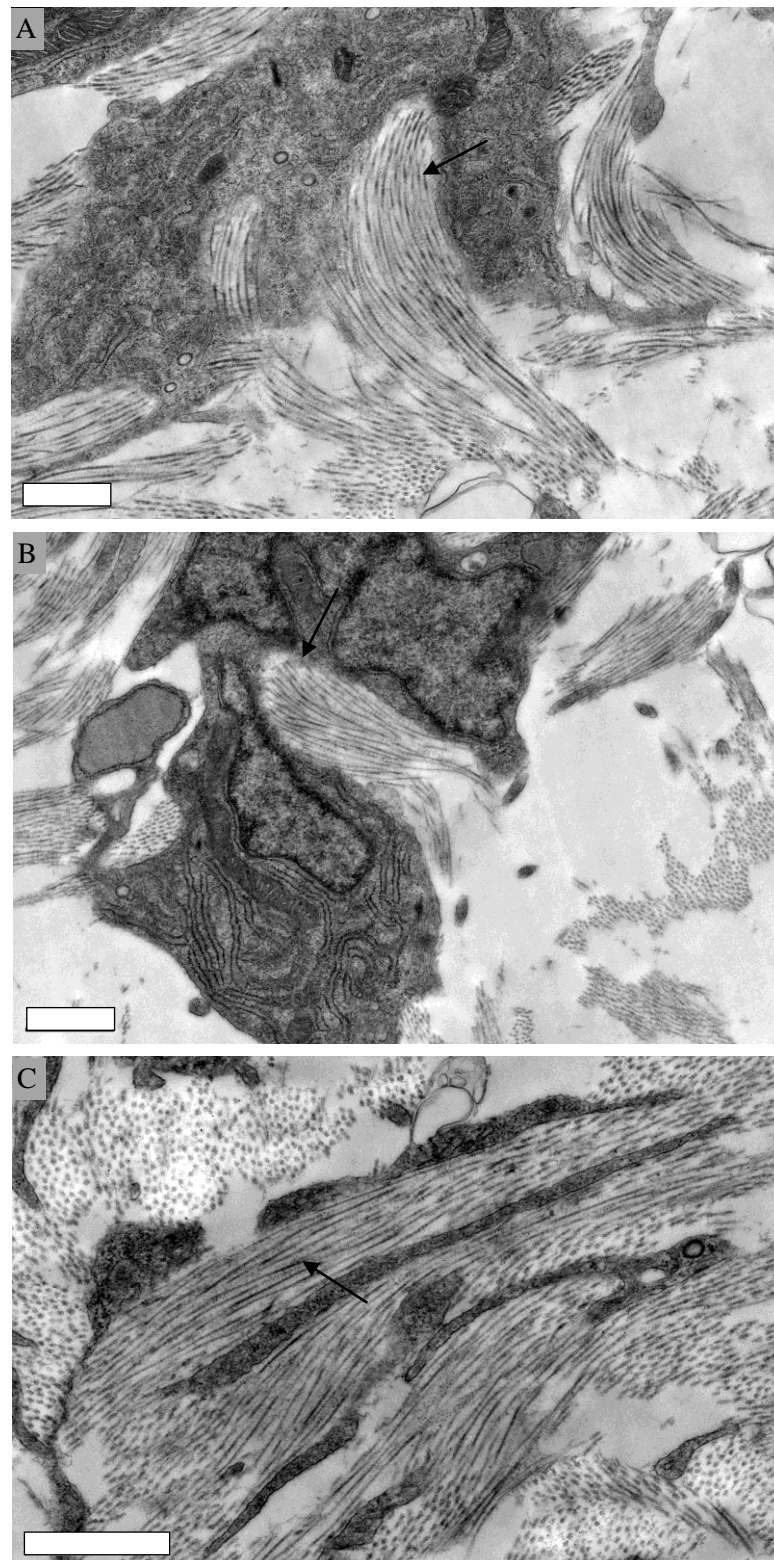


Figure 3.6: En face section of fibril bundles and keratocyte surface recesses.

(A) Mid day 14 corneal stroma at x3000 magnification. (B) Late day 14 corneal stroma at x3000 magnification. (C) Late day 14 corneal stroma at x5000 magnification. Arrows indicates keratocyte surface recesses and membrane bound compartments. Scale bar = 1 μ m.

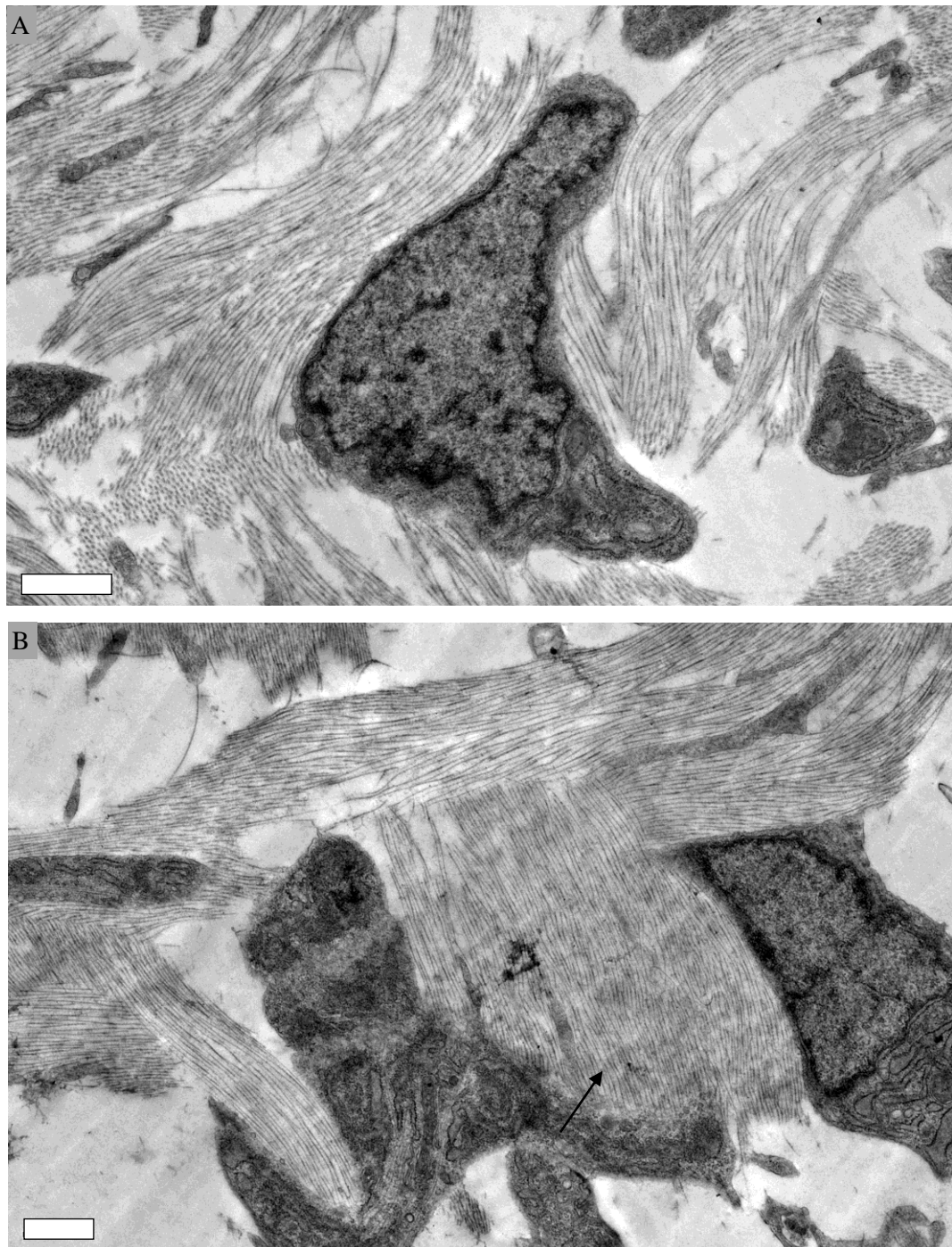


Figure 3.7: En face section of large fibril bundles and keratocyte compartments.

(A) Late day 14 corneal stroma at x2500 magnification. (B) Late day 14 corneal stroma at x2000 magnification. Arrow indicates keratocyte bound compartment. Scale bar = 1 μ m.

Finally, as evident in Figure 3.7, regions were observed where large fibril bundles coalesced into broader bundles and lamellae. These bundles would frequently contain well in excess of 50 fibrils. Occasionally it was evident that these bundles passed through spaces created between cell surfaces (Figure 3.7B). In Figure 3.7B orthogonally aligned sheets of collagen fibrils can be easily identified. Often these large sheets of fibrils were orientated at right angles, reminiscent of the orthogonally stacked lamellae of the mature corneal stroma.

Observed across day 14 at three different time points, the relative proportions of these different sized fibril bundles and recesses appeared to change. During early day 14, collagen fibril bundles largely contained around 10 fibrils, bundles of 25 fibrils were also present, as were occasional bundles of around 30 fibrils. By mid day 14 the relative proportions of these three bundle sizes were approximately equal. However, by late day 14 few of the smaller fibril bundles remained, with the predominant bundle size being around 30 fibrils. In addition at this developmental stage, the membrane compartments formed by the keratocytes were more commonly channels created between cell processes (see Figure 3.6C).

3.3.2 High magnification Study

Electron micrographs (Figure 3.8) show that throughout the developmental stages studied, Cuproinic blue-stained proteoglycans are present. They can be observed either associating with, or in the interfibrillar space between collagen fibrils (Figure 3.9). The fibrils themselves are seen initially in small bundles that progressively combine as development continues to form larger bundles, eventually coalescing into lamellae. Throughout development, even within these early bundles, a level of organisation in the collagen fibril packing can be seen.

Three-dimensional reconstructions of collagen fibrils and associated proteoglycans at developmental day 12, 14 and 16 were obtained in both longitudinal and transverse planes (Figure 3.10). Closer examination of the collagen fibrils within these reconstructions confirmed the regularity of fibril packing observed in the electron micrographs. At day 12, fibril packing is consistent with that of a loose hydrated stroma populated by independent bundles of collagen fibrils. At developmental day 14, interfibrillar spacing showed a temporary increase. However by day 16 interfibrillar spacing had decreased, and fibrillar packing was closer than at day 12.

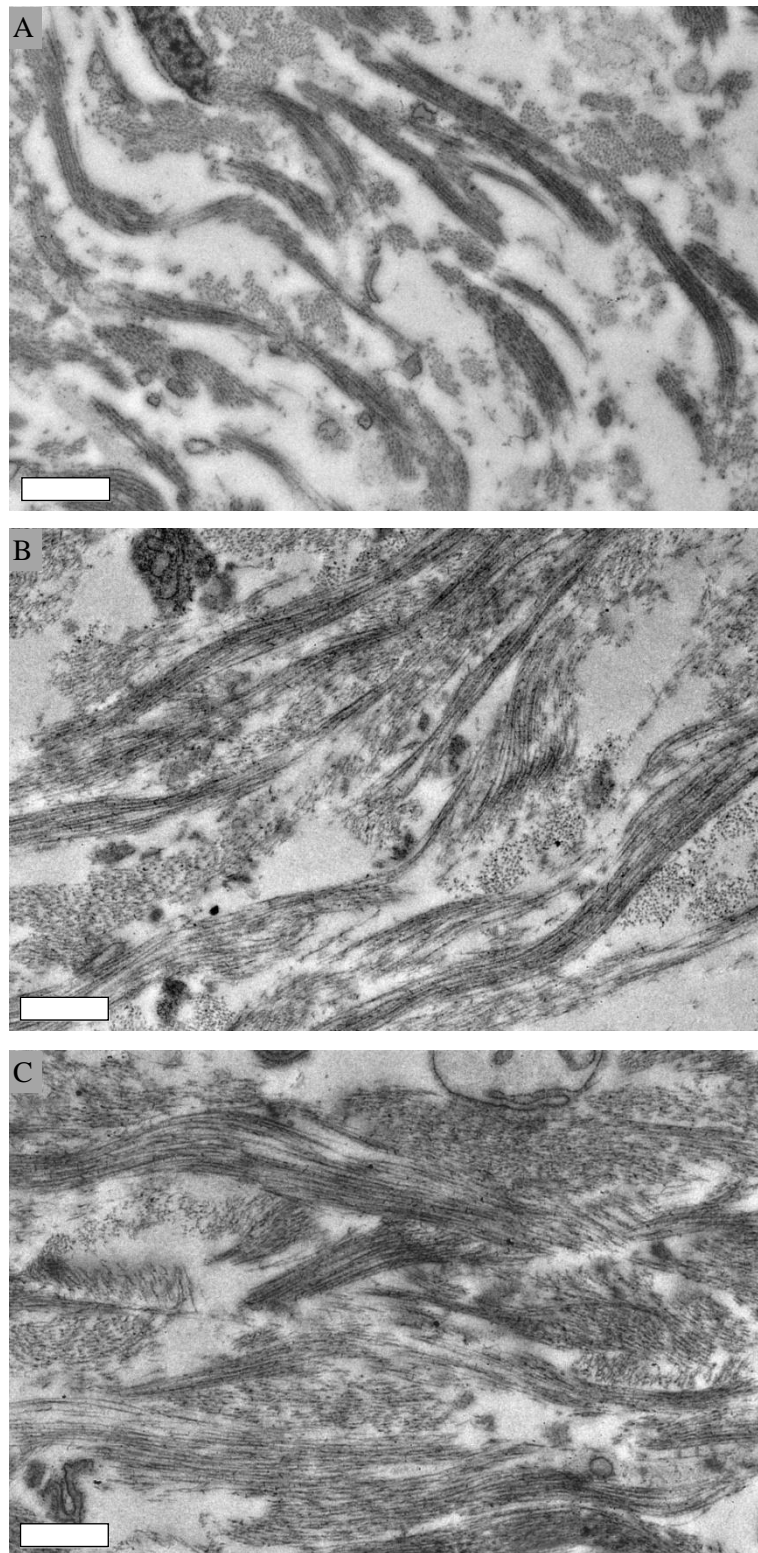


Figure 3.8: Transmission electron micrographs of the developing chick corneal stroma. Embryonic day 12 (A), day 14 (B) and day 16 (B) showing the progressive dehydration and compaction of the stroma at x3000 magnification. Collagen fibrils can be seen coalescing into larger bundles as development progresses. Scale bar = 1 μ m.

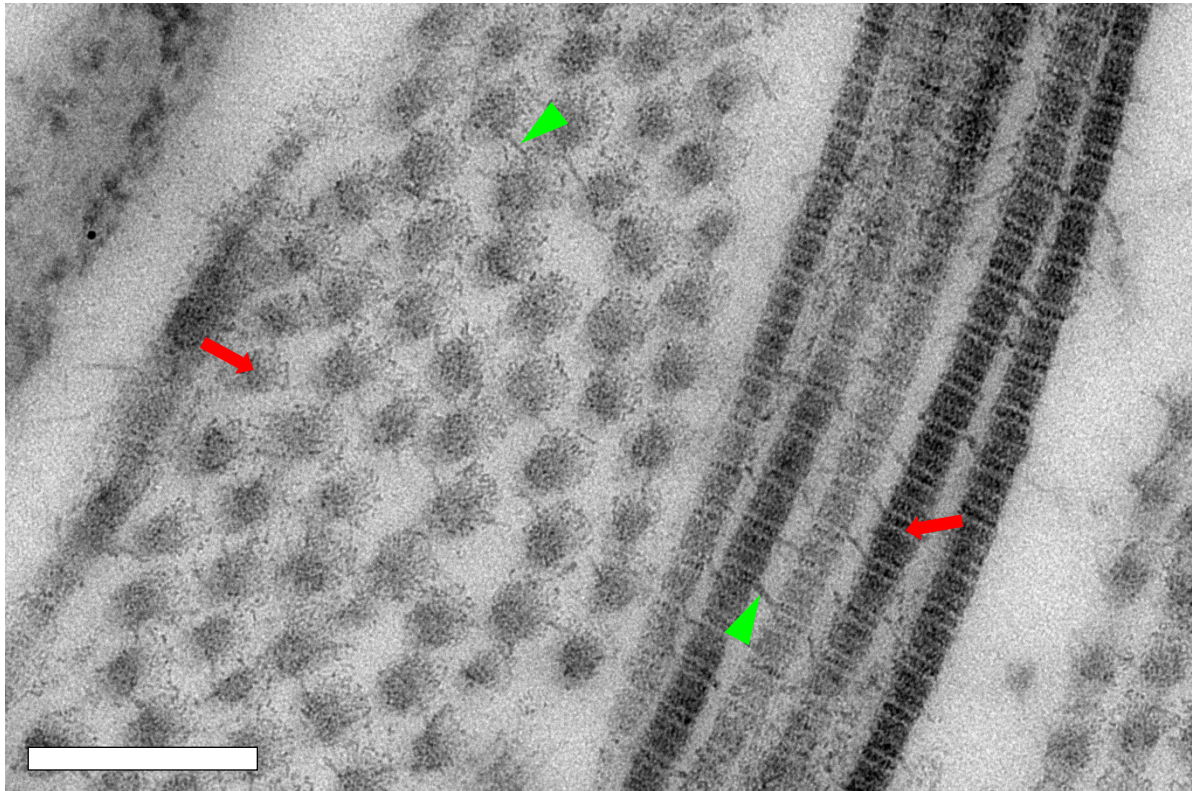


Figure 3.9: Transmission electron micrograph of collagen and proteoglycans in day 14 developing chick corneal stroma.

Collagen fibrils (red arrows) can be seen in a longitudinal and transverse plane at x20000 magnification. Proteoglycans (green arrow heads) can be seen spanning the gaps between fibrils, and binding to the longitudinally orientated collagen fibrils at regular spacings. The proteoglycans interacting with the transversely orientated fibrils shows no regularity or order in their arrangement. Scale bar = 250nm.

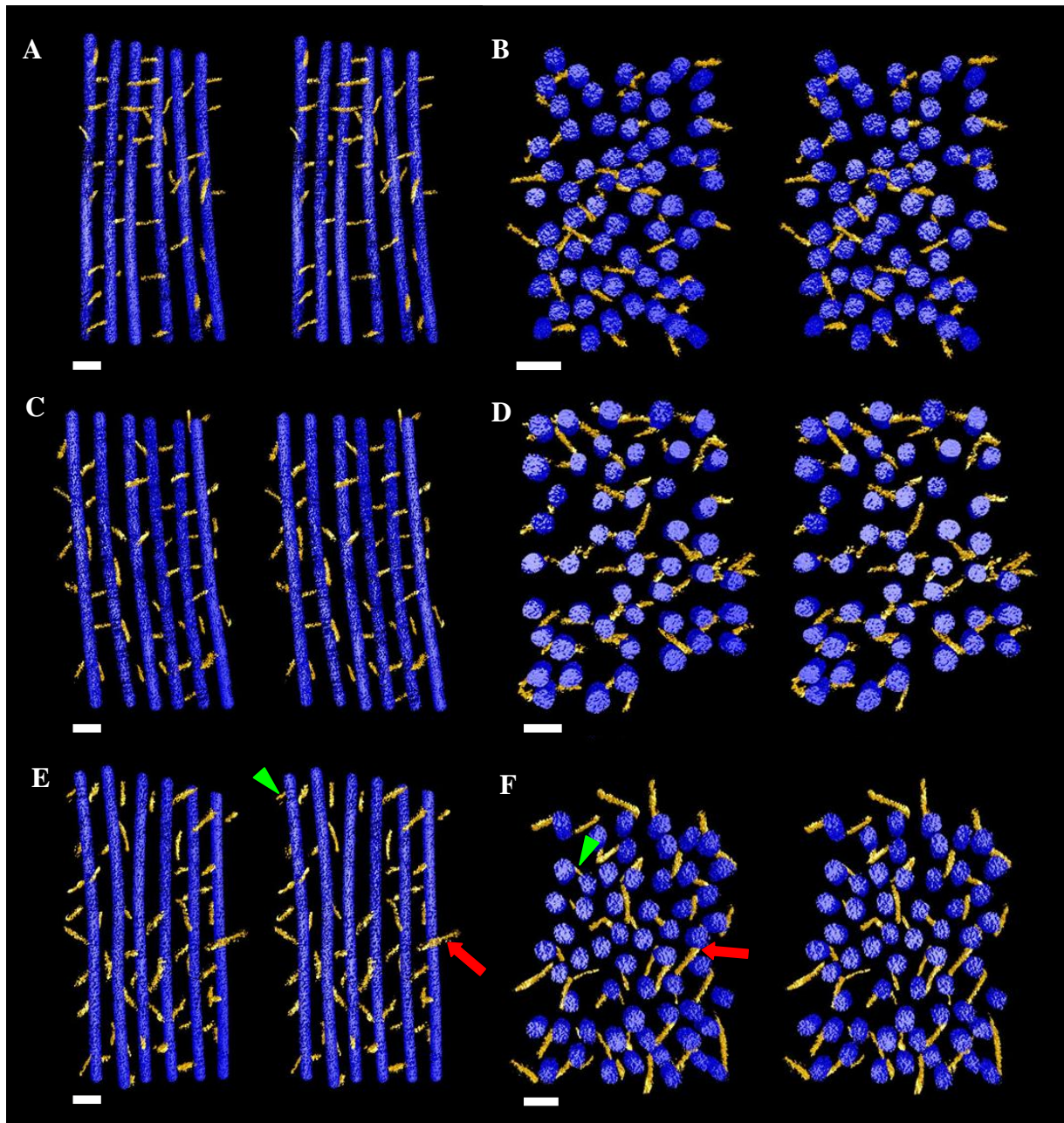


Figure 3.10: Stereo pairs of three-dimensional reconstructions.

Collagen (blue) and proteoglycan (yellow) interactions in the developing chick cornea at embryonic day 12 (A, B), day 14 (C, D), and day 16 (E, F). A, C and E show a longitudinal view, whilst B, D and F show a transverse view. Short proteoglycans are indicated by green arrowheads, whilst long proteoglycans are indicated by red arrows. Scale bar = 50nm.

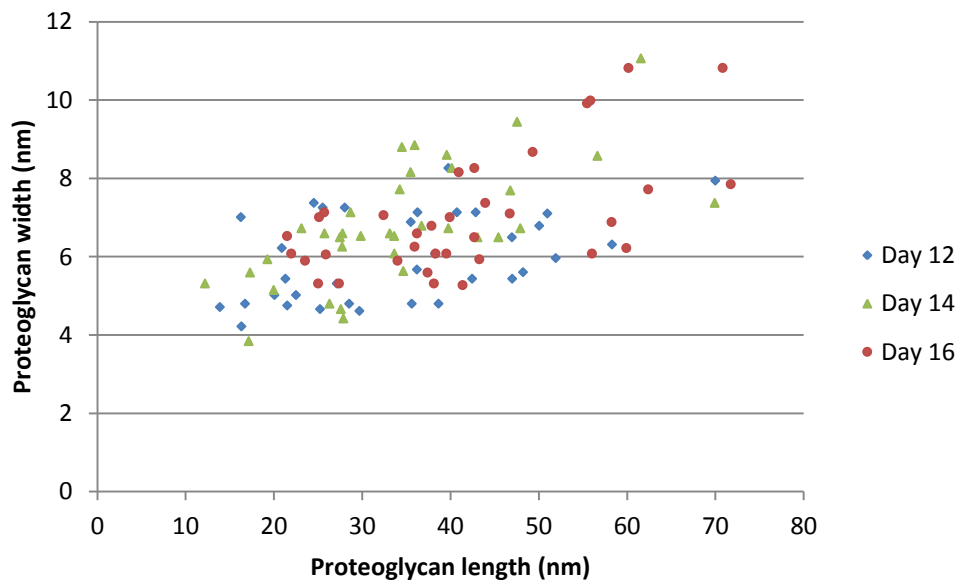


Figure 3.11: Proteoglycan size scatter graph.

Proteoglycan length versus width at embryonic days 12, 14 and 16. Only proteoglycans whose entire structure was present in a reconstruction were measured. Proteoglycans range from 12.2nm to 71.7nm in length, and from 3.8nm to 11.1nm in width.

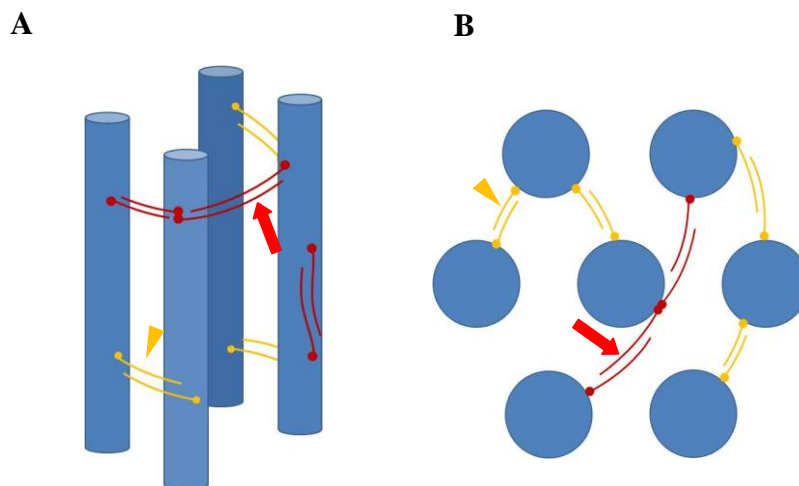


Figure 3.12: Models of collagen fibril and proteoglycan interactions in the chick cornea.

Collagen (blue) and proteoglycans (red and yellow) in a longitudinal view (A), and transverse view (B). Yellow arrowheads indicate short antiparallel keratan sulphate side chains. Red arrows indicate long antiparallel chondroitin sulphate/dermatan sulphate side chains.

Proteoglycan number increased as development progressed (Figure 3.10). A scatter graph comparing proteoglycan length and width revealed the range of sizes that proteoglycans can exhibit (Figure 3.11). Tables of proteoglycan dimensions across the developmental stages studied can be found in Appendix 1. Small and medium sized proteoglycans ranging from approximately 12nm to 50nm in length, were prevalent throughout the developmental days studied. However during the later stages, larger proteoglycans up to 75nm in length were also present. The ratio of smaller to larger proteoglycans appeared to shift as development progressed, with the larger proteoglycans present in greater numbers at day 14 and greater still at day 16 (Figures 3.10 and 3.11). However, the smaller and intermediate sized proteoglycans still remain more common. An overall trend can be seen in the scatter graph, showing that the width of the proteoglycan corresponds approximately to its length, in that the shorter proteoglycans were often thinner in width also. Conversely, the longer proteoglycans were present in a range of widths. The smaller proteoglycans can be seen projecting from the surface of collagen fibrils and spanning the interfibrillar gaps. The length of these proteoglycans was approximately equal to the distance between adjacent fibril surfaces. The larger proteoglycans were often observed passing around adjacent fibrils to interconnect a more distant neighbouring fibril (Figure 3.12). The three-dimensional reconstructions also make it possible to observe the orientation and positioning of the proteoglycans on the collagen fibrils. By observing the longitudinally sectioned reconstructions at day 12 and day 14, the orientation of the proteoglycans appears to be more orthogonal with respect to the long axis of the collagen fibril to which it is associated. By day 16, their orientation has taken on the characteristic appearance of more mature tissue, with proteoglycans pointing at more oblique angles from the collagen axis. These reconstructions also show distinct binding regions along the length of the fibril. Often two or more proteoglycans can be seen associating with the fibril at the same binding point along its length (Figure 3.10). In the transverse sectioned reconstructions, no distinct six-fold arrangement of the proteoglycans around a central fibril could be seen, nor did the proteoglycans appear to follow any set arrangement or azimuthal positioning.

3.4. Discussion

3.4.1. Low magnification Study

Whilst the synthesis and post translational modification of extracellular matrix components is well documented in fibroblasts, what is less well studied is the role these cells also have in the assembly and deposition of these matrix components.

Trelstad and Coulombre (1971) observed that in the primary stroma, thin bundles of collagen fibrils are secreted into an orthogonal array by similarly orientated vacuoles in epithelial basal cells. Equally, in the secondary stroma Birk and Trelstad (1984) suggested that collagen production and organisation occurs in close association with the surface of the keratocyte. Often the lateral fusion of cell surface recesses and the process of cell surface folding can create membrane bound compartments that then contain the fibrilizing collagen. This process would then facilitate the direct connection and regulation between the intracellular and extracellular mechanisms of collagen fibril production.

More recently this membrane compartmentalisation method was also discovered to be the predominant method of collagen production in embryonic tendon (Canty and Kadler, 2005). During embryonic development, tendon fibroblasts synthesise collagen through actin-rich fibripositors (Canty et al., 2004). A recent study investigated the role that tension has on the formation of fibripositors in embryonic tendon cells cultured in fibrin gel. The production of thin, axially aligned collagen fibrils from newly formed fibripositors was dependant on the receipt of a tension stimulus from the fibril gel matrix (Kapacee et al., 2008). This behaviour has also been simulated in adult human tendon fibroblasts, when cultured under tension in fibrin gels (Bayer et al., 2010). However, *in vivo*, the fibripositor mechanism appears to be active only during the short developmental period dedicated to the establishment of tissue architecture.

This study utilized en face sections through the corneal stroma. This technique facilitates the observation of collagen fibril bundles running in multiple directions across the same plane. Sections could be taken through cell membrane bound compartments that are orientated in different directions, and orthonally aligned sheets of collagen fibrils can be seen longitudinally.

In the corneal stroma, the keratocyte cell surface was partitioned into at least three major compartments within which collagen fibrillogenesis, bundle formation, and the deposition of fibril bundles into orthogonal lamellae are all regulated (Birk and Trelstad, 1984). The diameter of the collagen fibrils often corresponded directly to the size of the compartments that contain them, an observation also reported by Birk and Trelstad (1984).

The smallest cell surface recess usually contained 7 to 15 collagen fibrils. These small compartments may be the result of intracellular secretory vacuoles fusing with each other and the cell surface membrane (Birk and Trelstad, 1984). In these recesses, newly synthesised collagen undergoes extracellular modification (Trelstad and Hayashi, 1979). The clear presence of rough endoplasmic reticulum within the keratocytes is an indication of their high level of anabolic activity (Figure 3.5B).

Medium sized compartments, termed open fibripositors, were wide membrane bound channels (Figure 3.6C) that may have facilitated the formation of small fibril bundles of approximately 20 to 40 fibrils. These recesses may have formed through the fusion of smaller cell surface recesses.

Finally, large membrane bound channels were also observed, containing large fibril bundles coalescing into lamellae. These channels were often formed from large folds in the cell surface membrane and the spaces between adjacent cell processes. The collagen fibrils that could be seen running within these channels ran in a uniform direction, dictated by the long axis of the cell processes.

The fibripositor model implies that the production and deposition of collagen fibrils is controlled by individual cells. An important feature of fibripositors is that they are always orientated along the main axis of the cell and tissue. Subsequently, intracellular transport and the extracellular matrix organisation are connected. Corneal fibroblasts migrate into the stroma using the collagenous template of the primary stroma. Positional information gained from this scaffold may then help orientate the cells in the correct axis. Consequently, collagen extruded by these cells will also possess the correct spatial orientation. By examining en face sections of the corneal stroma it was possible to observe keratocytes, and the cell membrane bound channels they produce, aligning with two major orthogonally orientated axes. The

fibril bundles being synthesised may then gain a degree of orientation from the direction of these cellular compartments.

The compartmentalization of the intercellular space is well documented. Collagen fibrillogenesis, post-translational modification, and packing are all initiated within the cell cytoplasm, Golgi complex, and secretory vesicles (Prockop et al., 1979; Olsen, 1981; Trelstad and Silver, 1981; Trelstad et al., 1982). The compartmentalization of the extracellular space then allows a direct connection and continuation of this intracellular process, allowing cellular control over every aspect of collagen architecture, from fibril to lamellae, through the management of these unique micro-environments. These extracellular compartments facilitate both the spatial orientation and structural cohesion of the developing collagen lamellae that are so integral to proper corneal function.

3.4.2 High magnification Study

The reconstructions of collagen-proteoglycan interactions require careful analysis, as each developmental time point is only represented by one reconstruction. Therefore, any theories drawn from these results must take this into account. However, each reconstruction was taken from approximately the same region in the corneas. In addition, numerous micrographs were taken and compared, to ensure each reconstruction was representative and characteristic of stromal morphology at that particular point in development.

The reconstructions of developing corneas at embryonic days 12, 14 and 16 make it clear that whilst the collagen bundles possess increasingly regular and ordered packing throughout development, their relationship with proteoglycans appears much more complex and unsystematic. The diverse three-dimensional orientation of the proteoglycans, and their ability to interconnect adjacent and neighbouring fibrils seemingly without any set pattern or predisposed arrangement, points to a more mutable and dynamic matrix environment.

Previous studies have reported the interfibrillar spacing within collagen bundles decreases during development as the stroma progressively dehydrates and compacts. It is clear from the transverse sectioned reconstructions that, of the three developmental stages studied, interfibrillar spacing is greatest at day 14, followed by day 12, with day 16 showing the most compact fibril packing. This agrees with data from a recent study that used x-ray diffraction

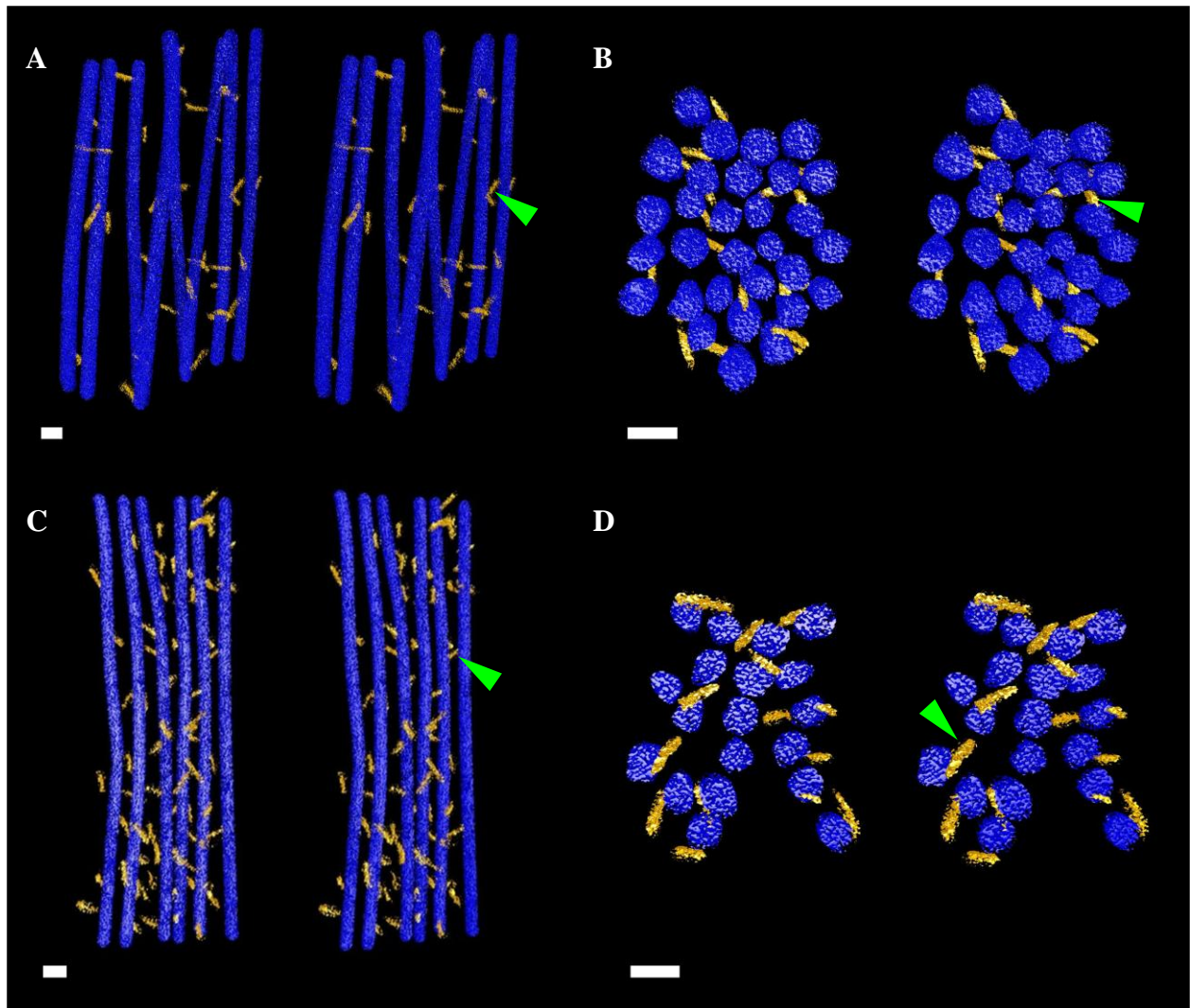


Figure 3.13: Stereo pairs of three-dimensional reconstructions following treatment with chondroitinase ABC.

Collagen (blue) and proteoglycan (yellow) in the developing chick cornea at embryonic day 14 (A, B), and day 16 (C, D). A and C show a longitudinal view, whilst B and D show a transverse view. After enzyme digestion of chondroitin sulphate/dermatan sulphate proteoglycans using chondroitinase ABC, only short proteoglycans remain (indicated by green arrowheads). Scale bar = 10nm. Data obtained in collaboration with Dr Satoshi Nakajima and Dr Barbara Palka.

to measure collagen fibril Bragg spacing. Compaction within the bundles of collagen fibrils was initiated after developmental day 14 (Liles et al., 2010). From electron microscopic study of this developmental period, it is clear that the compaction of fibrils within these bundles occurs simultaneously with the progressive coalescing of the bundles eventually

forming lamellae. Proteoglycan number was seen to increase as development progressed. Similarly the number of large proteoglycans was considerably increased at the later developmental stages. This increased proteoglycan presence may have a key role in the condensing of collagen fibril bundles, and the reduction in collagen interfibrillar spacing. The large proteoglycans are thought to be chondroitin sulphate/dermatan sulphate proteoglycans, as enzyme digestion using chondroitinase ABC left only small keratan sulphate proteoglycans (Figure 3.13). These short proteoglycans can be seen bridging the interfibrillar gap. After enzyme treatment, no proteoglycans were observed with sufficient length to pass around adjacent collagen fibrils to interconnect with more distant fibrils. The protocol for this enzyme treatment method is detailed in Liles et al., 2010. The increased presence of large proteoglycans following day 14 may correlate with the initiation of reduced interfibrillar spacing, as dermatan sulphate proteoglycans are considered to have a morphogenetic role in the developing chick (Hart, 1976; Hahn, 1992). For example, disruption of dermatan sulphate proteoglycan synthesis leads to abnormalities in collagen fibrils packing and lamellar organization. Therefore dermatan sulphate proteoglycans may control fibril-fibril spacing, but not the regulation of fibril diameter (Hahn, 1992; Danielson et al., 1997)

The large range in proteoglycan length and width that was observed (Figure 3.11) may be due to the varying intensity of Cuproinic blue staining resulting from different proteoglycan sulphation levels. However, individual glycan chains have a smaller width (<0.5nm) than what is observed (Scott, 1992), and the Cu^+ and WO_4^{2-} ions used to stain for proteoglycans are small enough to be measured in picometers. The proteoglycan chains are recorded in the reconstructions at much greater widths. It is therefore likely that these larger proteoglycans are the result of self-assembly or aggregation of glycosaminoglycan chains from individual proteoglycans to form anti-parallel multimers. It is not possible to determine the structure of the bond from these reconstructions, however several models have been proposed (Knupp et al., 2009; Lewis et al., 2010). In addition, the mediating role of other extracellular matrix components cannot be ruled out (Cooper et al., 2006). The mechanism by which these lateral associations form is not clear. The ionic balance of the stroma may be important for proteoglycan interactions. The formation of proteoglycan multimers in nasal cartilage have been reported previously, and have been shown to be sensitive to changes in the ionic balance *in vitro* (Roughley et al., 1995). It is possible that positively charged ions within the stroma

(K⁺, Na⁺) cancel out the negative charge of the glycosaminoglycan chains, allowing them to associate through hydrogen bonding and hydrophobic attraction (Scott, 2001).

Linear aggregation of glycosaminoglycan chains allow the proteoglycans to form large multimers that are able pass around adjacent fibrils and interconnect a third more distant neighbouring fibril. From previous studies, these longer proteoglycans have been identified as chondroitin sulphate/dermatan sulphate proteoglycans (Scott, 1992; Liles et al., 2010). Decorin, the predominant chondroitin sulphate/dermatan sulphate proteoglycan of the developing avian cornea, is known to have the ability of molecular self-recognition. The protein core of one decorin molecule can recognise and bind to the protein core of another, and so undergo dimerisation (Scott et al., 2004). However, some studies have rejected the theory that decorin exist as naturally occurring dimers in solution (Goldoni et al., 2004).

It has been previously reported that the arrangement of proteoglycans around a central collagen fibril follows a symmetrical six-fold organisation (Müller et al., 2004). However, concurrent with recent findings (Knupp et al., 2009; Lewis et al., 2010; Parfitt et al., 2010), the present reconstructions suggest that the proteoglycans have no set azimuthal positioning. However, some regularity was observed in the proteoglycan binding sites along the length of the collagen fibrils. The concept of proteoglycan specific binding sites is now widely accepted. Proteoglycans possessing chondroitin sulphate/dermatan sulphate glycosaminoglycan chains will bind to the 'd' and 'e' bands of the collagen fibril, whilst those containing keratan sulphate glycosaminoglycan chains bind to the 'a' and 'c' bands (Scott and Haigh, 1985; Young, 1985; Meek et al., 1986; Scott and Bosworth, 1990).

With no regular or symmetrical organisation, alternative theories for how proteoglycans are able to regulate interfibrillar spacing have emerged. This more disordered local arrangement of proteycans may suggest that long range regulation of interfibrillar spacing is more important. It has been suggested in recent studies that two equal but opposing forces are exerted simultaneously on collagen fibrils due to the presence of proteoglycans. The negatively charged proteoglycan glycosaminoglycan chains attract positively charged ions within the stroma resulting in an osmotic pull. This influx of water molecules into the interfibrillar spaces creates a repulsive force due to increased pressure between fibrils. Simultaneously, thermal motion of the glycosaminoglycan chain complexes, arising from the constant molecular collisions of the proteoglycans and other extracellular matrix molecules,

creates an attractive force (Lewis et al., 2010; Knupp et al., 2009). This force counteracts the repulsive force caused by increased osmotic pressure resulting in a balanced system. Together, these two proteoglycan subtype are able to regulate interfibrillar distances, and stabilize fibril architecture.

Chondroitin sulphate proteoglycans can achieve a much greater level of sulphation than keratan sulphate proteoglycans, due to a larger number of disaccharide motifs (Plaas et al., 2001). Chondroitin sulphate/dermatan sulphate proteoglycans are able to form large complexes capable of interconnecting multiple fibrils. The increased osmotic pressure between fibrils caused by the large number of sulphated glycosaminoglycan chains would then act as a repulsive force, pushing fibrils apart. Conversely, under-sulphated keratan sulphate proteoglycans form short bridges that span the interfibrillar gap, connecting neighbouring fibrils. Thermal motion within these bridges would act as an attractive force, pulling the ends of the glycosaminoglycan chains, and consequently the attached fibrils, closer together. Sulphation levels in keratan sulphate proteoglycans are subject to change during development. Previous studies have reported that as development progresses, highly sulphated keratan sulphate proteoglycans accumulate preferentially over the lesser sulphated isoform (Liles et al., 2010). Here, the increase in sulphated keratan sulphate proteoglycans is not considered to be the driving force behind stromal dehydration and compaction of interfibrillar spacing. Instead, this may occur through the action of the developing endothelial pump. These over-sulphated keratan sulphate proteoglycans may then share a common role with chondroitin sulphate/dermatan sulphate proteoglycans, in controlling interfibrillar spacing through the maintenance of local hydration levels.

3.5. Conclusions

In summary, these three-dimensional reconstructions show that proteoglycans in the developing chick cornea possess no symmetrical arrangement, or system of organisation. Self aggregation of these proteoglycans may result in the formation of multimers that are able to extend around adjacent collagens, interconnecting multiple fibrils. The pseudo-hexagonal arrangement of collagen fibrils is likely held in place through the combined attractive and repulsive forces exerted by the resident proteoglycans. This network of proteoglycans has a key role in the formation of the transparency and mechanical strong corneal tissue.

4. *IN VITRO* SYNTHESIS OF COLLAGEN GEL STROMAL EQUIVALENTS

4.1. Introduction

Having examined the radical structural changes that occur in the corneal stroma during developmental days 12-16, this knowledge can then be applied to the production of a stromal equivalent for use in grafting, or the production of a full thickness corneal substitute. Following the study of collagen organisation and its interactions with proteoglycans in the stroma, attempts were made to utilize similar, predominantly natural, biological materials in the construction of an artificial corneal stroma.

The transparency of the cornea is thought to be dependent on the regular short-range spatial order of the collagen fibril array within each lamella (Maurice, 1957; Hart and Farrell, 1969; Benedek, 1971). Interactions between proteoglycan macromolecules which associate with the collagen and occupy the extrafibrillar space (Zhang et al., 2009; Quantock et al., 2010; Lewis et al., 2010), and between different collagen subtypes (Birk et al., 1990), are thought to mediate the characteristic collagen fibril arrangement in the cornea. The biomechanical properties of the cornea are also largely due to the precisely ordered collagen fibrils and the orientation and architecture of the lamellae they form in the stroma (Meek and Boote, 2009). High concentrations of the water soluble proteins transketolase and aldehyde dehydrogenase type I within the keratocytes help minimize any light scattering that may occur due to their presence (Jester et al., 1999; Jester 2008).

The organization of collagen within the stroma plays a key role in the formation of a transparent and mechanically robust corneal stroma. However, the inherent complexity of the tissue's architecture has resulted in little progress being made in producing an effective construct that mimics corneal structure and function. Precise regulation of collagen fibril diameter, spacing and alignment would all be necessary in order to successfully engineer a construct that effectively resembles the stromal matrix and which has potential applications as a tissue substitute. At present this is difficult to achieve at the scale required for usable tissue construct size, although progress is being made (Griffith et al., 1999; Li et al., 2003; Orwin et al., 2003; Hu et al., 2005; Torbet et al., 2007).

Over the last decade, collagen gels have been investigated as scaffolds for use as potential stromal constructs (Germain et al., 1999; Schneider et al., 1999; Tegtmeier et al., 2001; Griffith et al., 2002). However, whilst highly biocompatible, these collagen gels often have reduced transparency and show mechanical instabilities. Gels that can effectively mimic the highly organized collagen architecture of the corneal stroma are essential to achieve proper optical and biomechanical function. Collagen gels have been developed as aligned sheets of collagen fibrils, in an attempt to recapitulate the structure of the corneal stroma. These aligned collagen gels have been engineered from monomeric collagen molecules by utilizing electron spinning (Zhong et al., 2006, Chew et al., 2007), strong magnetic fields (Guo et al., 2007; Torbet et al., 2007), dip pen nanolithography (Wilson et al., 2001), and flow manipulations (Koster et al., 2007; Lanfer et al., 2008). Recently, a mechanical improvement was achieved using electron spinning to produce a bilaminar, mesenchymal stem cell seeded collagen gel (Nerurkar et al., 2009). Whilst this construct fails to accurately reproduce stromal morphology or the cornea's optical and mechanical properties, it does highlight the importance of the relationship between tissue structure and function. Producing biomimetic multi-laminated collagen gels that accurately mirror stromal architecture may also result in improved mechanical properties, suitable for use as a tissue substitute in corneal grafting.

The addition of glycosaminoglycans and cross-linking agents has also been examined to determine their affect on the structural and functional properties of collagen constructs (Matsuda et al., 1990; Chen et al., 1995; Zhong et al., 2005), although fabricating and modulating a fibrillar arrangement using proteoglycan additions still remains a long way off. Comparatively, less research has been carried out on the structural and mechanical properties of type I collagen constructs formed at lower pH levels.

Type I collagen molecules, at high concentrations, will self assemble into a liquid crystalline array. By altering the environmental conditions under which this process takes place, it may be possible to produce a construct that is not only biocompatible, but can accurately reproduce the structural and functional characteristics of the corneal stroma. In this study I worked with a team of bioengineers in Tohoku University, Japan, producing gels from a telopeptide-free collagen molecule solution known as atelocollagen.

Although atelocollagen will naturally form a weakly cross-linked gel, for the purpose of constructing a mechanical stable stromal equivalent, covalent intermolecular cross-linking must be induced between collagen molecules. Glutaraldehyde, whilst one of the most effective cross-linkers of biological tissue (Lee et al., 2001), has an undesirable level of cytotoxicity. For the current study, 'zero-length' cross-linkers were used which, unlike glutaraldehyde and other bridge building cross-linkers, do not become incorporated into the cross-linking bonds. Instead, they induce covalent cross-linking to occur between collagen molecules directly, the cross-linking agent is then washed out of the tissue. To cross-link the gels, a mixture of ethyl (dimethylaminopropyl) carbodiimide (EDC) and N-hydroxysuccinimide (NHS) was applied. Using EDC in conjunction with an amine-rich compound such as NHS increases the efficiency by which EDC can induce cross-linking between collagen molecules. By manipulating the molecular assembly of highly concentrated atelocollagen solutions and optimizing the chemical environment, we were able to produce a transparent and mechanically stable cross-linked collagen gel using flow manipulation (Tanaka et al., 2011b). This study, carried out by the author in the laboratory of Professor Kohji Nishida (Tohoku University, Japan), reports the structural and functional characteristics of these constructs.

4.2. Methods

4.2.1. Collagen solution preparation

Acid freeze-dried type I porcine atelocollagen powder containing 5% type III collagen (Nippon Meat Packers) was dissolved at 4°C in distilled water using a syringe mixing technique (Liu et al., 2006a, 2006b; Rafat et al., 2008). Centrifugation overnight at 3500rpm was used to remove any air bubbles. The pH of the collagen solution was then adjusted by the addition, of a 1.0M NaOH (aq) solution, using the same syringe mixing method.

4.2.2. Cross-linking of collagen gels

To create the gels, the collagen solution was syringe mixed with a cross-linking solution of EDC/NHS (EDC:NHS = 2:1) until an homogeneous mixture was achieved. The final concentration of collagen was adjusted to 10 % wet weight.

4.2.3. Collagen fibril alignment within the gel

Within 3 minutes of mixing the cross-linking agent with the collagen solution, 0.5ml of the mixture was spread onto a glass slide in a 30mm oval configuration. An elastic film was then placed on top, and a roller was used to spread the mixture in a unilateral direction (Figure 4.2). Silicon rubber spacers placed between the glass slide and the elastic film regulated the thickness of the gel to 500 μ m. Incubation for 12 hours at 20 °C and for 12 hours at 37 °C was followed by phosphate buffered saline (PBS) washing at 4 °C.

4.2.4. Collagen laminate gel preparation

The atellocollagen solution was extruded in a line onto a tilted glass slide. This slide was placed on a hand-crafted stage attached to a swing type centrifugation machine (Figure 4.6). After centrifugation at 3500 rpm, the wet collagen layer was then incubated at 37 °C for 30 min and dehydrated at 4-8°C until a dry rigid film is produced. Incubation before drying created thicker microfibre-like structures within the gel and a smoother surface texture. The reduction in thickness achieved by this method improved the visible light transmission through the collagen constructs (Takezawa et al., 2004). Subsequent collagen layers were added by rotating the collagen coated slide by 90° or 180° (Figures 1D, E), before extruding a new line of the collagen solution on top of the dried layer and repeating the centrifugation, incubation and drying processes. The final thickness of the laminated gel was proportional to the number of collagen layers it contained. Gels containing up to 20 layers were constructed. The thickness of each layer was consistently 2–5 μ m (Figure 1F).

4.2.4.1 Optical clearing and cross-linking of collagen laminate gels

Once dry, the collagen laminate gels were cross-linked at room temperature for 2 hours using a 2:1 mixture of EDC (Wako pure chemicals, Osaka, Japan) and NHS (Thermo science, Rockford, IL, USA) solutions. Washing with distilled water was then followed by drying at 4°C. This process of low temperature drying, cross-linking, and washing in distilled water was then repeated until a desirable level of transparency was achieved.

4.2.5. Polarized Light Microscope imaging

Constructs were placed on a glass slide, then covered with a glass cover slip. These were then inserted between an LCD monitor and a polarized filter set in an orthogonal direction. The transmitted light was then recorded with a digital camera (Canon, Japan).

4.2.6. Mechanical testing

The mechanical characteristics of the collagen gels were tested in directions parallel to and at right angles to the direction of flow manipulation. The 500 μ m-thick gels were formed into dumb-bell shapes to prevent rupture at the point of attachment and to provide a larger area on which to attach the apparatus. A Universal Testing Instrument (EZ Test, SHIMADZU, Japan) was used at a rate of 100mm/min to measure a 10mm by 3mm region of the gels. The stress was measured as a function of strain, and by analyzing the linear (elastic) region of the resulting stress-strain curve the Young's modulus was calculated.

4.2.7. Transparency testing

500 μ m thick collagen gels, and samples of non cross-linked atelocollagen, were placed between two glass slides, separated by 500 μ m thick silicon rubber spacers and held together with Parafilm. At room temperature, the transparency of the gels was measured using UV/vis-spectroscopy (UV-2550/2450, SHIMAZU, Japan) for narrow spectral regions centred at 400, 450, 500, 550, 600, 650, and 700nm.

4.2.8. Transmission electron microscopy

All samples underwent routine processing as described in Chapter 2 'General Methods'.

4.3. Results

From Figure 4.1 it is clear that by increasing the amount of NaOH used in the formation of the collagen solutions had the effect of increasing the pH but reduced their transparency. However, the effect on transparency was not linear, with a marked decrease in transparency at NaOH levels above 40mM. Below 40mM of NaOH, transparency remained approximately

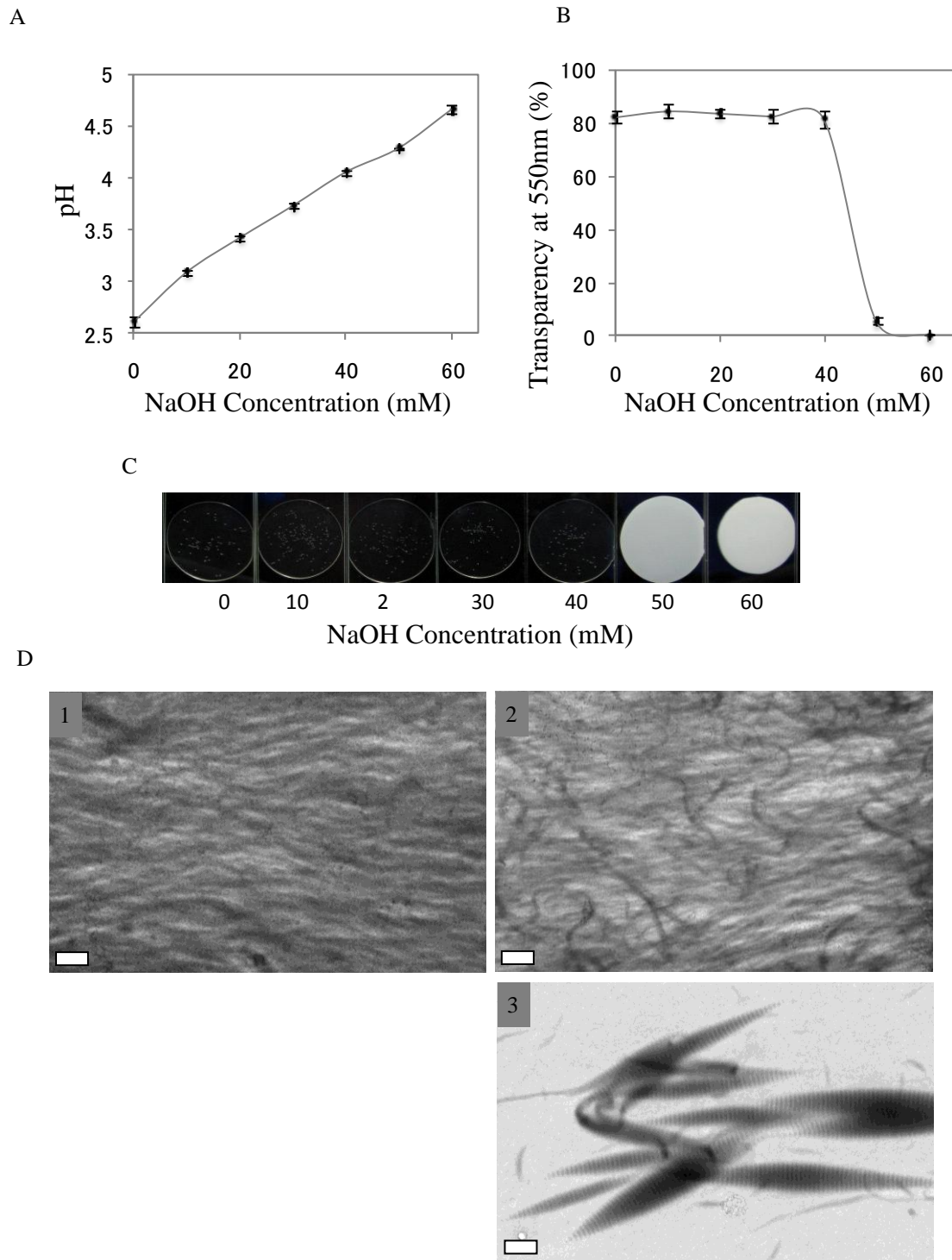


Figure 4.1: Deacidification of a 10% (w/w) collagen solution through the addition of NaOH.

(A) pH changes in the collagen solution upon NaOH addition. (B) Transparency changes in the collagen solution upon NaOH addition. (C) Photo images of collagen solutions at with different NaOH levels. (D) Transmission electron micrographs of collagen solutions using (1) 20mM, (2) 40mM, and (3) 60mM of NaOH. The thickness of specimens in (A), (B) and (C) is 500 μ m. Scale bar = 500nm.

constant at above 80% light transmission at 550nm. An increase in NaOH concentration from 40mM to 50mM was accompanied by an increase of pH from 4.05 to 4.29. However, the effect on transparency was a more profound, dropping from 82% to 6% light transmission (Figure 4.1B). At 60mM of NaOH (the highest used in these experiments) transparency measured less than 1%. Below 40mM of NaOH, the collagen solutions showed some aggregation or coalescing of the collagen. Only at 60mM of NaOH were any fibril like structures formed, demonstrating characteristic D-banding. These resembled large tactoid structures that have been previously reported in other studies (Bard and Chapman, 1968; Leibovich and Weiss, 1970), (Figure 4.1D).

4.3.1. Single layer gels

Gels were formed by adding cross-linking agents to the collagen solution and spreading the mixture over a flat plate. Polarized light microscopy revealed birefringence of the collagen gel constructs (Figure 4.2). Dark areas indicate collagen fibrils orientated in the same axes as the polarizer or analyzer ($\pm 45^\circ$ to the horizontal axis). Light areas denote collagen fibrils orientated horizontally (0°) or vertically (90°). Light and dark areas were observed in irregularly, non-uniform patterns in the thicker collagen gels, whilst the thinnest gels produced clear and regular birefringence patterns. Whilst the two non-rolled samples demonstrated more than one axis of symmetry with both dark and light regions, the thinnest unilaterally rolled gel (Figure 4.2) showed a light region over its entire surface.

The transparency of the gels reduced as NaOH levels were increased (Figure 4.3). This mirrors the results shown in Figure 4.1 for the collagen solutions. In addition it was found that increasing the levels of cross-linking also reduced the transparency of the gels. As a result, as NaOH levels were increased in the gels, the amount of cross-linking needed to be reduced accordingly in order to keep desirable levels of transparency (Figure 4.3).

Only those gels whose transparency was above 70% were tested for mechanical stability. As expected, increasing the cross-linking of the collagen gels improved their mechanical properties, enhancing their tensile strength and decreasing the strain at rupture (Figure 4.4). Concurrent with the transparency data presented in Figure 4.3, at higher NaOH levels less cross-linking was required to produce a mechanically stable gel. Similar stress levels at rupture were seen in gels made with 30mM NaOH and 0.5% EDC concentration, compared

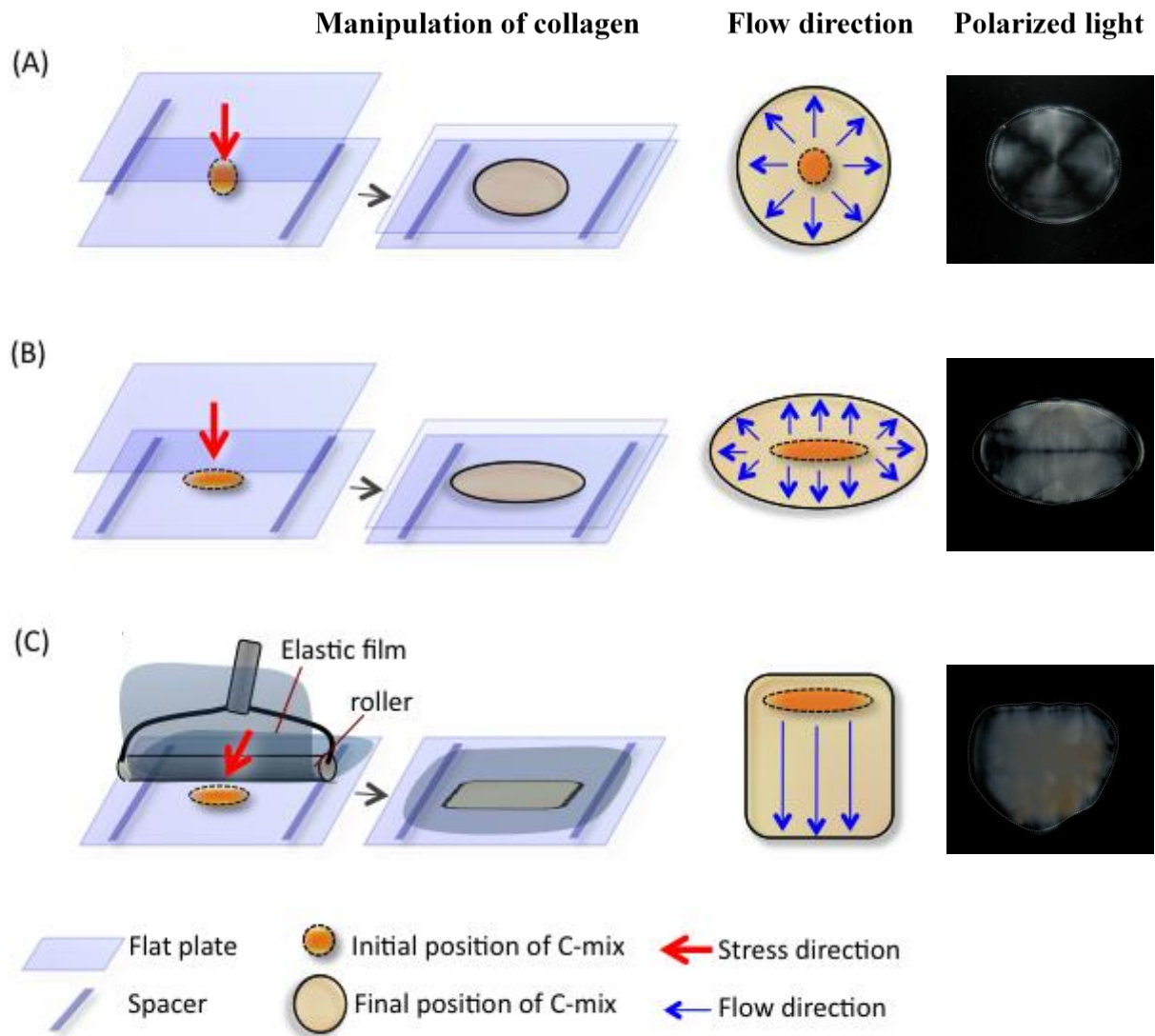


Figure 4.2: Flow-manipulation of collagen mixture to form aligned collagen gels.

(A) Collagen mixture was expanded radially from a droplet, resulting in a precise circular shape. (B) Collagen mixture was expanded radially from a rod shape, resulting in an ellipsoidal shape. (C) Collagen mixture was spread unidirectionally from a rod shape in an orthogonal direction.

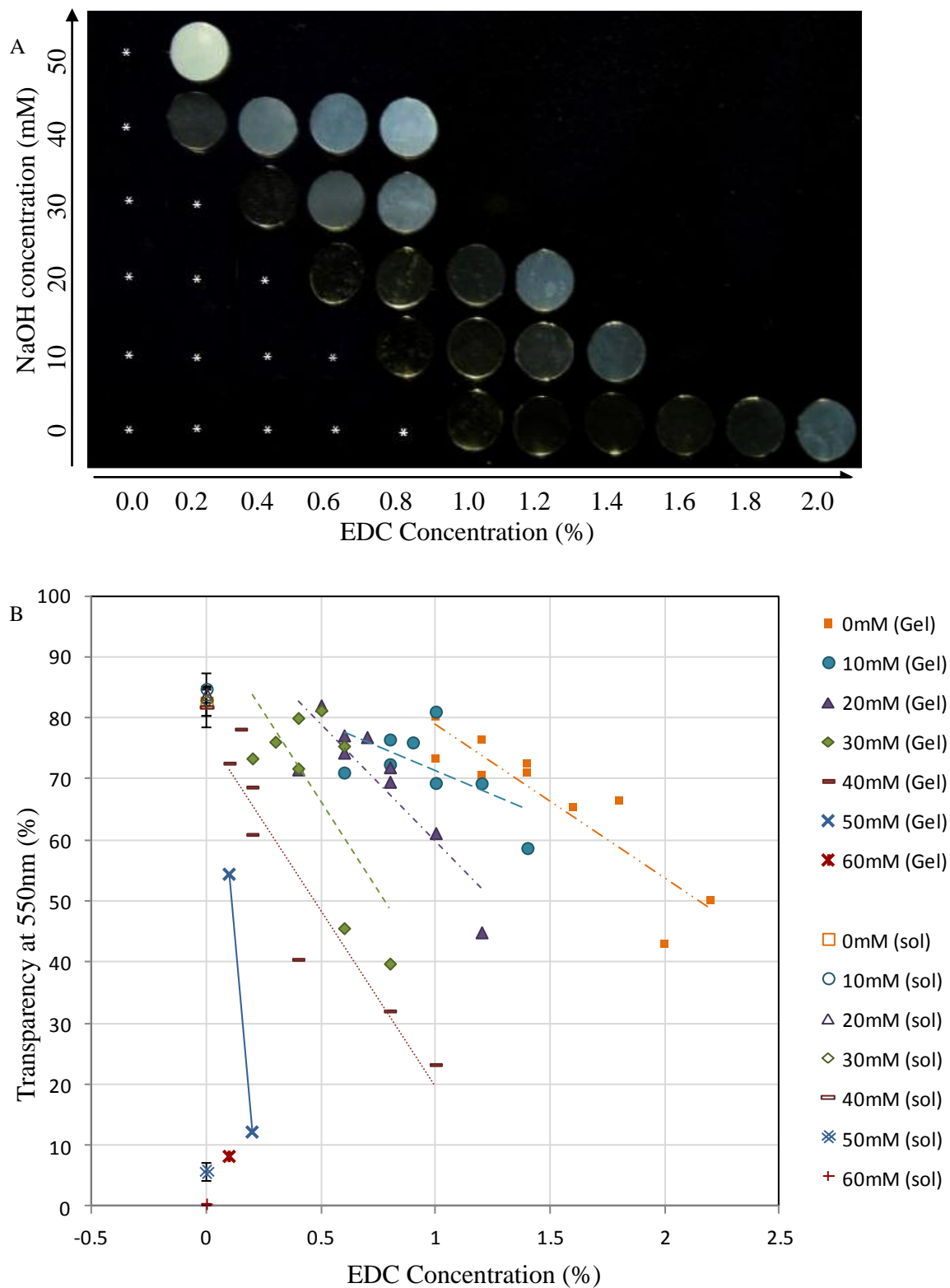


Figure 4.3: Cross-linked collagen gels transparency data.

(A) Photo image of collagen gels made using different NaOH and cross-linker levels. * denotes inadequate gel formation. (B) Transparency of collagen gels with lines of best fit, and uncrosslinked collagen solutions (sol). All samples are 500 μ m thick, with a final collagen concentration of 10% (w/w), and a 2:1 weight ratio of EDC and NHS cross-linking agents.

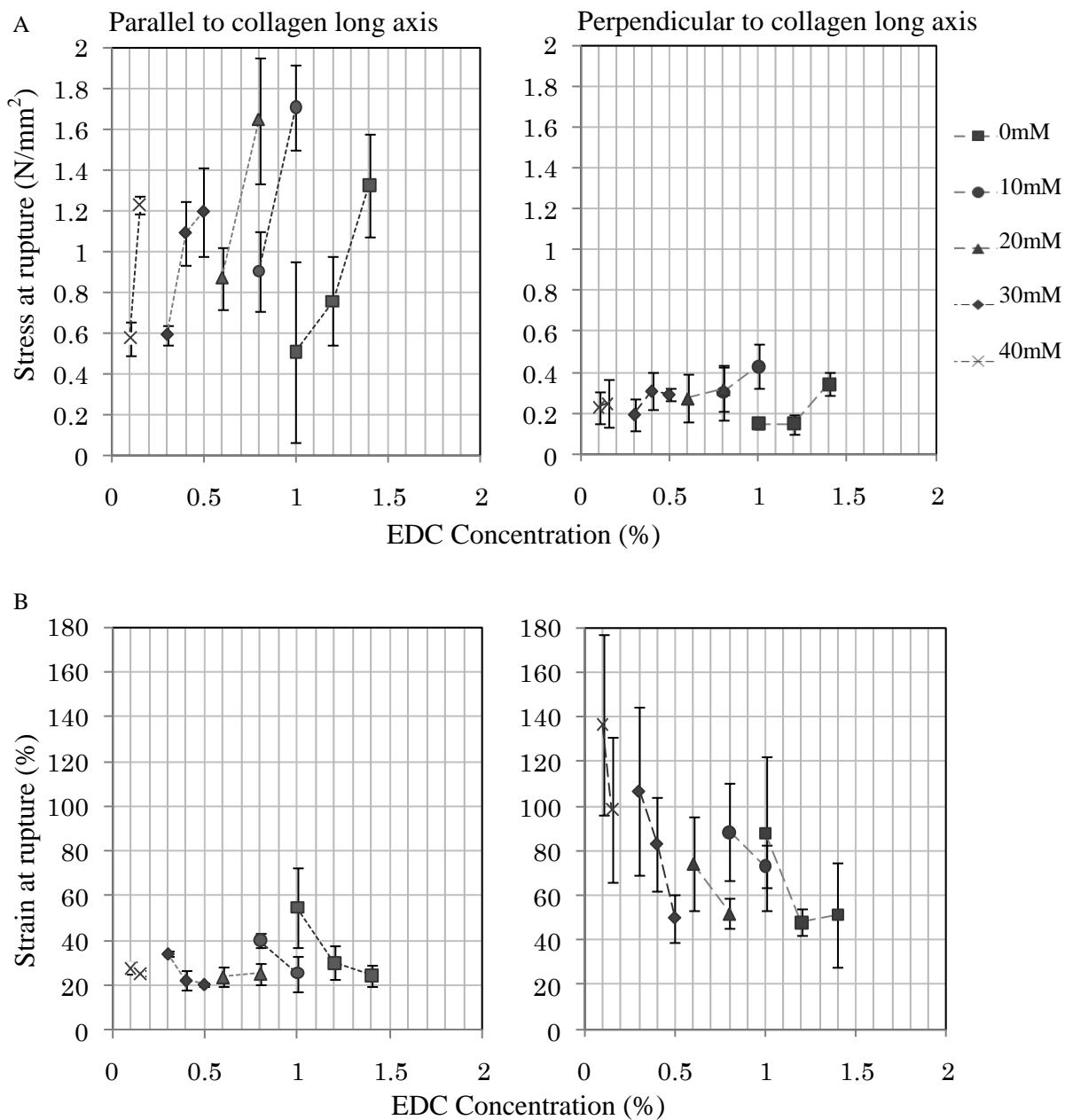


Figure 4.4: Mechanical properties of collagen gels.

(A) Stress (tensile strength) measured in a direction parallel to and perpendicular to collagen alignment.

(B) Strain (deformation) measured in a direction parallel to and perpendicular to collagen alignment.

Samples had transparency levels above 70%. All samples were 500 μ m thick, with a final collagen concentration of 10% (w/w), and a 2:1 weight ratio of EDC and NHS cross-linking agents.

to gels made with 40mM NaOH but with only 0.15% EDC. As NaOH levels were increased in the gels, the improvement in mechanical strength that accompanied cross-linker addition responded to smaller increases in cross-linker percentage. For example, in a 0mM NaOH gel, when the cross-linker concentration was increased by 0.2% (from 1.2% to 1.4%), the tensile strength of the gel almost doubled (from 0.75N/mm² to 1.32N/mm²). However, in a 40mM NaOH gel, a similar magnitude rise in tensile strength (from 0.57N/mm² to 1.22N/mm²) was achieved through just a 0.05% increase (from 0.1% to 0.15%) in cross-linker concentration (Figure 4.4). Mechanical testing also confirmed that uniaxial alignment of the collagen using flow manipulation affects the mechanical behaviour of the constructs. When tested in a direction parallel to the long axis of the collagen, the tensile strength of gels was approximately three fold higher than in the perpendicular direction. Strain levels were approximately doubled when tensile loading was applied in a direction perpendicular to the collagen long axis compared to the parallel direction. Increasing the amount of cross-linking or NaOH reduced the level of strain at rupture (Figure 4.4).

Transmission electron micrographs of the gels were taken at each different NaOH condition used: 0mM, 10mM, 20mM, 30mM, 40mM, 50mM and 60mM (Figure 4.5). This clearly shows that increasing NaOH levels were accompanied by a progressive condensation of the collagen into filamentous structures. With no NaOH added, the gels contained a loose matrix of collagen with no overall structure. Using 10mM of NaOH resulted in the formation of aggregates or bundles of collagen. These showed a degree of directionality due to the flow manipulation used in the gel manufacture, which manifests itself in the preferential strength of the gel along the long axis of the collagen. Repeated addition of 10mM NaOH resulted in increased levels of collagen aggregation (Figure 4.5). The gel made using 50mM of NaOH demonstrated more compact bundled structures than seen in the 30mM or 40mM NaOH gels. However, as with the uncross-linked collagen solutions (Figure 4.1D), only in the gels made with 60mM of NaOH were more mature fibrils present, with characteristic D-periodicity banding (Figure 4.5).

Chapter 4 - *In vitro* synthesis of collagen gel stromal equivalents

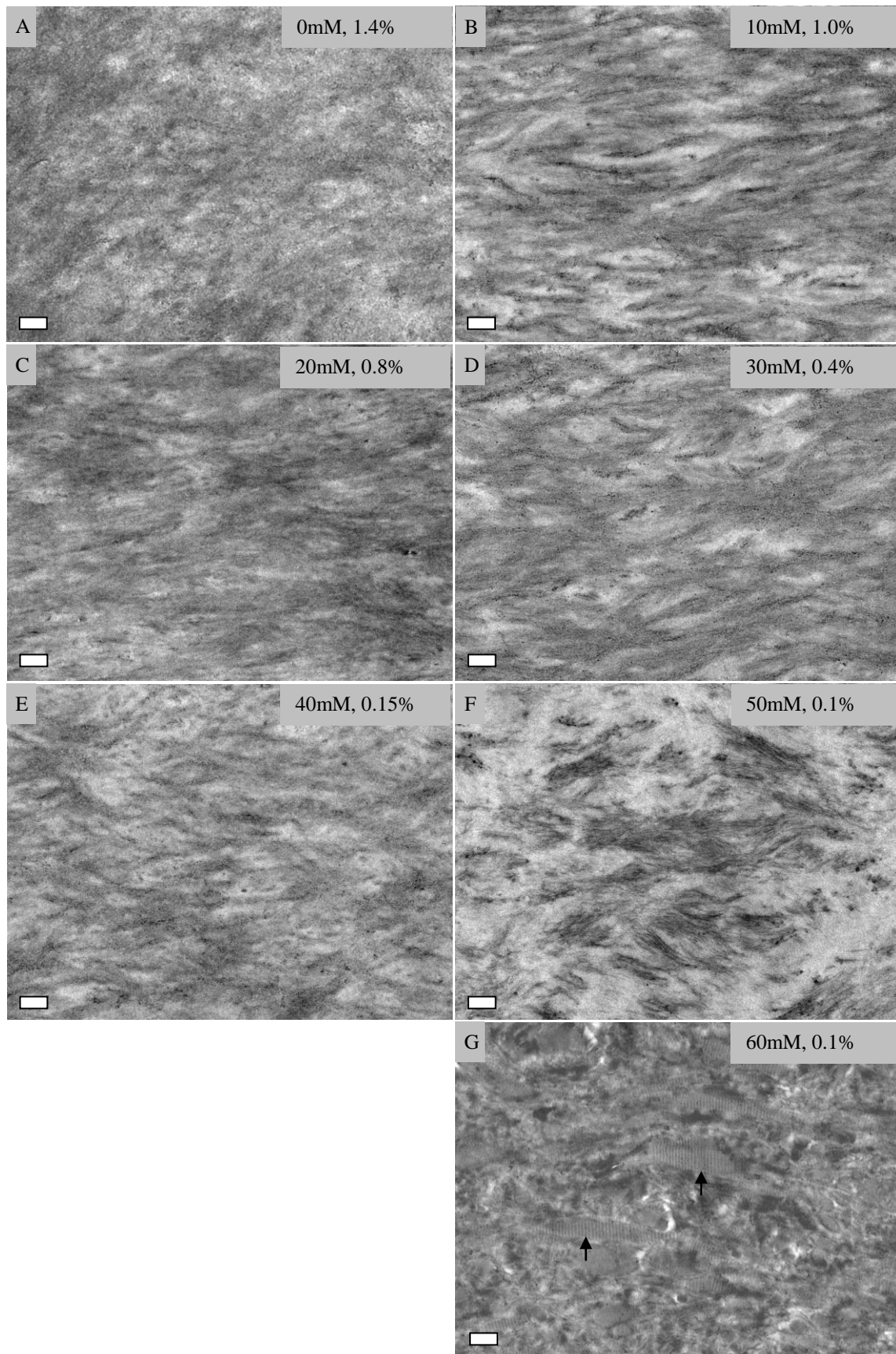


Figure 4.5: Transmission electron micrographs of collagen gels at x3500 magnification.

Gel conditions are shown as mM of NAOH, and % of cross-linker used. Black arrows in micrograph indicate tactoid structures. All samples were 500 μ m thick. Scale bar = 500nm.

4.3.2. *Laminated gels*

The laminated gels were cross-linked in order to inhibit the collagen layers from swelling during rehydration which would negatively affect light transmission, and to increase their mechanical stability by promoting chemical bonding between collagen molecules. However, a single cross-linking treatment resulted in only 55% transparency to visible light at 550nm.

Therefore repeat cycles of chemical cross-linking, washing and low temperature drying were performed (Figure 4.6). Repeated cycles of this process increased the transparency of the laminated gels to 75% (in the 8 layer gel) and 68% (in the 20 layer gel). Light transmission was independent of the orientation of the collagen layers. Laminated gels containing 20 collagen layers orientated in both parallel and orthogonal directions underwent six cycles of the cross linking, washing and drying process. Under transmission electron microscopy a clear difference in morphology can be seen between the orthogonal and parallel laminated gels (Figure 4.7). Furthermore, in the boundary zones of the orthogonally laminated gels some interlacing and fusion between adjacent orthogonal collagen layers was seen (Figure 4.7D).

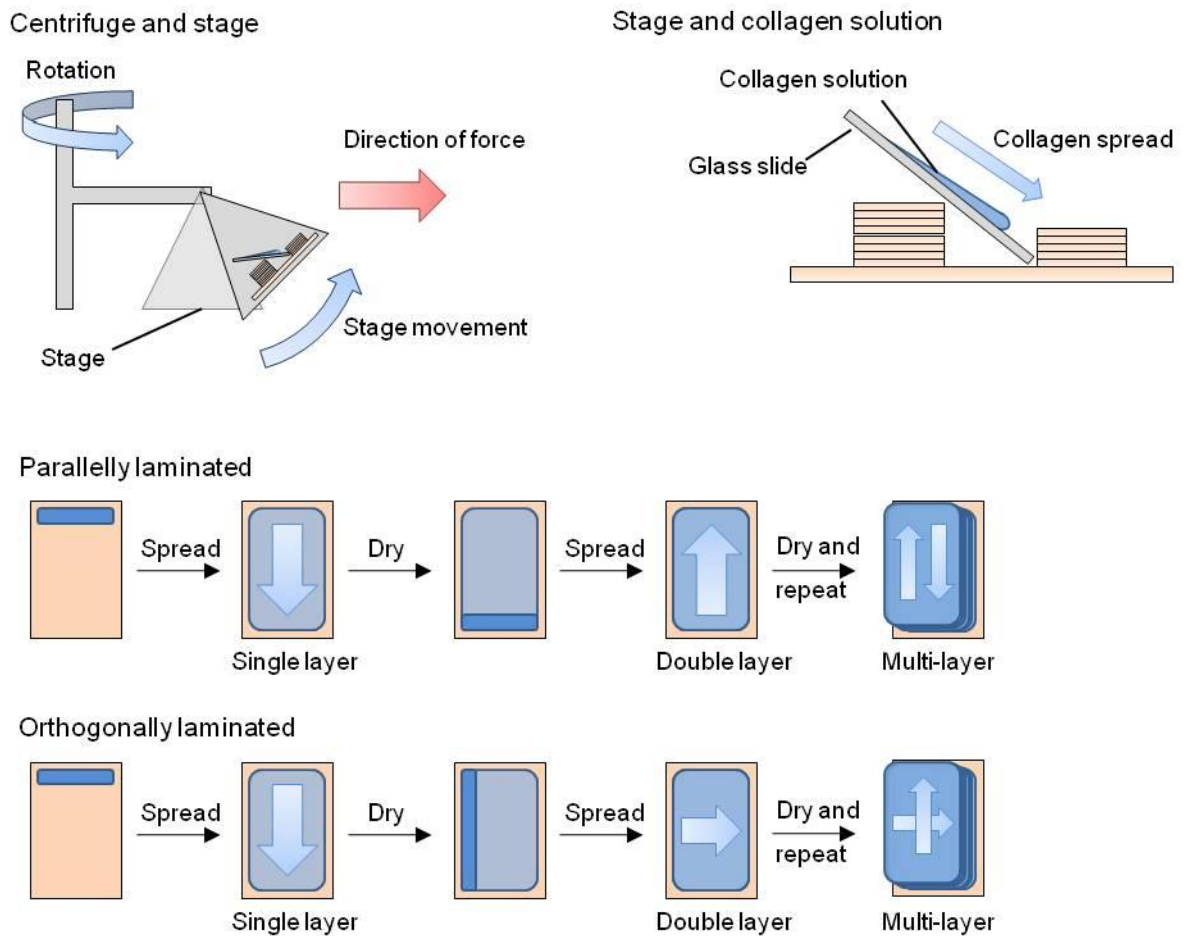


Figure 4.6: Formation of laminated gels by centrifugation.

(A) Centrifugal force causes the stage to tilt upwards, orientating the glass slide into a horizontal position. (B) The collagen solution spreads across the surface of the glass slide due to centrifugal force. (C) Parallel aligned laminated collagen sheets are made by repeating the process of collagen spreading and drying without changing the axis of collagen orientation. Orthogonally aligned laminated collagen sheets are made by repeating the process of collagen spreading and drying, whilst changing the axis of the collagen orientation by 90° for each new layer (Adapted from Tanaka et al., 2011a).

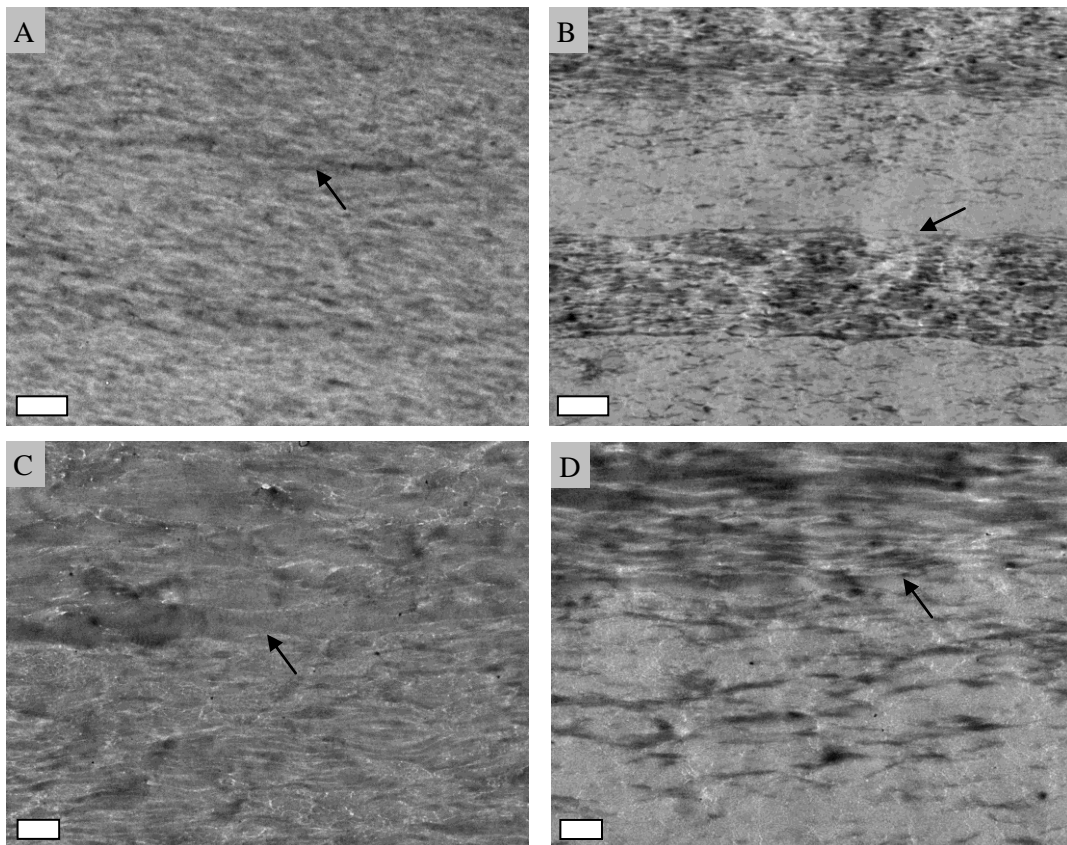


Figure 4.7: Transmission electron micrographs of multi layer collagen gels.

Parallel (A and C) and orthogonal (B and D) aligned gels at x4000 (A and B) and x1200 (C and D). Arrow indicates boundary zones between collagen layers. Scale bar = 500nm.

4.4. Discussion

4.4.1. Single layer gels

It is clear from these results that a suitable chemical environment is vital in order to fabricate a functional and implantable biomimetic collagen construct for use in corneal repair. It was necessary to find a balance between the level of fibrillogenesis within the gel, and the amount of cross-linker used. Light transmission and the mechanical strength of the gels were dependent on both these factors.

The transmission electron micrographs show that as NaOH levels, and therefore pH levels, within the gels are increased the diameter of the condensing collagen structures appear to decrease. Other studies that have focused on higher pH levels and later stages of fibril assembly have also recorded similar observations (Trelstad et al., 1976; Christiansen et al., 2000). From these micrographs it is also possible to identify a range of subfibrillar intermediates - from a matrix of largely disorganized collagen, through intermittent molecular aggregations, to the formation of progressively condensing filamentous structures. The intermediate aggregations seen in gels containing 30mM and 40mM of NaOH resembled the pathologically unravelling collagen fibrils that are found in necrotizing scleritis (Watson and Young, 2004). At 60mM of NaOH, the high pH levels resulted in the collagen condensing into tactoid-like structures (Bard and Chapman, 1968). Other studies have reported similar results, although no fully mature collagen fibrils were observed (Harris and Reiber, 2007). Only under much greater pH levels are mature collagen fibrils, possessing the characteristic D-banded periodicity, formed *in vitro* during fibrillogenesis (Gelman et al., 1979; Graham et al., 2000; Cisneros et al., 2006).

Transparency in the cornea is thought to be dependent on the major components of the matrix, namely the collagen fibrils, having diameters below that of the wavelength of visible light, and crucially a degree of short-range order (Farrell, 1994). In the gels with NaOH levels above 40mM, the matrix appears considerably more heterogeneous. The loss of ultrastructural uniformity might be responsible for the subsequent reduction in transparency above this level of NaOH. Loose collagen has associated into groups, forming filamentous structures with a higher degree of compaction. The assembly of larger macro-fibrillar structures would destructively scatter the light as it passes through the gel (Farrell, 1994). The

homogenous appearance of the gels below this level may result in a fairly uniform refractive index. With only small size aggregations of collagen, low levels of light scattering would occur, resulting in good transparency.

The biomechanical properties of the cornea are largely dependent on collagen architecture and organization, and the ability to exploit the natural tensile properties of fibrillar collagen. Aligning the collagen within these gels provides greater mechanical strength along the long axis of the fibril. In addition, cross-linking the collagen gels, as expected, enhanced their mechanical strength. Both tensile strength in the direction parallel to collagen alignment, and the elastic properties of the gels in the perpendicular direction showed improvement. The mechanical properties of the single layer gels, when measured in the parallel direction, approached those recorded in human corneal tissue: $3.81 \pm 0.40 \text{ N/mm}^2$ in tensile strength (Zeng et al., 2001) and $3\text{-}13 \text{ N/mm}^2$ in Young's modulus (Crabb et al., 2006).

Gels formed under increasingly greater pH levels demonstrated higher stress and strain readings at rupture in both the parallel and perpendicular directions to the collagen long axis of the initial layer. Other studies involving collagen gels have also reported the stress-strain relationship as being a function of pH (Christiansen et al., 2000; Roeder et al., 2002). In these studies, the length, diameter and organization of the forming collagen fibrils had a significant impact on the mechanical properties of the gels. Raising pH levels were found to increase fibril length and decrease fibril diameter, consequently improving the mechanical properties of the collagen matrices (Roeder et al., 2002). Increased levels of small diameter collagen fibrils in tendon were believed to have a protective role against the plastic deformation of the tissue structure (Parry, 1988). In addition, the viscoelastic properties of a collagenous matrix are considered to be more dependent on fibril length rather than diameter (Parry, 1988; Roeder et al., 2002). In particular the longitudinal fusion of fibril subunits increases the resistance to high strain level deformation. Conversely, resistance to low strain level deformation was thought to be specific to the lateral fusion of fibril subunits (Christiansen et al., 2000).

4.4.1. Laminated gels

During construction of the laminated gels, it was found that centrifugation at lower speeds was not sufficient to spread the collagen across the length of the glass slide. However,

increasing the incline of the glass slide improved the collagen spread (Tanaka et al., 2011a). The addition of successive collagen layers (in both the parallel and orthogonal orientations) increased total gel thickness as expected (Tanaka et al., 2011a).

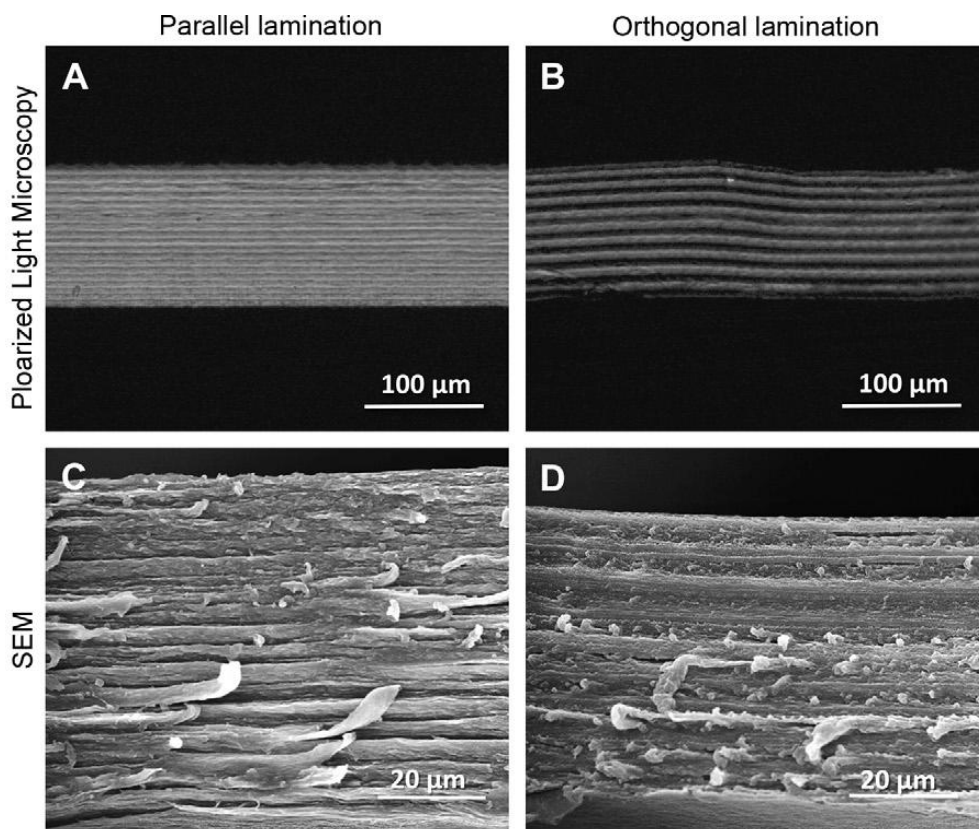


Figure 4.8: Cross sections through parallel and orthogonal laminated gels.

Parallel aligned collagen layers seen by polarized light (A) and scanning electron microscopy (C). Orthogonally aligned collagen layers seen by polarized light (B) and scanning electron microscopy (D). (A) and (C) cross sections obtained by cryosection, (B) and (D) cross sections obtained by microtome (Adapted from Tanaka et al., 2011a).

Under polarized microscopy the parallel aligned laminated gels showed uniformly thin bright stripes representing each of the individual collagen layers that run longitudinally through the gel (Figure 4.8A). These results were then published in Tanaka et al., 2011a. The orthogonally aligned laminated gels showed alternating dark and light stripes, with the dark stripes representing those collagen layers running in an orthogonal orientation. Under scanning electron microscopy, the parallel orientated gels demonstrated smooth, fibrous structures running in a uniform direction. The orthogonally orientated gels showed both long

fibrous structures, and rounded dot like structures that represent the orthogonally orientated collagen.

Transparency testing of these laminated gels shows them to have near human corneal transparency. In addition, they possessed greater transparency than either human donor corneal tissue or amniotic membrane which is commonly used for grafting during ocular surface repair (Liu et al., 2006a, 2006b; Connon et al., 2009).

In collaboration with Dr Yuji Tanaka, the tensile strength of these laminated gels was also tested, to determine the effect fibril architecture has on their biomechanical properties. The results were then published in Tanaka et al., 2011a. Laminate gels containing 8 layers of either parallel or orthogonally aligned collagen were measured along both axes, in the plane of the collagen layers (Figure 4.9). The stress-strain curve of the orthogonally aligned gels demonstrated similar result in both axes, with a maximum strength of 5.98 N/mm² in the parallel axis, and 5.35 N/mm² in the perpendicular axis. The elastic property of the gels was 47.8 N/mm² in the parallel axis and 50.7 N/mm² in the perpendicular axis. Conversely, the parallel aligned gels showed greater stress-strain levels at rupture when tested in the axis parallel to collagen orientation than in the perpendicular axis. They demonstrated a maximum strength of 9.38 N/mm² in the parallel axis, and only 2.86 N/mm² in the perpendicular axis. The elastic property of the parallel aligned gels was 74.8 N/mm² in the parallel axis, and only 24.1 N/mm² in the perpendicular axis. The parallel axis readings were considerable larger than the perpendicular axis readings for these parallel aligned gels. In addition, the orthogonally aligned gels demonstrated readings that were approximately three fold greater than the readings for the parallel aligned gels in the perpendicular axis.

The mechanical stability of the laminated gels allowed them to be handled and manipulated with tweezers, without incurring visible damage. They possessed mechanical properties greater than that of the original single layer gels, and greater than that of other collagen scaffolds (Cheema et al., 2007), cross-linked gels (Liu et al., 2009), or laminated constructs (Nerurkar et al., 2009) currently under development. In addition, their mechanical strength and elastic modulus exceeds that of human corneal tissue: 3.81 ± 0.40 N/mm² in tensile strength (Zeng et al., 2001) and 3-13 N/mm² in Young's modulus (Crabb et al., 2006). This increased stability may be due in part to interlacing between adjacent orthogonally aligned collagen layers that was observed under transmission electron microscopy.

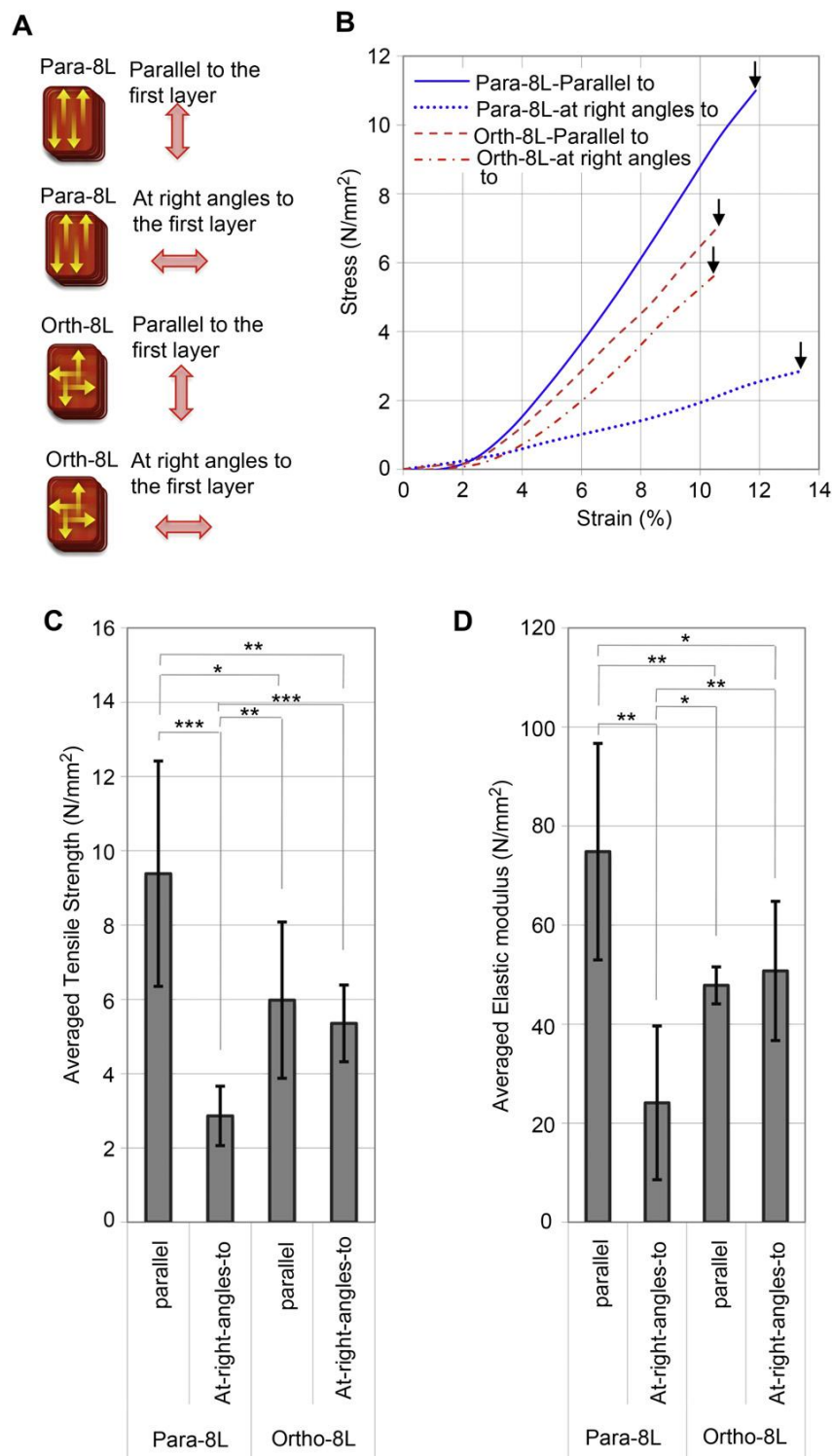


Figure 4.9: Mechanical properties of laminated gels.

(A) Direction of applied tensile load to both parallel and orthogonally aligned 8 layer lamellae gels. Yellow arrow show collagen flow direction, red arrows indicate direction of applied force. (B) Stress-strain curve, with arrows indicating the point of rupture. Average readings for tensile strength (C) and elastic modulus (D) of both gels testing both at parallel and at right angles to the flow axis (means \pm SD, $n = 7$, * $P < 0.05$, ** $P < 0.01$, and *** $P < 0.001$) (Taken from Tanaka et al., 2011a).

4.5. Conclusions

Type I collagen is ubiquitous and possesses excellent properties for use in tissue engineering. This study primarily focused on the ability of collagen fibril organization and structure to be manipulated *in vitro* by altering conditions, such as pH, during its formation. Whilst *in vitro* analysis can highlight the fundamental processes that govern fibrillogenesis, we must be careful to observe the limitations of any comparisons made to *in vivo* collagen assembly. The complex arrangement of other stromal cells and extracellular matrix macromolecules creates a unique three-dimensional environment that interacts with and influences the forming collagen fibrils. This represents a significant spatial system that cannot currently be replicated *in vitro*. Consequently, whilst our engineering method produces biocompatible stromal implants with desirable mechanical and optical properties, producing a stromal equivalent that effectively mirrors the structural architecture of the host stroma remains a challenge.

Nevertheless, it is clear that the assembly of type I collagen filaments within these gels, can be manipulated over a wide pH range. In addition, even minor changes in the environmental conditions of the gels (such as pH), dramatically affects the optical and mechanical properties of the constructs. The variety of subfibrillar intermediates that are produced are similar to those seen in previous collagen self assembly studies (Harris and Reiber, 2007; Merrett et al., 2009).

In summary, these simple optically transparent cross-linked collagen gels provide a basis for the future production of more complex biomimetic stromal constructs. They have potential clinical use as cell or drug carriers, as protective membranes for corneal surface damage, and stromal implantation for tissue replacement and regeneration. This study has also developed a unique and mass production-friendly processes for obtaining more complex laminated collagen gels with improved optical and mechanical properties. This novel method of repeated cycles of cross-linking, washing and low temperature drying, significantly improved light transmission through the gels. Additionally, the manipulation of collagen orientation, and lamina architecture enhanced the mechanical strength of the gels. These gels have potential use in the field of tissue engineering and regenerative medicine, including the production of stromal equivalent constructs for use in corneal grafting.

5. *IN VIVO* CHARACTERISTICS OF COLLAGEN GEL STROMAL EQUIVALENTS

5.1. Introduction

Opacification of the cornea caused from injury or disease is second only to cataracts as the leading causes of blindness worldwide. As such damage is usually irreversible, current treatment involves keratoplasty and the use of allografted corneal tissue. However, lack of donor tissue and the high rate of transplant rejection, limit the application of this treatment. Alternative approaches to these issues have involved using synthetic implants. These keratoprosthesis are designed principally to restore a functional level of vision rather than facilitate corneal regeneration. There is currently no one accepted keratoprosthesis that can effectively act as a corneal substitute. The two most successful implants are the AlphaCor, and the Boston KPro. The Boston KPro is a collar button design constructed from medical grade polymethylmethacrylate (PMMA). It features a front plate that contains the donor corneal tissue, and a back plate perforated with holes that serve to increase its permeability to the flow of oxygen and nutrients to the anterior chamber and the cellular component of the cornea (Sweeney et al., 1998). The AlphaCor is constructed from a porous and opaque outer skirt that provides anchorage to the host tissue, and a transparent central gel region, both of which are made from a polymer network of poly-2-hydroxyethyl methacrylate (pHEMA). However, these keratoprotheses also suffer from high rejection rates, with neovascularisation, stromal melt, and the formation of retroprosthetic membranes commonplace, reflective of their low level of biocompatibility.

As an alternative to the use of synthetic polymers, biodegradable scaffolds have been used to promote tissue regeneration. Extracellular matrix macromolecules are known to play a role in directing cell growth and differentiation during development. This function can then be exploited to promote tissue repair and regeneration. As type I collagen is the primary constituent of the corneal stroma, representing 70% of the extracellular matrix dry weight, it has been widely used in engineering scaffolds for tissue repair and regeneration (Germain et al., 1999; Chen et al., 2001; Shimmura et al., 2003). Easily isolated and purified, collagen is available in a range of subtypes that possess low toxicity and good cell and tissue biocompatibility (Stegman et al., 1987; Kilgman, 1988; Wallace et al., 1988).

Early experiments in the 1960's first established the potential of collagen gels for implantation. Gels were produced by neutralizing acidic collagen solutions, and injected into animal tissue *in vivo* (Grillo and Gross, 1962). Of particular significance was the observation that injecting the collagen gels into living tissue elicited no immune response. This then led the way for collagen gels to be used in the *in vitro* culturing of cells (Elsdale and Bard, 1972). In 1985, Stopack et al demonstrated that collagen gels placed with the limb bud of a developing chick will be remodelled by the host cells to form natural tissue structures such as tendon. This remodelling effect has since proved to be a popular method of producing biomimetic constructs by combining the collagen gels with cell populations. Collagen gels have been preloaded with stromal cells (Hu et al., 2005), used to support the migration of host stromal cells, and used as acellular supports to facilitate the natural repair and regeneration of corneal tissue (Li et al., 2003; Liu et al., 2006a, 2006b).

Cross-linked collagen gel scaffolds have been used in the construction of full thickness, functioning corneal equivalents (Minami et al., 1993; Griffith et al., 1999; Germain et al., 1999). However, mechanical instabilities and complications at the graft/host interface still remain. More recently, a full thickness corneal equivalent was constructed from a cross-linked collagen sponge. This scaffold was able to co-culture both epithelial and stromal cells when seeded with primary and progenitor cell populations (Vrana et al., 2008).

Combining collagen gels with cross-linking agents such as 1-ethyl-3-(3-dimethylaminopropyl) carbodiimide hydrochloride (EDC) and N-hydroxysuccinimide (NHS), has produced stable biomimetic constructs that demonstrate successful implantation and graft-host integration. Recently type III collagen, similar in structure to type I, have also been used to produce collagen gels for corneal implantation. These type III gels showed good integration and optical transparency 1 year post-implantation, with migration of host stromal cells and nerve fibres into the construct (Merrett et al., 2008; Liu et al., 2008). In this study, the chemical composition of cross-linked type I collagen gels was altered during their production, to determine if varying the amounts of cross-linker and NaOH used, would have an effect on the morphology and long term survival of the constructs *in vivo*.

5.2. Methods

5.2.1. Collagen solution preparation

Acid freeze-dried type I porcine atelocollagen powder containing 5% type III collagen (Nippon Meat Packers) was dissolved at 4°C in an HCl aqueous solution (pH 3.0) using a syringe mixing technique (Liu et al., 2006a, 2006b; Rafat et al., 2008). Centrifugation overnight at 3500rpm was used to remove any air bubbles that were present. The pH of the collagen solution was then tuned to 3.5 by the addition, in an ice-water bath, of a NaOH 1.0M aqueous solution using the same syringe mixing method.

5.2.2. Cross-linking of collagen gels

To create the gels, the collagen solution was syringe mixed with a cross-linking solution of EDC /NHS (EDC:NHS = 2:1) until an homogeneous mixture was achieved. The final collagen concentration was adjusted to 10% wet weight.

5.2.3. Collagen fibril alignment within the gel

Within 3 minutes of mixing the cross-linking agent with the collagen solution, 0.5 ml of the mixture was spread onto a glass slide in a 30mm oval configuration. An elastic film was then placed on top, and a roller was used to spread the mixture in a unilateral direction. Silicon rubber spacers placed between the glass slide and the elastic film regulated the thickness of the gel to 500µm. Incubation for 12 hours at 20 °C and for 12 hours at 37 °C was followed by phosphate buffered saline (PBS) washing at 4 °C.

5.2.4. In vivo implantation

Three circular collagen gels with unilateral collagen orientation, 8mm in diameter and approximately 135µm thick were implanted into mid-depth stromal pockets of six male New Zealand White rabbits (2.0 to 3.5kg; Kitayama Labs Co., Nagano, Japan). This procedure was carried out by my colleague and ophthalmic surgeon, Dr Dong Shi at Tohoku Univeristy Hospital, Japan. To achieve this, the rabbits were anesthetized intramuscularly with a mixture of ketamine hydrochloride (60mg/kg; Sankyo, Tokyo, Japan) and xylazine (10mg/kg; Bayer,

Munich, Germany). A 6mm-long circumferential incision was then made at the limbus and a stromal pocket created throughout the cornea at mid-stromal depth after which a rolled up gel was inserted and unfolded *in situ*. The following gels were implanted: 30mM of NaOH with 0.8% EDC concentration, 30mM of NaOH with 0.4% EDC concentration, and 10mM of NaOH with 0.8% EDC. Post-operatively, antibiotic medication (Tarivid and Levofloxacin ophthalmic ointment) was administered daily. All experimental procedures conformed to the ARVO (Association for Research in Vision and Ophthalmology) Statement for the Use of Animals in Ophthalmic and Vision Research and to local ethical rules.

5.2.5. Corneal thickness measurements

An ultrasonic pachymeter was used to measure corneal thickness *in vivo* at regular intervals during the post-implantation period. The ultrasonic transducer was pressed onto the corneal surface, and five measurements were used to give an average corneal thickness reading.

5.2.6. Histology

After fixation in 4% paraformaldehyde for 24 hours, the samples underwent dehydration in a series of graded alcohols: 70%, 95%, 100%, and 100% for 2 hours each. This was followed by clearance in histoclear for 2 hours. Three cycles of paraffin wax infiltration were then carried out at 60°C for 2 hours each. Following this, the samples were dried and embedded into the holding block.

The block was trimmed, and sections were cut at 8µm thick through the central portion of the cornea, using an LKB bromma 2218 historange microtome. All sections were mounted on individual slides. Slides were then placed into a slide holder, deparaffinised by two repeats of 5 minutes in Xylene, and rehydrated by 5 minutes in a series of graded alcohols (100%, 90%, 70%, 50%).

The slides were then stained in haematoxylin for 15minutes, followed by rinsing in (mildly alkaline) tap water. Then, counterstaining in eosin for 5 minutes was followed by a few seconds in 70% ethanol to remove any excess stain. Following this, dehydration through a series of graded alcohols for 5 minutes each (50%, 70%, 90%, 100%,) was carried out. Finally the slides went into two repeats of Xylene for 5 minutes, before being mounted with

DPX mounting fluid and cover slips. Images were taken on a BZ-9000 Series All-in-One Fluorescent Microscope (Keyence, Japan, Osaka).

5.2.7. Transmission electron microscopy

All samples underwent routine processing as described in Chapter 2 ‘General Methods’.

5.3. Results

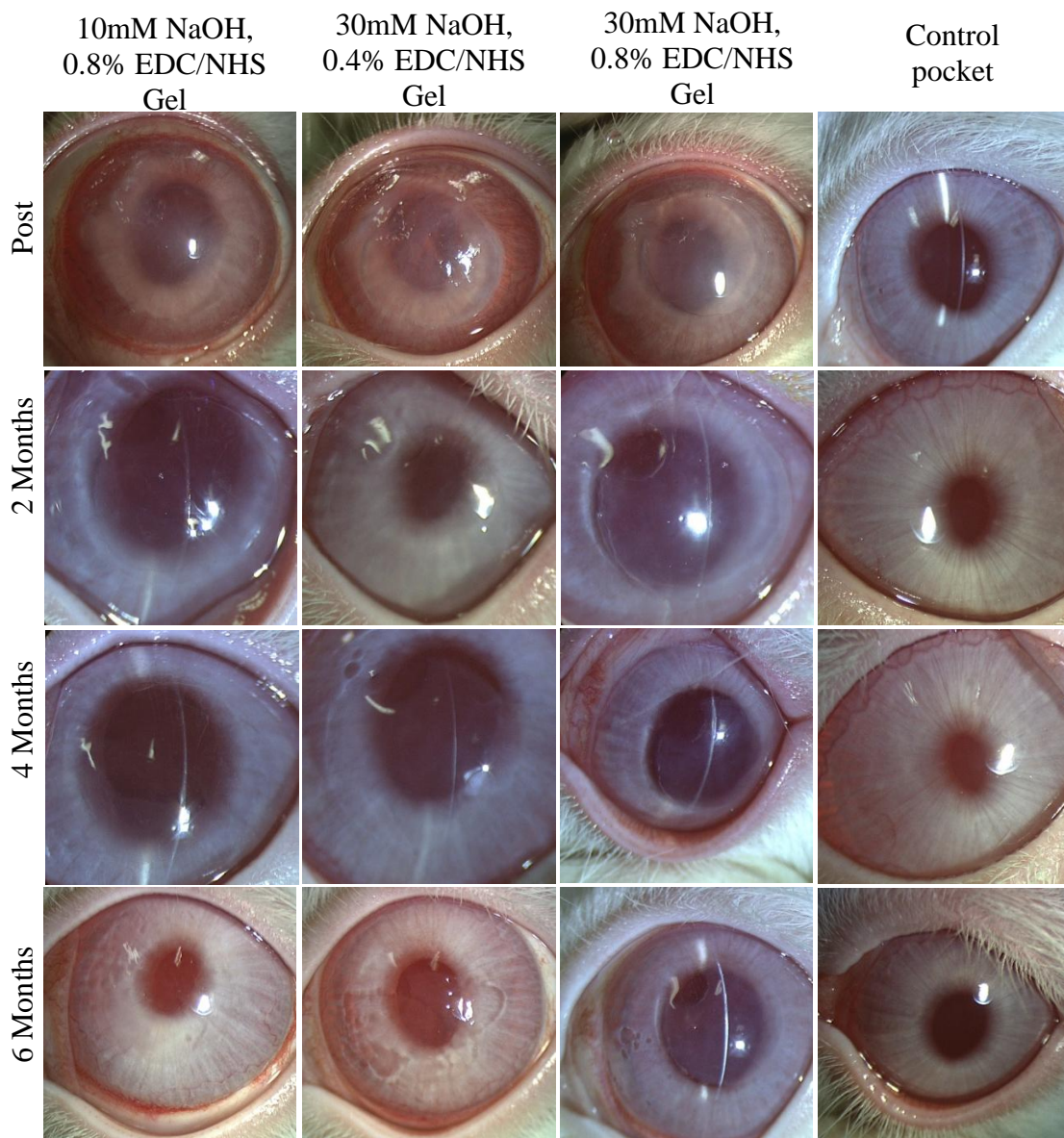


Figure 5.1: Six month implantation of collagen gels into rabbit intra-stromal pockets.

The implanted collagen gels were 8mm in diameter and 100-200µm in thickness.

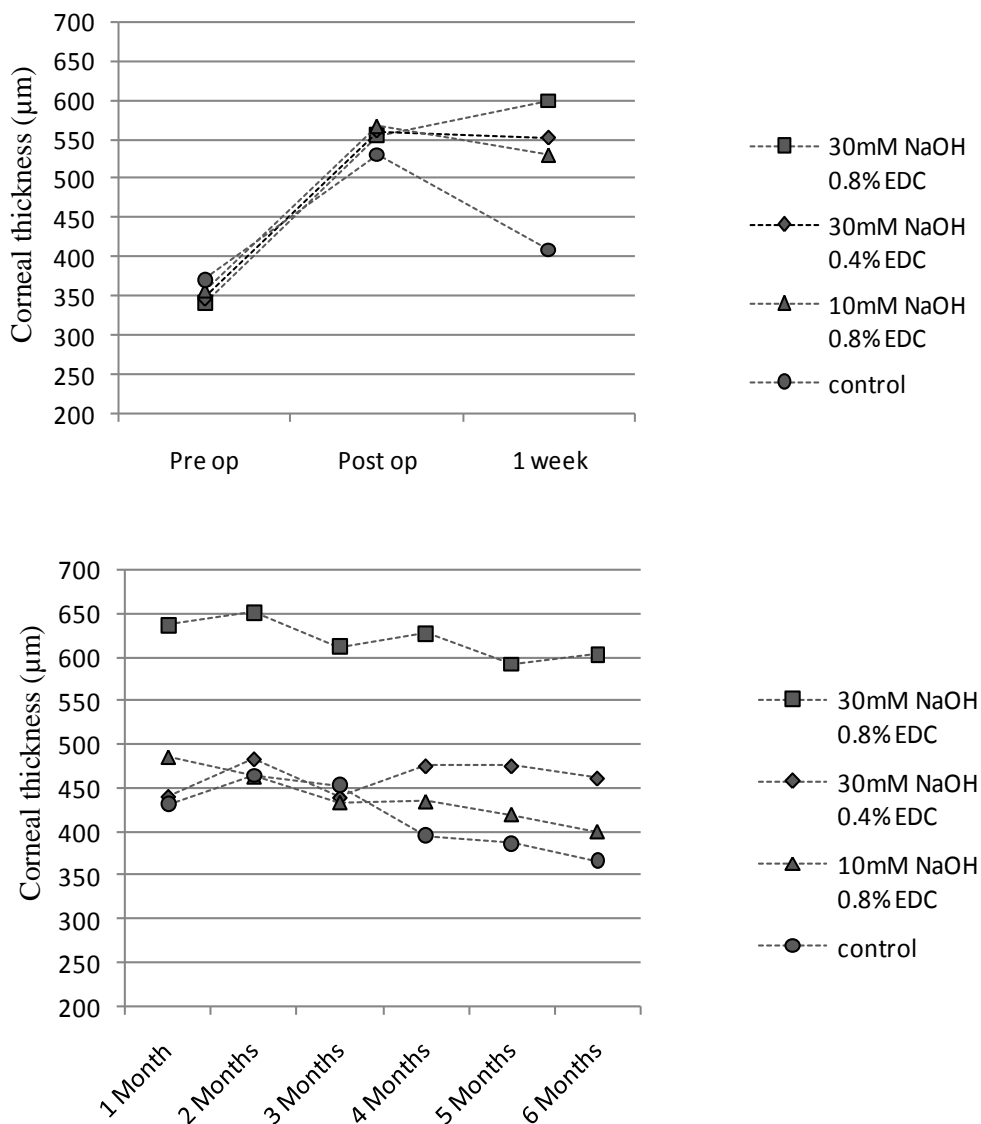


Figure 5.2: Rabbit corneal thickness measurements following implantation of collagen gels.

For each time point, an average reading was taken from three thickness measurements using an ultrasonic pachymetry.

No evidence of long term inflammation or rejection could be seen in the implanted corneas (Figure 5.1). All collagen gel types were well tolerated when implanted into mid-depth rabbit corneal intra-stromal pockets. Slit-lamp investigation detected no aberrations within the epithelium or endothelium during the period of gel implantation. No neovascularisation or immune reaction was observed in any of the eyes studied. The host stroma superficial and deep to the implant maintained a normal morphology in all but one case. In Figure 5.3F, some oedema can be seen in the anterior region of the stroma above the implant, indicated by

the region of paler staining and more loosely packed matrix. Good biocompatibility and transparency was seen in all three gel types, even up to 6 months post-implantation (Figure 5.1). The transparency of the gels was dependant on the amount of cross-linker and NaOH used during production. The 10mM/0.8% gel demonstrated the best optical properties, whilst under a slit lamp observation the 30mM/0.8% gel was visible due to its lower transparency to light (Figure 5.1).

The thickness of the operated corneas was measured in the immediate post-operative period by ultrasonic pachymetry (Figure 5.2). There was a significant increase in corneal thickness due to the addition of the gel into the stroma and because of the intrusive nature of the surgical procedure itself producing some temporary inflammation. The sham-operated cornea had a pocket made, but no gel inserted. This cornea measured approximately 150µm thicker after surgery indicative of post-operative inflammation and general trauma. However, one week after surgery, the control cornea had returned to pre-operative thickness, while the corneas containing collagen gels all remained significantly thicker than at pre-implantation (Figure 5.2). Following this, over the 6 month period of implantation, a gradual reduction in corneal thickness can be observed in the 30mM/0.4% gel and 10mM/0.8% gel implanted corneas. Conversely, the cornea containing the 30mM/0.8% gel remained at approximately the same thickness as immediately post-implantation over the duration of the 6 month implantation period.

The reduction in gel thickness was confirmed by histological analysis (Figure 5.3). Both the 30mM/0.8% and 30mM/0.4% gels remained prominent in the intra-stromal pockets, even 6 months after implantation. The 10mM NaOH gel, even at 1 month after implantation, had reduced in thickness. By 6 months post-implantation the gel was barely visible, with only a small trace remaining indicating the location where the intra-stromal pocket was made. In addition, Figure 5.3, images B and C show several host cells that appeared to have migrated to within the collagen gel.

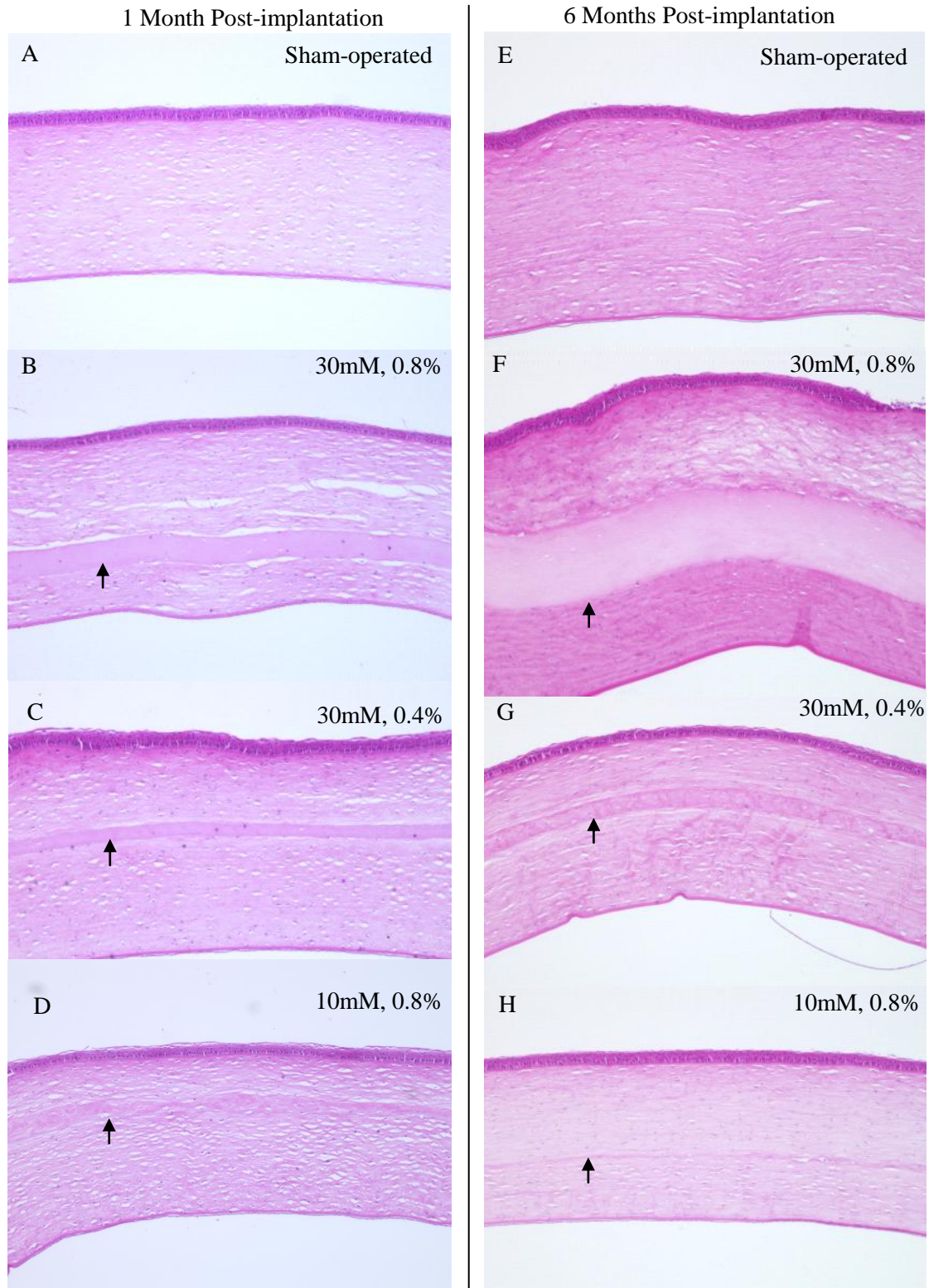


Figure 5.3: Rabbit corneal cross sections 1 and 6 months post-implantation of collagen gels into intra-stromal pockets.

Corneas were stained with haematoxylin and eosin. Gel conditions are shown as mM of NaOH, and % of cross-linker used. Black arrows indicate the posterior surface of the implant.

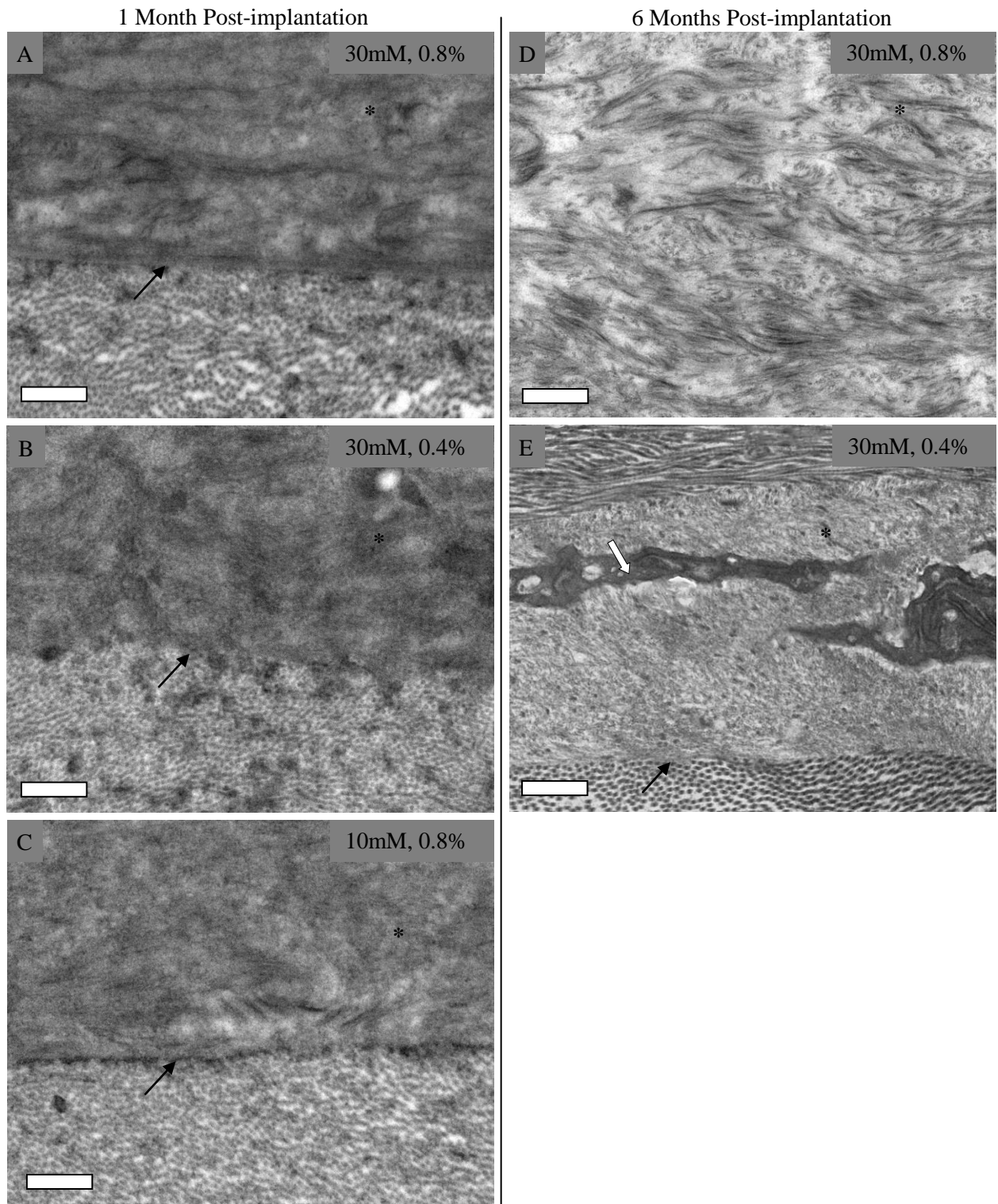


Figure 5.4: Transmission electron micrographs of rabbit corneal stroma 1 and 6 months post-implantation of collagen gels into intra-stromal pockets.

Gel conditions are shown as mM of NaOH, and % of cross-linker used. * indicate collagen gel implant, Black arrow indicates boundary between host stroma and gel implant. White arrow indicates invading host stromal cell. 10mM NaOH, 0.8% EDC/NHS gel was no longer present in the stroma at 6 months post-implantation. Micrographs are at x 6000 magnification. Scale bar = 500nm.

The implanted gels were analyzed *in situ* by electron microscopy. Host stromal cells could clearly be seen having migrated into the collagen gel. This migration was often accompanied by the remodelling or digestion of the gels (Figures 5.4). Migration of stromal cells was more prevalent in the 10mM/0.8%, and 30mM/0.4% gels. Despite cross-linking the gels during their production, their morphological appearance was still able to change after long term implantation in the host stroma. The 30mM/0.8% gel showed a greater level of collagen fibrillogenesis at 6 months post-implantation compared to 1 month post-implantation. The morphology of the gels varied depending on the amounts of NaOH and cross-linker used during production. Lower levels of NaOH and cross-linker produced gels with a matrix of more loosely associated collagen filaments. As confirmed by histological examination (Figure 5.3), under transmission electron microscopy, remnants of the 10mM/0.8% gel were observed in the host stroma at 1 month post-implantation (Figure 5.4). However by 6 months post-implantation, the collagen gel could not be located. At the boundary zone of the 30mM/0.4% gel a degree of interlacing could be seen between the gel implant and the host stroma. At this interface region, collagen from the gel could be seen interspersed with mature collagen fibrils. However in the two 0.8% cross-linked gels, the boundary zone of the gel appeared as a straight line, and was occasionally separated from the host stroma, with no integration seen between the gel and the stroma.

5.4. Discussion

Several key parameters define the production of collagen gels for use in corneal stroma tissue engineering. These include both physical factors such as their mechanical strength and survival *in vivo*, and biological factors such as cell migration and adhesion. The biocompatibility of the gel *in vivo* is an essential criterion for the production of a functioning stromal equivalent. An inflammatory response has the potential to not only compromise the function of the gel, but also to spread to any transplanted cells. Collagen-based gels are commonly used in tissue engineering, in part because naturally derived polymers usually exhibit sufficient biocompatibility. The cornea itself is somewhat immune privileged, and can subsequently accept allografts, such as the collagen gel used in this study, with minimal rejection. In addition, the amino acid composition of atelocollagen shows little variation across mammalian species (Angele et al., 2003). Consequently, as seen in this study, it is possible to produce collagen gel implants from purified animal collagen for use in tissue

engineering. In addition during implantation, taking care not to penetrate the anterior chamber also reduces the rate of implant rejection, minimizes the potential risk of intraocular infection, and improves the long term stability of the graft (Terry, 2000).

Collagen turnover within the corneal stroma is very slow. However, in response to injury, the production of matrix metalloproteinases including collagenases quickly remodels the matrix to form opaque scar tissue. Stromal equivalent collagen gels must be able to resist this natural process of matrix digestion and remodelling. To achieve this, a frequently used method involves cross-linking the collagen molecules to increase both the mechanical strength of the gel and its stability *in vivo*. This study used EDC, a water-soluble carbodiimide, in combination with NHS to effectively cross-link the collagen gel by forming a stable amide link between the carboxyl group of one collagen molecule and the amine group of another. NHS increases the efficacy of EDC mediated cross-link formation by reacting with the initial carbodiimidecarboxylic acid product (Damink et al., 1996). However, despite undergoing cross-linking, the morphology of the 30mM/0.8% gel was still able to change during the 6 months of implantation. What is not clear is whether this change was due to remodelling of the construct by the migrating host stromal cells, or whether collagen fibrillogenesis was still able to progress despite the gel being cross-linked. A recent study using similar cross-linked collagen gels implanted into pig cornea, demonstrated remodelling of the gel implants by host stromal cells, with regeneration of normal stromal extracellular matrix after one year *in vivo* (Liu et al., 2008).

Corneas implanted with the 30mM/0.4% and 10mM/0.8% gels showed a reduction in total corneal thickness over the course of the implantation period. It is clear from transmission electron microscopy and histological examination that these gels have been digested by host stromal cells. Only the gel containing 30mM of NAOH and 0.8% EDC was sufficiently stable enough to resist biodegradation. This was due to the greater degree of cross-linking and fibrillogenesis it underwent during construction. This level of cross-linking was however, detrimental to the gel's optical properties. A possible solution would be to perforate the gel with large pores. This may serve to increase light transmission through direct removal of some of the slightly opaque gel matrix. But it may also compensate for the fixed nature of the gel, by allowing greater access for host cells to migrate within the gel, whilst providing a greater surface area for integration into the host stromal matrix. Furthermore, as atelocollagen is a naturally derived substance, during production of collagen gels one is able to covalently

incorporate certain ligands and other extracellular matrix molecules in order to stimulate cell growth, migration or adhesion. For example, covalently binding the laminin pentapeptide motif YIGSR has been found to stimulate nerve growth into, and epithelial cell adhesion and proliferation across the surface of implanted collagen gels (Li et al., 2005; Duan et al., 2007). The addition of ligands that encourage stromal cell proliferation and migration within the matrix of the gel would complement the production of a perforated collagen gel into which they can gain easier access.

The oedema seen in Figure 5.3F is affecting the anterior portion of the cornea that had the 30mM/0.8% gel implanted. No swelling was observed in any of the corneas containing the other gel types. The more advanced fibrillogenesis and cross-linking that this gel possesses may have also affected its permeability to water and nutrients. Corneal epithelial nutrition is reliant on the diffusion of metabolites, primarily glucose, through the stroma from the aqueous humour. The diffusion of glucose through the implant is directly dependant on the diffusion coefficient of the gel, and inversely proportional to the thickness of the implant (McCarey and Schimidt, 1990). The gel's increased resistance to digestion resulted in it maintaining its original thickness whilst *in vivo*. Consequently, this may then have reduced its permeability to glucose compared to the other, thinner implants. Improving the implants permeability to glucose could be achieved by increasing the water content of the gels. However, an increase in water content would detrimentally affect other properties of the gel, such as their mechanical stability. Despite the odema seen by histological examination, no other pathological signs were seen that might indicate reduced nutrient diffusion. Any disruption of the flow of nutrients to the epithelium would result in stromal thinning and the formation of epithelial and stromal ulcerations anterior to the implant (Cardona et al., 1964; Maurice et al., 1969; Sweeney et al., 1998). Histological examination of the epithelium and anterior stroma revealed no pathologies other than a slight swelling of the tissue, suggesting that the implant had sufficient permeability to glucose.

5.5. Conclusions

Previous *in vivo* studies have shown that cross-linked collagen gels possess satisfactory biocompatibility for integration into stromal tissue and re-growth of host epithelial cells (Liu et al., 2006a, 2006b, 2008; Merrett et al., 2009). Our findings support the potential use of collagen based constructs for clinical use as corneal stromal implants. The enhanced stability

of the 30mM NaOH, 0.8% EDC cross-linked gel within the intra-stromal pocket suggests that higher cross-linker levels, when coupled with greater levels of collagen fibrillogenesis, delay the digestion or degradation of the construct. However, the detrimental effect that these levels have on transparency of the gel must be taken into consideration. In addition, edema in the anterior stroma suggests that the most stable gel (30mM of NaOH, 0.8% EDC/NHS) may act as a barrier, preventing the endothelial pump from properly regulating anterior stromal hydration.

Further work will be aimed at introducing other macromolecules such as proteoglycans and other collagen types with a view to enhancing the optical and mechanical properties of the gels, and improving their long term *in vivo* characteristics. The production of more biomimetic collagen gels will also be investigated, utilizing orthogonally stacked layers of aligned collagen.

These optically transparent cross-linked collagen gels provide a basis for the future production of more complex biomimetic stromal constructs. They have potential clinical use as cell or drug carriers, as protective membranes for corneal surface damage, and stromal implantation for tissue replacement and regeneration.

6. CONCLUDING DISCUSSION

The focus of this study was the engineering of a corneal stromal equivalent from predominantly natural biological materials. By studying the developmental period during which the cornea undergoes the most radical structural and functional changes, this information could then be applied to the production of a stromal equivalent for therapeutic treatments. Chapter 3 centres on the development of the corneal stroma, investigating how the collagenous matrix is constructed naturally. Transmission electron microscopy was used to examine how collagen is deposited into the extracellular matrix, and the method by which it gains its spatial orientation. Three-dimensional tomography was then used to observe the interactions between collagen and other extracellular matrix components, namely proteoglycans, and to examine how these interactions changed as development progressed.

Collagen fibrillogenesis has been shown to be a complex process that occurs both intracellularly and extracellularly (Trelstad, 1982). What is now evident is that cellular control over collagen fibrillogenesis also extends into the extracellular processes. As in developing tendon (Canty and Kadler, 2005), keratocytes in the developing cornea have a key role in the assembly and deposition of collagen fibrils.

During the developmental time period studied, the keratocyte plasma membrane was seen to be highly convoluted. Collagen fibrils were often seen in close association with the keratocyte surface, within the recesses and compartments formed by the convoluted plasma membrane. It has been hypothesized that collagen excretion into the extracellular matrix occurs via membrane bound tunnels known as 'fibripositors' (Canty et al., 2004). The lateral fusion of surface recesses creates larger compartments capable of containing fibril bundles, indeed the fusion of small fibril bundles into a larger bundle may be facilitated by these cellular compartments. In tendon, fibripositor are seen aligned along the long axis of the cell, which in turn is aligned along the long axis of the tendon. Consequently, collagen extruded from the fibroblast fibripositor gains positional information and is correctly orientated within the extracellular matrix (Canty et al., 2004). This process is also thought to occur in corneal keratocytes, with the membrane bound channels aligned along the two orthogonal axes of the cell, thus conferring orthogonality to the collagen being synthesized (Birk and Trelstad, 1984). However, recent transmission electron microscopy of the chick cornea around developmental

day 14 revealed cell-associated collagen running in multiple directions within a loose stroma (Young et al., 2007).

The fibrilpositor model implies that the production and deposition of collagen fibrils is controlled by individual cells. Compartmentalization of the extracellular space allows for direct connection between the intracellular and extracellular processes. The orientation and topography of these cell membrane bound compartments confers spatial orientation to the synthesized collagen, as well as facilitating the fusion of fibril bundles into collagen lamellae.

Having initially observed the assembly of collagen fibril bundles, and the involvement of the keratocyte in this process, Chapter 3 continued to study the developing corneal stroma by going within the fibril bundles to observe the relationship between collagen and proteoglycans in the developing stroma.

Considerable research has gone into understanding the importance of regular collagen fibril organisation to the transparency of the cornea (Maurice, 1957; Hart and Farrell, 1969; Farrell, 1994). However, the mechanism which this level of organisation is achieved and maintained in the corneal stroma is still not widely understood. Proteoglycans are known to play a key role in collagen fibril assembly, mediating collagen fibril size, spacing and organization (Scott, 1985; Scott, 1988). Routine transmission electron microscopy of proteoglycan organisation has revealed two distinct populations of proteoglycans in the developing corneal stroma (Bianco et al., 1990; Blochberger et al., 1992; Li et al., 1992; Funderburgh et al., 1997; Corpuz et al., 1996). However, examining proteoglycan structure and organisation using two-dimensional microscopy may lead to inaccuracies (Scott, 1992). Utilizing three-dimensional tomography gave a unique insight into how proteoglycans and collagen fibrils interact within fibril bundles in the developing corneal stroma.

A large range in proteoglycan width and length was observed throughout the developmental days studied. Short, thin proteoglycans were observed bridging the interfibrillar gap between adjacent neighbouring fibrils. Longer, thicker proteoglycans could be seen passing around adjacent fibrils to interconnect more distant neighbouring fibrils. Previous studies have identified these large proteoglycans to be chondroitin sulphate/dermatan sulphate proteoglycans (Scott, 1992; Liles et al., 2010). The shorter proteoglycans are likely to be keratan sulphate proteoglycans such as keratocan.

The sizes of the Cu^- and WO_4^{2-} ions used to stain for proteoglycans are on a picometer scale, and are therefore unlikely to be the cause behind the presence of these large proteoglycans. The large range in proteoglycan sizes may be the result of self-assembly or aggregation of individual proteoglycan chains. The exact configuration of these complexes has not been established, although potential structures have been modelled (Knupp et al., 2009; Lewis et al., 2010). In addition, the mechanism by which these multimers form is not clear, and whether other extracellular matrix molecules have a facilitating role cannot be ruled out (Cooper et al., 2006). Within the corneal stroma of knock-out mice lacking the keratan sulphotransferase enzyme, large chondroitin sulphate/dermatan sulphate proteoglycan complexes have been observed, resulting from increased lateral and end-to-end aggregation of this proteoglycan type (Parfitt et al., 2011). Consequently, a regulatory mechanism must exist in the normal cornea in order to produce the more discrete proteoglycan multimers that have been observed in the murine, bovine, and now developing avian corneal stroma.

Previous studies have suggested that proteoglycans are organised into a symmetrical six-fold arrangement around a central collagen fibril (Farrell and Hart, 1969; Müller et al., 2004). However, the three-dimensional reconstructions revealed no specific organisation or set pattern of orientation. Large proteoglycans were observed passing around adjacent fibrils to interconnect more distant neighbouring fibrils. Whilst, smaller proteoglycans were frequently observed bridging interfibrillar gaps, often at regular axial positions - this is in agreement with the theory of specific proteoglycan binding regions along the length of a collagen fibril (Scott and Haigh, 1985; Young, 1985; Meek et al., 1986; Scott and Bosworth, 1990). A small number of proteoglycans were also seen running along the long axis of the fibril. These results are consistent with three dimension reconstructions of collagen and proteoglycan organisation in both bovine and murine corneal stroma (Lewis et al., 2010; Parfitt et al., 2010). Overall these findings imply that the proteoglycans and collagen fibrils of the corneal stroma may have a more dynamic relationship than previously thought. This research suggests that the corneal stroma is a more fluid system, where the organisation and interactions of these two extracellular matrix components are dynamic and flexible.

One key role of proteoglycans in the corneal stroma is the maintenance of collagen interfibrillar spacing. The previously suggested model of six-fold symmetrical proteoglycan organisation would provide a simple answer as to how this role is carried out, whereby each

fibril is connected to its adjacent neighbouring fibril by a short proteoglycan, forming a lattice-like configuration. However, three-dimensional reconstructions of bovine, murine and avian corneal stroma have shown this six-fold theory of organisation to be incorrect. Consequently, the method by which proteoglycans maintain collagen fibril spacing has yet to be established. Despite the lack of local proteoglycan organisation, long range regulation of interfibrillar spacing may be maintained through a combination of attractive and repulsive forces generated by the presence of negatively charged proteoglycans in the interfibrillar region (Lewis et al., 2010; Parfitt et al., 2010). The negatively charged sulphate groups present on a glycosaminoglycan chain would attract positively charged ions into the interfibrillar space. The resulting osmotic pull would create an increase in osmotic pressure in the area surrounding the proteoglycan, generating a repulsive force between the adjacent collagen fibrils.

In order to restrict the expansion of interfibrillar spacing, proteoglycans must generate an attractive force capable pulling adjacent fibrils together. Proteoglycans spanning the interfibrillar gap would serve to physically tether adjacent fibrils together. In addition the thermal motion of the glycosaminoglycan chains, resulting from constant bombardment by other molecules and ions, would cause retraction of the two terminal ends of the proteoglycans. As the proteoglycans are bound to the collagen fibrils via their protein core, the fibrils would experience an attractive force, pulling them closer together. Equilibrium of both these repulsive and attractive forces generated by the proteoglycans would serve to maintain collagen interfibrillar spacing, enabling the transmission of light through the cornea. The magnitude of these generated forces is dependent on several characteristics of the proteoglycans present. Sulphation pattern, charge density, glycosaminoglycan chain length and the degree of self-aggregation would all affect the magnitude of the forces involved, and therefore influence collagen fibril spacing. Consequently, the proportions of different proteoglycan subtypes present in the stroma would be an important determining factor in establishing interfibrillar spacing. This may explain the varying proteoglycan compositions and interfibrillar spacing observed in the corneal stromas of different species (Gyi et al., 1988; Scott and Bosworth, 1990).

Having examined how collagen is organised in the corneal stroma, and the significance of its interactions with proteoglycans, attempts were made to utilize similar biological materials in the construction of an artificial corneal stroma. Chapters 4 and 5 are an attempt to tissue

engineer a stromal equivalent using type I collagen, and to record its structural and functional properties both *in vitro* and *in vivo* (following implantation into rabbit corneal stroma). A range of analytical tools were used to determine the optical, mechanical and morphological properties of the collagen constructs including transmission electron microscopy, polarized light microscopy, histology, spectrophotometry and mechanical testing. This fundamental study is then open to further investigation as future research attempts to improve the functional properties of the constructs.

Disease or injury to the cornea can result in opacification and, in extreme cases, causes irreversible blindness. Affecting over 10 million people worldwide (The Vision Share Consortium of Eye Banks, USA) the only treatment for corneal blindness is transplantation using donated corneal tissue. An alternative option to donated corneal tissue is the use of a manufactured or engineered substitute that attempts to recapitulate the structural and functional properties of a healthy human cornea. Current attempts at manufacturing such replacements can be divided into two broad categories. The first approach involves the production of a keratoprosthesis - a synthetic polymer which replaces the damaged tissue and is designed to recreate the functional properties of the cornea. They have the advantage of reduced risk of disease transmission, consistent availability, and lack of postoperative remodelling. The second approach involves tissue engineering corneal equivalents from more natural biological materials. These constructs are designed to mimic the structure and properties of normal corneal tissue. They can then be implanted into the cornea to either replace damaged or diseased tissue, or to facilitate the repair and regeneration of healthy corneal tissue by the host's own cells. Whilst these two approaches are fundamentally quite different, the criteria for replicating proper corneal function are common to both. They must be optically transparent, mechanically strong, and biocompatible. They must also possess a functioning epithelium or support re-epithelialisation, be permeable to the diffusion of nutrients and gases, and promote re-innervation.

Currently, there are numerous approaches being developed based on utilizing natural biological materials with or without cellular assistance, in order to tissue engineer a construct capable of replacing or aiding in the repair of damaged and disease corneal tissue. Whilst extensive research has been focused on the inclusion of a cellular component into engineered constructs (Minami et al., 1993; Germain et al., 1999; Griffith et al., 1999), there has also been considerable breakthroughs in the production of collagen based scaffolds which, when

implanted, become populated by migrating host cells *in vivo* (Liu et al., 2008; Merrett et al., 2008). A third approach involves the isolation and expansion of corneal cell types *in vitro* (Du et al., 2007). These cell populations can then be manipulated into forming cell sheets for transplantation (Nishida et al., 2004), or into expressing stromal extracellular matrix *in vitro* in an attempt to construct a corneal equivalent for use in implantation. The addition of ascorbic acid to a cultured population of keratocytes induces an increase in collagen synthesis - the primary constituent of the corneal stroma and of most engineered corneal constructs (Grinnell et al., 1989). The cultured keratocytes then produce fibrous sheets that can be combined to form a stromal equivalent, or seeded with a surface layer of epithelial cells.

Cultured corneal cells have also been used in conjunction with engineered stromal constructs. In 1994, Zieske et al developed a full thickness rabbit corneal equivalent using rabbit epithelial cells and keratocytes, and immortalized mouse endothelial cells grown around a three-dimensional type I collagen gel matrix. They were able to confirm the presence of anchoring fibrils, hemidesmosomes, and a continuous epithelial basement membrane following culture of their full thickness construct. Similarly, a full thickness bovine corneal equivalent was constructed from isolated bovine corneal cells in a collagen gel culture (Minami et al 1993).

Using a similar method, Griffith et al (1999) constructed the first full thickness human corneal equivalent containing all three layers. Immortalized human corneal cells were characterized then seeded onto a glutaraldehyde cross-linked, chondroitin sulphate-collagen gel matrix. The morphological and physiological properties of the constructs were shown to be similar to that of normal corneal tissue, including stromal swelling, gene expression, wound healing response, transparency, and nerve re-growth.

Recently, collagen gels have been used in phase I clinical trials as cell-free corneal substitutes to aid in the regeneration of stromal tissue (Fagerholm et al., 2009). Chondroitin sulphate-collagen type III gels crosslinked with EDC/NHS were implanted into the anterior cornea of 10 patients who had significant loss of vision. After an anterior lamellar keratoplasty, the implants were sutured into place and antibiotics were administered for a 5 week post-operative period. 2 years post-implantation the constructs remain well integrated, populated by host stromal cells and innervated by nerve re-growth. The gels showed good transparency,

with re-epithelialisation over the surface of the constructs occurring in all patients, and the restoration of functioning tear films (Fagerholm et al., 2010).

The hydrophilic properties of collagen gels, as well as their high level of transparency and permeability to nutrients, make them ideally suited for use in engineering corneal equivalents. However, due to their relatively poor mechanical properties, cross-linking is necessary in order to make the constructs robust enough to withstand implantation, and to function as corneal equivalents. In addition, cross-linking will also slow the rate of digestion by host collagenases to a more desirable level for tissue regeneration. However, cross-linking type I collagen gels was found to have a detrimental effect on their transparency. Consequently only low levels of cross-linker were used, and the pH of the gels was increased. A more advanced stage of fibrillogenesis in the gels would then compensate for the lower cross-linking levels.

By increasing the pH of the gels a range of subfibrillar intermediates could be observed, from a largely disorganized matrix of loose collagen, through intermittent molecular aggregations, to the formation of progressively condensing filamentous structures (Chapter 4). At extreme levels of fibrillogenesis, short lengths of banded collagen fibrils could be seen within the gel matrix. However, as fibrillogenesis progressed, the increase in thickness of these aggregating filaments, coupled with a more heterogeneous matrix, led to a reduction in gel transparency. Establishing the correct balance between cross-linker levels and the degree of fibrillogenesis within the gels was key to constructing a transparent and mechanically stable collagen gel.

A range of clinical suitable gels, demonstrating good transparency and mechanical strength, were implanted into rabbit cornea intra-stromal pockets (Chapter 5). Only those gels which had undergone the higher degree of cross-linking survived for 6 months implantation period, the mechanically weaker gels were digested *in vivo*.

Consequently, future work is being focused on increasing the mechanical stability of the collagen gels without having to rely on extensive cross-linking or fibrillogenesis which would be detrimental to the gel transparency. One such method involved producing thinner collagen gels which could be stacked orthogonally, in an attempt to recapitulate the natural corneal architecture and to improve the mechanical properties of the gels (Chapter 4). These laminate gels demonstrated greater mechanical stability than the uniformly aligned gels that were used

during the *in vivo* implantation (Chapter 5). Moreover, their mechanical properties exceed that of other crosslinked collagen gels or scaffold, and even that of human corneal tissue.

Alternatively, introducing other elements which may control and limit fibril diameter would allow fibrillogenesis to progress further, without negatively impacting on the gel transparency. This would increase the mechanical stability of the gel, without the need for extensive cross-linking. Type V collagen is known to have a mediating role in collagen fibrillogenesis, naturally forming heterotypic fibrils with collagen type I in the corneal stroma, limiting fibril diameter by inhibiting the addition of additional collagen molecules. Proteoglycans are known to have a similar effect. The addition of either of these extracellular matrix components may be beneficial to the production of an effective corneal stromal equivalent. Previous unpublished data revealed that the addition of commercially available glycosaminoglycan chains such as chondroitin sulphate, dermatan sulphate and hyaluronic acid only served to decrease the transparency of the gels. However, future work may involve utilizing naturally expressed proteoglycans from cultured or implanted cell populations (Funderburgh et al., 1996; Long et al., 2000).

Modifying the predominant collagen type used in constructing a collagen gel may affect its transparency and mechanical properties. As discussed previously, a team led by Griffith have recently developed a stromal substitute using crosslinked chondroitin sulphate-collagen type III gels (Fagerholm et al., 2009). They reported that the smaller diameter type III fibrils resulted in improved transparency, whilst the greater amount of hydroxyproline residues present in type III collagen molecules led to increased intermolecular hydrogen bonding and consequently greater mechanical stability over type I collagen gels (Liu et al., 2008).

Collagen gel based constructs are now commonly used in the production of corneal equivalents of a sufficient quality to be suitable for implantation into animal models, and in some cases into humans (Liu et al., 2006a; Fagerholm et al., 2009). However, the long term characteristics of these gels are still unknown. Research is now focused on improving the morphological and physiological properties of corneal equivalents to more closely match the structural and functional characteristics of a healthy human cornea. Combining different methods of cross-linking, such as using γ -irradiation and carbodiimide-based cross-linking are being investigated as potential means to increasing the mechanical stability of collagen

gels whilst still providing access into the construct for migrating stromal cells (Griffith et al 2002).

Optimizing the properties of engineered corneal equivalents may vary depending on the intended application of the construct. *In vitro* applications, such as tissue models, may not require a full thickness corneal equivalent containing all three layers. For example, investigating the link between mechanical stimuli and extracellular matrix organisation would require only the stroma to be replicated (Petroll et al., 2004; Karamichos et al., 2007). Artificial constructs can also be used in the advancement of surgery technology, whereby a realistic corneal equivalent can be used in place of corneal tissue, which is of limited availability. Collagen gels have a potential use as stromal equivalents for developing and training with new surgical tools and techniques. The constructs developed in Chapter 4 are now being used as a practice material for a newly developed tool designed for DSEK surgery.

Engineered corneas may also have other uses *in vivo*, for example in promoting wound healing. If used as a temporary dressing, the construct would not need to integrate with the host cornea. It would serve to protect the wound, whilst promoting host cell migration and tissue repair through the secretion of specific growth and signalling factors. Engineered skin grafts have proved effective in treating skin wounds, and have been shown to accelerate the healing process when impregnated with growth factors (Kawai et al., 2000).

Whilst considerable research has gone into the production of synthetic keratoprotheses, current attempts still demonstrate adverse side effects with failure still commonplace. Recently however, focus has shifted towards tissue engineering of corneal equivalents. The significant progress being made in this field of research suggests that these constructs may, in the near future, provide a new approach to the treatment of corneal injury and disease.

REFERENCES

- Akama T O, Misra A K, Hindsgaul O and Fukuda M N (2002) Enzymatic synthesis *in vitro* of the disulfated disaccharide unit of corneal keratan sulfate. *J Biol Chem* 277 (45) 42505-42513.
- Akama T O, Nishida K, Nakayama J, Watanabe H, Ozaki K, Nakamura T, Dota A, Kawasaki S, Inoue Y, Maeda N, Yamamoto S, Fujiwara T, Thonar E J, Shimomura Y, Kinoshita S, Tanigami A and Fukuda M N (2000) Macular corneal dystrophy type I and type II are caused by distinct mutations in a new sulphotransferase gene. *Nat Genet* 26 (2) 237-241.
- Akimoto Y, Yamakawa N, Furukawa K, Kimata K, Kawakami H and Hirano H (2002) Changes in distribution of the long form of type XII collagen during chicken corneal development. *J Histochem Cytochem* 50 (6) 851-862.
- Alberts B, Bray D, Lewis J, Raff M, Roberts K and Watson J D (2002) The cell. V. Cells in Their Social Context, 19. Cell Junctions, Cell Adhesion, and the Extracellular Matrix. In: Molecular Biology of the Cell 4th Edition. *Garland Science Publishers*, New York, NY.
- Ameye L and Young M F (2002) Mice deficient in small leucine-rich proteoglycans: novel *in vivo* models for osteoporosis, osteoarthritis, Ehlers-Danlos syndrome, muscular dystrophy, and corneal diseases. *Glycobiology* 12 (9) 107R-116R.
- Angele P, Abke J, Kujat R, Faltermeier H, Schumann D, Nerlich M, Kinner B, Englert C, Ruszczak Z, Mehrl R and Mueller R (2004) Influence of different collagen species on physico-chemical properties of cross-linked collagen matrices. *Biomaterials* 25 (14) 2831-2841.
- Anseth A (1961) Studies on corneal polysaccharides. III. Topographic and comparative biochemistry. *Exp Eye Res* 1 106-115.
- Bard J B, Bansal M K and Ross A S (1988) The extracellular matrix of the developing cornea: diversity, deposition and function. *Development* 103 Suppl 195-205.

References

- Bard J B and Chapman J A (1968) Polymorphism in collagen fibrils precipitated at low pH. *Nature* 219 (5160) 1279-1280.
- Bard J B and Hay E D (1975) The behavior of fibroblasts from the developing avian cornea. Morphology and movement *in situ* and *in vitro*. *J Cell Biol* 67 (2PT.1) 400-418.
- Bard J B and Kratochwil K (1987) Corneal morphogenesis in the Mov13 mutant mouse is characterized by normal cellular organization but disordered and thin collagen. *Development* 101 (3) 547-555.
- Barry F P, Rosenberg L C, Gaw J U, Koob T J and Neame P J (1995) N- and O-linked keratan sulfate on the hyaluronan binding region of aggrecan from mature and immature bovine cartilage. *J Biol Chem* 270 (35) 20516-20524.
- Baumeister W, Grimm R and Walz J (1999) Electron tomography of molecules and cells. *Trends Cell Biol* 9 (2) 81-85.
- Bayer M L, Yeung C Y, Kadler K E, Qvortrup K, Baar K, Svensson R B, Magnusson S P, Krogsgaard M, Koch M and Kjaer M (2010) The initiation of embryonic-like collagen fibrillogenesis by adult human tendon fibroblasts when cultured under tension. *Biomaterials* 31 (18) 4889-4897.
- Beecher N, Carlson C, Allen B R, Kipchumba R, Conrad G W, Meek K M and Quantock A J (2005) An x-ray diffraction study of corneal structure in mimecan-deficient mice. *Invest Ophthalmol Vis Sci* 46 (11) 4046-4049.
- Bell E, Ehrlich H P, Buttle D J and Nakatsuji T (1981) Living tissue formed *in vitro* and accepted as skin-equivalent tissue of full thickness. *Science* 211 (4486) 1052-1054.
- Bell E, Ivarsson B and Merrill C (1979) Production of a tissue-like structure by contraction of collagen lattices by human fibroblasts of different proliferative potential *in vitro*. *Proc Natl Acad Sci U S A* 76 (3) 1274-1278.
- Benedek G B (1971) Theory of transparency of the eye. *Appl Opt* 10 (3) 459-473.

References

- Bergmanson J P G, Horne J, Doughty M J, Garcia M, and Gondo M (2005) Assessment of the number of lamellae in the central region of the normal human corneal stroma at the resolution of the transmission electron microscope. *Eye & contact lens* 31 (6) 281.
- Berryhill B L, Kader R, Kane B, Birk D E, Feng J and Hassell J R (2002) Partial restoration of the keratocyte phenotype to bovine keratocytes made fibroblastic by serum. *Invest Ophthalmol Vis Sci* 43 (11) 3416-3421.
- Bettelheim F A and Plessy B (1975) The hydration of proteoglycans of bovine cornea. *Biochim Biophys Acta* 381 (1) 203-214.
- Bianco P, Fisher L W, Young M F, Termine J D and Robey P G (1990) Expression and localization of the two small proteoglycans biglycan and decorin in developing human skeletal and non-skeletal tissues. *J Histochem Cytochem* 38 (11) 1549-1563.
- Birk D E, Fitch J M, Babiarz J P, Doane K J and Linsenmayer T F (1990) Collagen fibrillogenesis *in vitro*: interaction of types I and V collagen regulates fibril diameter. *J Cell Sci* 95 (Pt 4) 649-657.
- Birk D E, Fitch J M, Babiarz J P and Linsenmayer T F (1988) Collagen type I and type V are present in the same fibril in the avian corneal stroma. *J Cell Biol* 106 (3) 999-1008.
- Birk D E, Nurminskaya M V and Zycband E I (1995) Collagen fibrillogenesis *in situ*: fibril segments undergo post-depositional modifications resulting in linear and lateral growth during matrix development. *Dev Dyn* 202 (3) 229-243.
- Birk D E and Trelstad R L (1984) Extracellular compartments in matrix morphogenesis: collagen fibril, bundle, and lamellar formation by corneal fibroblasts. *J Cell Biol* 99 (6) 2024-2033.
- Birk D E and Trelstad R L (1985) Fibroblasts create compartments in the extracellular space where collagen polymerizes into fibrils and fibrils associate into bundles. *Ann N Y Acad Sci* 460 258-266.
- Birk D E and Trelstad R L (1986) Extracellular compartments in tendon morphogenesis: collagen fibril, bundle, and macroaggregate formation. *J Cell Biol* 103 (1) 231-240.

References

- Blochberger T C, Vergnes J P, Hempel J and Hassell J R (1992) cDNA to chick lumican (corneal keratan sulfate proteoglycan) reveals homology to the small interstitial proteoglycan gene family and expression in muscle and intestine. *J Biol Chem* 267 (1) 347-352.
- Bonaventure J, Zylberberg L, Cohen-Solal L, Allain J C, Lasselin C and Maroteaux P (1989) A new lethal brittle bone syndrome with increased amount of type V collagen in a patient. *Am J Med Genet* 33 (3) 299-310.
- Borcherding M S, Blacik L J, Sittig R A, Bizzell J W, Breen M and Weinstein H G (1975) Proteoglycans and collagen fibre organization in human corneoscleral tissue. *Exp Eye Res* 21 (1) 59-70.
- Bromsel M and Alfsen A (2003) Entry of viruses through the epithelial barrier: pathogenic trickery. *Nature Reviews Molecular Cell Biology* 4, 57-68.
- Butticè G, Kaytes P, D'Armiento J, Vogeli G and Kurkinen M (1990) Evolution of collagen IV genes from a 54-base pair exon: a role for introns in gene evolution. *J Mol Evol* 30 (6) 479-488.
- Cai C X, Fitch J M, Svoboda K K, Birk D E and Linsenmayer T F (1994) Cellular invasion and collagen type IX in the primary corneal stroma *in vitro*. *Dev Dyn* 201 (3) 206-215.
- Cai C X, Gibney E, Gordon M K, Marchant J K, Birk D E and Linsenmayer T F (1996) Characterization and developmental regulation of avian corneal beta-1,4-galactosyltransferase mRNA. *Exp Eye Res* 63 (2) 193-200.
- Canty E G and Kadler K E (2005) Procollagen trafficking, processing and fibrillogenesis. *J Cell Sci* 118 (Pt 7) 1341-1353.
- Canty E G, Lu Y, Meadows R S, Shaw M K, Holmes D F and Kadler K E (2004) Coalignment of plasma membrane channels and protrusions (fibripositors) specifies the parallelism of tendon. *J Cell Biol* 165 (4) 553-563.
- Cardona H (1964) Plastic keratoprosthesis: A description of plastic material and comparative histologic study of recipient. *Am J Ophthalmol* 58 247-252.

References

- Chakravarti S, Magnuson T, Lass J H, Jepsen K J, LaMantia C and Carroll H (1998) Lumican regulates collagen fibril assembly: skin fragility and corneal opacity in the absence of lumican. *J Cell Biol* 141 (5) 1277-1286.
- Chakravarti S, Petroll W M, Hassell J R, Jester J V, Lass J H, Paul J and Birk D E (2000) Corneal opacity in lumican-null mice: defects in collagen fibril structure and packing in the posterior stroma. *Invest Ophthalmol Vis Sci* 41 (11) 3365-3373.
- Cheema U, Chuo C B, Sarathchandra P, Nazhat S N and Brown R A (2007) Engineering functional collagen scaffolds: cyclical loading increases material strength and fibril aggregation. *Advanced Functional Materials* 17 (14) 2426-2431.
- Chen C S, Yannas I V and Spector M (1995) Pore strain behaviour of collagen-glycosaminoglycan analogues of extracellular matrix. *Biomaterials* 16 (10) 777-783.
- Chen J, Zhang S, Guo L, Zheng H, Lin J and Zheng J (2001) Primary research about reconstruction of cornea in three-dimensional collagen gel *in vitro*. *Zhonghua Yan Ke Za Zhi* 37 (4) 244-247.
- Cheng F, Yoshida K, Heinegård D and Fransson L A (1992) A new method for sequence analysis of glycosaminoglycans from heavily substituted proteoglycans reveals non-random positioning of 4- and 6-O-sulphated N-acetylgalactosamine in aggrecan-derived chondroitin sulphate. *Glycobiology* 2 (6) 553-561.
- Chew S Y, Mi R, Hoke A and Leong K W (2007) Aligned Protein-Polymer Composite Fibers Enhance Nerve Regeneration: A Potential Tissue-Engineering Platform. *Adv Funct Mater* 17 (8) 1288-1296.
- Christiansen D L, Huang E K and Silver F H (2000) Assembly of type I collagen: fusion of fibril subunits and the influence of fibril diameter on mechanical properties. *Matrix Biol* 19 (5) 409-420.
- Cintron C, Gregory J D, Damle S P and Kublin C L (1990) Biochemical analyses of proteoglycans in rabbit corneal scars. *Invest Ophthalmol Vis Sci* 31 (10) 1975-1981.

References

- Cisneros D A, Hung C, Franz C M and Muller D J (2006) Observing growth steps of collagen self-assembly by time-lapse high-resolution atomic force microscopy. *J Struct Biol* 154 (3) 232-245.
- Comper W D (1996) *Extracellular matrix*. Harwood Academic Publishers.
- Comper W D and Laurent T C (1978) Physiological function of connective tissue polysaccharides. *Physiol Rev* 58 (1) 255-315.
- Connon C J, Douth J, Chen B, Hopkinson A, Mehta J S, Nakamura T, Kinoshita S and Meek K M (2010) The variation in transparency of amniotic membrane used in ocular surface regeneration. *Br J Ophthalmol* 94 (8) 1057-1061.
- Connon C J, Siegler V, Meek K M, Hodson S A, Caterson B, Kinoshita S and Quantock A J (2003) Proteoglycan alterations and collagen reorganisation in the secondary avian cornea during development. *Ophthalmic Res* 35 (4) 177-184.
- Conrad A H and Conrad G W (2003) The keratocan gene is expressed in both ocular and non-ocular tissues during early chick development. *Matrix Biol* 22 (4) 323-337.
- Conrad G W (1970) Collagen and mucopolysaccharide biosynthesis in mass cultures and clones of chick corneal fibroblasts *in vitro*. *Dev Biol* 21 (4) 611-635.
- Cooper L J, Bentley A J, Nieduszynski I A, Talabani S, Thomson A, Utani A, Shinkai H, Fullwood N J and Brown G M (2006) The role of dermatopontin in the stromal organization of the cornea. *Invest Ophthalmol Vis Sci* 47 (8) 3303-3310.
- Corpuz L M, Funderburgh J L, Funderburgh M L, Bottomley G S, Prakash S, and Conrad G W (1996) Molecular cloning and tissue distribution of keratocan. Bovine corneal keratan sulfate proteoglycan 37A. *J Biol Chem* 271 (16): 9759-9763.
- Coulombre A J and Coulombre J L (1958a) Corneal development. I. Corneal transparency. *J Cell Physiol* 51 (1) 1-11.
- Coulombre A J and Coulombre J L (1958b) The role of intraocular pressure in the development of the chick eye. IV. Corneal curvature. *AMA Arch Ophthalmol* 59 (4) 502-506.

References

- Cox J L, Farrell R A, Hart R W and Langham M E (1970) The transparency of the mammalian cornea. *J Physiol* 210 (3) 601-616.
- Crabb R A, Chau E P, Evans M C, Barocas V H and Hubel A (2006) Biomechanical and microstructural characteristics of a collagen film-based corneal stroma equivalent. *Tissue Eng* 12 (6) 1565-1575.
- Craig A S and Parry D A (1981) Collagen fibrils of the vertebrate corneal stroma. *J Ultrastruct Res* 74 (2) 232-239.
- Craig A S, Robertson J G and Parry D A (1986) Preservation of corneal collagen fibril structure using low-temperature procedures for electron microscopy. *J Ultrastruct Mol Struct Res* 96 (1-3) 172-175.
- Danielson K G, Baribault H, Holmes D F, Graham H, Kadler K E and Iozzo R V (1997) Targeted disruption of decorin leads to abnormal collagen fibril morphology and skin fragility. *J Cell Biol* 136 (3) 729-743.
- Davies Y, Lewis D, Fullwood N J, Nieduszynski I A, Marcyniuk B, Albon J and Tullo A (1999) Proteoglycans on normal and migrating human corneal endothelium. *Exp Eye Res* 68 (3) 303-311.
- Doane K J and Birk D E (1991) Fibroblasts retain their tissue phenotype when grown in three-dimensional collagen gels. *Exp Cell Res* 195 (2) 432-442.
- Doane K J, Ting W H, McLaughlin J S and Birk D E (1996) Spatial and temporal variations in extracellular matrix of periocular and corneal regions during corneal stromal development. *Exp Eye Res* 62 (3) 271-283.
- Du Y, SundarRaj N, Funderburgh M L, Harvey S A, Birk D E, and Funderburgh J L (2007) Secretion and organization of a cornea-like tissue in vitro by stem cells from human corneal stroma. *Investigative ophthalmology & visual science* 48 (11) 5038-5045.
- Duan X, McLaughlin C, Griffith M and Sheardown H (2007) Biofunctionalization of collagen for improved biological response: scaffolds for corneal tissue engineering. *Biomaterials* 28 (1) 78-88.

References

- Dunlevy J R, Beales M P, Berryhill B L, Cornuet P K and Hassell J R (2000) Expression of the keratan sulfate proteoglycans lumican, keratocan and osteoglycin/mimecan during chick corneal development. *Exp Eye Res* 70 (3) 349-362.
- Dunlevy J R, Neame P J, Vergnes J P and Hassell J R (1998) Identification of the N-linked oligosaccharide sites in chick corneal lumican and keratocan that receive keratan sulfate. *J Biol Chem* 273 (16) 9615-9621.
- Edelhauser H F (2006) The balance between corneal transparency and edema: the Proctor Lecture. *Invest Ophthalmol Vis Sci* 47 (5) 1754-1767.
- Elsdale T and Bard J (1972) Collagen substrata for studies on cell behavior. *J Cell Biol* 54 (3) 626-637.
- Fagerholm P, Lagali N S, Carlsson D J, Merrett K, and Griffith M (2009) Corneal Regeneration Following Implantation of a Biomimetic Tissue Engineered Substitute. *Clinical and Translational Science* 2 (2) 162-164.
- Fagerholm P, Lagali N S, Merrett K, Jackson W B, Munger R, Liu Y, Polarek J W et al. (2010) A biosynthetic alternative to human donor tissue for inducing corneal regeneration: 24-month follow-up of a phase 1 clinical study. *Science translational medicine* 2 (46) 46ra61.
- Farrell R and McCally R (1994) Corneal transparency. *Principles and Practice of Ophthalmology* 64-81.
- Farrell R A and Hart R W (1969) On the theory of the spatial organization of macromolecules in connective tissue. *Bull Math Biophys* 31 (4) 727-760.
- Fisher L W, Termine J D and Young M F (1989) Deduced protein sequence of bone small proteoglycan I (biglycan) shows homology with proteoglycan II (decorin) and several nonconnective tissue proteins in a variety of species. *J Biol Chem* 264 (8) 4571-4576.
- Fitch J M, Birk D E, Linsenmayer C and Linsenmayer T F (1990) The spatial organization of Descemet's membrane-associated type IV collagen in the avian cornea. *J Cell Biol* 110 (4) 1457-1468.

References

- Fitch J M, Birk D E, Linsenmayer C and Linsenmayer T F (1991) Stromal assemblies containing collagen types IV and VI and fibronectin in the developing embryonic avian cornea. *Dev Biol* 144 (2) 379-391.
- Fitch J M, Gordon M K, Gibney E P and Linsenmayer T F (1995) Analysis of transcriptional isoforms of collagen types IX, II, and I in the developing avian cornea by competitive polymerase chain reaction. *Dev Dyn* 202 (1) 42-53.
- Fitch J M, Gross J, Mayne R, Johnson-Wint B and Linsenmayer T F (1984) Organization of collagen types I and V in the embryonic chicken cornea: monoclonal antibody studies. *Proceedings of the National Academy of Sciences of the United States of America* 81 (9) 2791.
- Fitch J M, Linsenmayer C M and Linsenmayer T F (1994) Collagen fibril assembly in the developing avian primary corneal stroma. *Invest Ophthalmol Vis Sci* 35 (3) 862-869.
- Fitch J M, Mentzer A, Mayne R and Linsenmayer T F (1988) Acquisition of type IX collagen by the developing avian primary corneal stroma and vitreous. *Dev Biol* 128 (2) 396-405.
- Fitzgerald J and Bateman J F (2001) A new FACIT of the collagen family: COL21A1. *FEBS Lett* 505 (2) 275-280.
- Fitzsimmons T D, Fagerholm P, Härfstrand A and Schenholm M (1992) Hyaluronic acid in the rabbit cornea after excimer laser superficial keratectomy. *Invest Ophthalmol Vis Sci* 33 (11) 3011-3016.
- Forrester J V (2002) *The eye: basic sciences in practice*. London: Saunders
- Frank J (2006) *Electron tomography: methods for three-dimensional visualization of structures in the cell*. Springer Verlag.
- Freearg T J (1997) The physical basis of transparency of the normal cornea. *Eye (Lond)* 11 (Pt 4) 465-471.
- Funderburgh J L (2000) Keratan sulfate: structure, biosynthesis, and function. *Glycobiology* 10 (10) 951-958.

References

- Funderburgh J L (2002) Keratan sulfate biosynthesis. *IUBMB Life* 54 (4) 187-194.
- Funderburgh J L, Cintron C, Covington H I and Conrad G W (1988) Immunoanalysis of keratan sulfate proteoglycan from corneal scars. *Invest Ophthalmol Vis Sci* 29 (7) 1116-1124.
- Funderburgh J L, Corpuz L M, Roth M R, Funderburgh M L, Tasheva E S and Conrad G W (1997) Mimecan, the 25-kDa corneal keratan sulfate proteoglycan, is a product of the gene producing osteoglycin. *J Biol Chem* 272 (44) 28089-28095.
- Funderburgh J L, Funderburgh M L, Mann M M and Conrad G W (1991) Unique glycosylation of three keratan sulfate proteoglycan isoforms. *J Biol Chem* 266 (22) 14226-14231.
- Funderburgh J L, Funderburgh M L, Mann M M, Prakash S, and Conrad G W (1996) Synthesis of corneal keratan sulfate proteoglycans by bovine keratocytes in vitro. *Journal of Biological Chemistry* 271 (49) 31431-31436.
- Funderburgh J L, Funderburgh M L, Rodrigues M M, Krachmer J H and Conrad G W (1990) Altered antigenicity of keratan sulfate proteoglycan in selected corneal diseases. *Invest Ophthalmol Vis Sci* 31 (3) 419-428.
- Funderburgh J L, Hevelone N D, Roth M R, Funderburgh M L, Rodrigues M R, Nirankari V S and Conrad G W (1998) Decorin and biglycan of normal and pathologic human corneas. *Invest Ophthalmol Vis Sci* 39 (10) 1957-1964.
- Funderburgh J L, Mann M M and Funderburgh M L (2003) Keratocyte phenotype mediates proteoglycan structure: a role for fibroblasts in corneal fibrosis. *J Biol Chem* 278 (46) 45629-45637.
- Garrett R H and Grisham C M (2005) 7.6 How do proteoglycans modulate processes in cell organisms? Chapter 7. Carbohydrates and the Glycoconjugates of Cell Surfaces. In: *Biochemistry 3rd Edition*. *Thompson Brooks/Cole*, London.
- Gealy E C, Kerr B C, Young R D, Tudor D, Hayes A J, Hughes C E, Caterson B, Quantock A J and Ralphs J R (2007) Differential expression of the keratan sulphate

References

- proteoglycan, keratocan, during chick corneal embryogenesis. *Histochem Cell Biol* 128 (6) 551-555.
- Gelman R A, Poppke D C and Piez K A (1979) Collagen fibril formation *in vitro*. The role of the nonhelical terminal regions. *J Biol Chem* 254 (22) 11741-11745.
- Germain L, Auger F A, Grandbois E, Guignard R, Giasson M, Boisjoly H and Guérin S L (1999) Reconstructed human cornea produced *in vitro* by tissue engineering. *Pathobiology* 67 (3) 140-147.
- Gipson I K, Spurr-Michaud S J and Tisdale A S (1987) Anchoring fibrils form a complex network in human and rabbit cornea. *Invest Ophthalmol Vis Sci* 28 (2) 212-220.
- Glasser A and Howland H C (1996) A history of studies of visual accommodation in birds. *Q Rev Biol* 71 (4) 475-509.
- Glasser A, Troilo D and Howland H C (1994) The mechanism of corneal accommodation in chicks. *Vision Res* 34 (12) 1549-1566.
- Goldman J N, Benedek G B, Dohlman C H and Kravitt B (1968) Structural alterations affecting transparency in swollen human corneas. *Invest Ophthalmol* 7 (5) 501-519.
- Goldoni S, Owens R T, McQuillan D J, Shriver Z, Sasisekharan R, Birk D E, Campbell S and Iozzo R V (2004) Biologically active decorin is a monomer in solution. *J Biol Chem* 279 (8) 6606-6612.
- Goodfellow J M, Elliott G F and Woolgar A E (1978) X-ray diffraction studies of the corneal stroma. *J Mol Biol* 119 (2) 237-252.
- Gordon M K, Fitch J M, Foley J W, Gerecke D R, Linsenmayer C, Birk D E and Linsenmayer T F (1997) Type XVII collagen (BP 180) in the developing avian cornea. *Invest Ophthalmol Vis Sci* 38 (1) 153-166.
- Gordon M K, Foley J W, Birk D E, Fitch J M and Linsenmayer T F (1994) Type V collagen and Bowman's membrane. Quantitation of mRNA in corneal epithelium and stroma. *J Biol Chem* 269 (40) 24959-24966.

References

- Gordon M K, Foley J W, Lisenmayer T F and Fitch J M (1996) Temporal expression of types XII and XIV collagen mRNA and protein during avian corneal development. *Dev Dyn* 206 (1) 49-58.
- Gordon M K, Gerecke D R, Dublet B, van der Rest M and Olsen B R (1989) Type XII collagen. A large multidomain molecule with partial homology to type IX collagen. *J Biol Chem* 264 (33) 19772-19778.
- Gordon M K, Gerecke D R and Olsen B R (1987) Type XII collagen: distinct extracellular matrix component discovered by cDNA cloning. *Proc Natl Acad Sci U S A* 84 (17) 6040-6044.
- Gottlieb M D, Fugate-Wentzek L A and Wallman J (1987) Different visual deprivations produce different ametropias and different eye shapes. *Invest Ophthalmol Vis Sci* 28 (8) 1225-1235.
- Graham H K, Holmes D F, Watson R B and Kadler K E (2000) Identification of collagen fibril fusion during vertebrate tendon morphogenesis. The process relies on unipolar fibrils and is regulated by collagen-proteoglycan interaction. *J Mol Biol* 295 (4) 891-902.
- Gregory J D, Cöster L and Damle S P (1982) Proteoglycans of rabbit corneal stroma. Isolation and partial characterization. *J Biol Chem* 257 (12) 6965-6970.
- Greiling H, Scott J E and . B S (1989) *Keratan Sulphate*. Biochemical Society.
- Griffith M, Hakim M, Shimmura S, Watsky M A, Li F, Carlsson D, Doillon C J, Nakamura M, Suuronen E, Shinozaki N, Nakata K and Sheardown H (2002) Artificial human corneas: scaffolds for transplantation and host regeneration. *Cornea* 21 (7 Suppl) S54-61.
- Griffith M, Osborne R, Munger R, Xiong X, Doillon C J, Laycock N L, Hakim M, Song Y and Watsky M A (1999) Functional human corneal equivalents constructed from cell lines. *Science* 286 (5447) 2169-2172.

References

- Grillo H C and Gross J (1962) Thermal reconstitution of collagen from solution and the response to its heterologous implantation. *J Surg Res* 2 69-82.
- Grinnell F, Fukamizu H, Pawelek P, and Nakagawa S (1989) Collagen processing, crosslinking, and fibril bundle assembly in matrix produced by fibroblasts in long-term cultures supplemented with ascorbic acid. *Experimental cell research* 181 (2) 483-491.
- Guo C and Kaufman L J (2007) Flow and magnetic field induced collagen alignment. *Biomaterials* 28 (6) 1105-1114.
- Gyi T J, Meek K M, and Elliott G F (1988) Collagen interfibrillar distances in corneal stroma using synchrotron X-ray diffraction: a species study. *International Journal of Biological Macromolecules* 10 (5) 265-269.
- Hahn R A and Birk D E (1992) beta-D xyloside alters dermatan sulfate proteoglycan synthesis and the organization of the developing avian corneal stroma. *Development* 115 (2) 383-393.
- Handley C J and Phelps C F (1972) The biosynthesis *in vitro* of keratan sulphate in bovine cornea. *Biochem J* 128 (2) 205-213.
- Harris J R and Reiber A (2007) Influence of saline and pH on collagen type I fibrillogenesis *in vitro*: fibril polymorphism and colloidal gold labelling. *Micron* 38 (5) 513-521.
- Hart G W (1976) Biosynthesis of glycosaminoglycans during corneal development. *J Biol Chem* 251 (21) 6513-6521.
- Hart R W and Farrell R A (1969) Light scattering in the cornea. *J Opt Soc Am* 59 (6) 766-774.
- Hassell J R, Cintron C, Kublin C and Newsome D A (1983) Proteoglycan changes during restoration of transparency in corneal scars. *Arch Biochem Biophys* 222 (2) 362-369.
- Hassell J R, Newsome D A, Krachmer J H and Rodrigues M M (1980) Macular corneal dystrophy: failure to synthesize a mature keratan sulfate proteoglycan. *Proc Natl Acad Sci U S A* 77 (6) 3705-3709.

References

- Hay E D (1991) *Cell biology of extracellular matrix*. Springer US.
- Hay E D and Revel J P (1969) Fine structure of the developing avian cornea. *Monogr Dev Biol* 1 1-144.
- Hayashi M, Ninomiya Y, Hayashi K, Linsenmayer T F, Olsen B R and Trelstad R L (1988) Secretion of collagen types I and II by epithelial and endothelial cells in the developing chick cornea demonstrated by *in situ* hybridization and immunohistochemistry. *Development* 103 (1) 27-36.
- Hayashida Y, Akama T O, Beecher N, Lewis P, Young R D, Meek K M, Kerr B, Hughes C E, Caterson B, Tanigami A, Nakayama J, Fukada M N, Tano Y, Nishida K and Quantock A J (2006) Matrix morphogenesis in cornea is mediated by the modification of keratan sulfate by GlcNAc 6-O-sulfotransferase. *Proc Natl Acad Sci U S A* 103 (36) 13333-13338.
- Hedblom E E (1961) The role of polysaccharides in corneal swelling. *Exp Eye Res* 1 81-91.
- Hendrix M J, Hay E D, von der Mark K and Linsenmayer T F (1982) Immunohistochemical localization of collagen types I and II in the developing chick cornea and tibia by electron microscopy. *Invest Ophthalmol Vis Sci* 22 (3) 359-375.
- Henriksson J T, McDermott A M and Bergmanson J P (2009) Dimensions and morphology of the cornea in three strains of mice. *Invest Ophthalmol Vis Sci* 50 (8) 3648-3654.
- Hirsch M, Noske W, Prenant G and Renard G (1999) Fine structure of the developing avian corneal stroma as revealed by quick-freeze, deep-etch electron microscopy. *Exp Eye Res* 69 (3) 267-277.
- Hocking A M, Shinomura T and McQuillan D J (1998) Leucine-rich repeat glycoproteins of the extracellular matrix. *Matrix Biol* 17 (1) 1-19.
- Hodge A and Petruska J (1963) Recent studies with the electron microscope on ordered aggregates of the tropocollagen molecule. *Aspects of protein structure* 289-300.
- Hodson S and Miller F (1976) The bicarbonate ion pump in the endothelium which regulates the hydration of rabbit cornea. *J Physiol* 263 (3) 563-577.

References

- Holmes D F, Gilpin C J, Baldock C, Ziese U, Koster A J and Kadler K E (2001) Corneal collagen fibril structure in three dimensions: Structural insights into fibril assembly, mechanical properties, and tissue organization. *Proc Natl Acad Sci U S A* 98 (13) 7307-7312.
- Horton H R, Moran L A, Ochs R S, Rawn J D and Scrimgeour K G (2002) *Principles of biochemistry*. Prentice Hall Upper Saddle River, NJ.
- Hu X, Lui W, Cui L, Wang M and Cao Y (2005) Tissue engineering of nearly transparent corneal stroma. *Tissue Eng* 11 (11-12) 1710-1717.
- Hulmes D J and Miller A (1979) Quasi-hexagonal molecular packing in collagen fibrils. *Nature* 282 (5741) 878-880.
- Ide T, Nishida K, Yamato M, Sumide T, Utsumi M, Nozaki T, Kikuchi A, Okano T and Tano Y (2006) Structural characterization of bioengineered human corneal endothelial cell sheets fabricated on temperature-responsive culture dishes. *Biomaterials* 27 (4) 607-614.
- Iozzo R V (1997) The family of the small leucine-rich proteoglycans: key regulators of matrix assembly and cellular growth. *Crit Rev Biochem Mol Biol* 32 (2) 141-174.
- Iozzo R V (1998) Matrix proteoglycans: from molecular design to cellular function. *Annu Rev Biochem* 67 609-652.
- Ivarsen A, Fledelius W and Hjortdal J (2009) Three-year changes in epithelial and stromal thickness after PRK or LASIK for high myopia. *Invest Ophthalmol Vis Sci* 50 (5) 2061-2066.
- Jakus M A (1956) Studies on the cornea. II. The fine structure of Descemet's membrane. *J Biophys Biochem Cytol* 2 (4 Suppl) 243-252.
- Jester J V (2008) Corneal crystallins and the development of cellular transparency. *Semin Cell Dev Biol* 19 (2) 82-93.

References

- Jester J V, Moller-Pedersen T, Huang J, Sax C M, Kays W T, Cavanagh H D, Petroll W M and Piatigorsky J (1999) The cellular basis of corneal transparency: evidence for 'corneal crystallins'. *J Cell Sci* 112 (Pt 5) 613-622.
- Kapacee Z, Richardson S H, Lu Y, Starborg T, Holmes D F, Baar K and Kadler K E (2008) Tension is required for fibripositor formation. *Matrix Biol* 27 (4) 371-375.
- Karamichos D, Lakshman N, and Petroll W M (2007) Regulation of corneal fibroblast morphology and collagen reorganization by extracellular matrix mechanical properties. *Investigative ophthalmology & visual science* 48 (11) 5030 - 5037.
- Kawai K, Suzuki S, Tabata Y, Ikada Y, and Nishimura Y (2000) Accelerated tissue regeneration through incorporation of basic fibroblast growth factor-impregnated gelatin microspheres into artificial dermis. *Biomaterials* 21 (5) 489-499.
- Keene D R, Lunstrum G P, Morris N P, Stoddard D W and Burgeson R E (1991) Two type XII-like collagens localize to the surface of banded collagen fibrils. *J Cell Biol* 113 (4) 971-978.
- Keene D R, Sakai L Y, Lunstrum G P, Morris N P and Burgeson R E (1987) Type VII collagen forms an extended network of anchoring fibrils. *J Cell Biol* 104 (3) 611-621.
- Kligman A (1988) Histologic responses to collagen implants in human volunteers: Comparison of Zyderm collagen with Zyplast implant. *J Dermatol Surg Oncol* 14 (Suppl 1) 35-38.
- Klintworth G K and Smith C F (1977) Macular corneal dystrophy. Studies of sulfated glycosaminoglycans in corneal explant and confluent stromal cell cultures. *Am J Pathol* 89 (1) 167-182.
- Knupp C, Pinali C, Lewis P N, Parfitt G J, Young R D, Meek K M and Quantock A J (2009) The architecture of the cornea and structural basis of its transparency. *Adv Protein Chem Struct Biol* 78 25-49.
- Kobe B and Deisenhofer J (1993) Crystal structure of porcine ribonuclease inhibitor, a protein with leucine-rich repeats. *Nature* 366 (6457) 751-756.

References

- Koch M, Foley J E, Hahn R, Zhou P, Burgeson R E, Gerecke D R and Gordon M K (2001) alpha 1(Xx) collagen, a new member of the collagen subfamily, fibril-associated collagens with interrupted triple helices. *J Biol Chem* 276 (25) 23120-23126.
- Koch M, Veit G, Stricker S, Bhatt P, Kutsch S, Zhou P, Reinders E, Hahn R A, Song R, Burgeson R E, Gerecke D R, Mundlos S and Gordon M K (2006) Expression of type XXIII collagen mRNA and protein. *J Biol Chem* 281 (30) 21546-21557.
- Koizumi N, Sakamoto Y, Okumura N, Okahara N, Tsuchiya H, Torii R, Cooper L J et al. (2007) Cultivated corneal endothelial cell sheet transplantation in a primate model. *Investigative ophthalmology & visual science* 48(10) 4519-4526.
- Komai Y and Ushiki T (1991) The three-dimensional organization of collagen fibrils in the human cornea and sclera. *Invest Ophthalmol Vis Sci* 32 (8) 2244-2258.
- Kremer J R, Mastronarde D N and McIntosh J R (1996) Computer visualization of three-dimensional image data using IMOD. *J Struct Biol* 116 (1) 71-76.
- Kurkinen M, Alitalo K, Vaheri A, Stenman S and Saxén L (1979) Fibronectin in the development of embryonic chick eye. *Dev Biol* 69 (2) 589-600.
- Kusche-Gullberg M and Kjellén L (2003) Sulfotransferases in glycosaminoglycan biosynthesis. *Curr Opin Struct Biol* 13 (5) 605-611.
- Köster S, Leach J B, Struth B, Pfohl T and Wong J Y (2007) Visualization of flow-aligned type I collagen self-assembly in tunable pH gradients. *Langmuir* 23 (2) 357-359.
- Lanfer B, Freudenberg U, Zimmermann R, Stamov D, Körber V and Werner C (2008) Aligned fibrillar collagen matrices obtained by shear flow deposition. *Biomaterials* 29 (28) 3888-3895.
- Lee C R, Grodzinsky A J and Spector M (2001) The effects of cross-linking of collagen-glycosaminoglycan scaffolds on compressive stiffness, chondrocyte-mediated contraction, proliferation and biosynthesis. *Biomaterials* 22 (23) 3145-3154.

References

- Lehninger A L, Nelson D L and Cox M M (2005) Chapter 4: The Three-dimensional Structure of Proteins. In: *Lehninger Principles of Biochemistry* 5th Edition. *Worth Publishers*, New York, NY.
- Leibovich S J and Weiss J B (1970) Electron microscope studies of the effects of endo- and exopeptidase digestion on tropocollagen. A novel concept of the role of terminal regions in fibrillogenesis. *Biochim Biophys Acta* 214 (3) 445-454.
- Leonard D W and Meek K M (1997) Refractive indices of the collagen fibrils and extrafibrillar material of the corneal stroma. *Biophys J* 72 (3) 1382-1387.
- Lewis P N, Pinali C, Young R D, Meek K M, Quantock A J and Knupp C (2010) Structural interactions between collagen and proteoglycans are elucidated by three-dimensional electron tomography of bovine cornea. *Structure* 18 (2) 239-245.
- Li F, Carlsson D, Lohmann C, Suuronen E, Vascotto S, Kobuch K, Sheardown H, Munger R, Nakamura M and Griffith M (2003) Cellular and nerve regeneration within a biosynthetic extracellular matrix for corneal transplantation. *Proc Natl Acad Sci U S A* 100 (26) 15346-15351.
- Li F, Griffith M, Li Z, Tanodekaew S, Sheardown H, Hakim M and Carlsson D J (2005) Recruitment of multiple cell lines by collagen-synthetic copolymer matrices in corneal regeneration. *Biomaterials* 26 (16) 3093-3104.
- Li W, Vergnes J P, Cornuet P K and Hassell J R (1992) cDNA clone to chick corneal chondroitin sulphate/dermatan sulfate proteoglycan reveals identity to decorin. *Arch Biochem Biophys* 296 (1) 190-197.
- Liles M, Palka B P, Harris A, Kerr B, Hughes C, Young R D, Meek K M, Caterson B and Quantock A J (2010) Differential relative sulfation of Keratan sulfate glycosaminoglycan in the chick cornea during embryonic development. *Invest Ophthalmol Vis Sci* 51 (3) 1365-1372.
- Lindahl B, Eriksson L, Spillmann D, Caterson B and Lindahl U (1996) Selective loss of cerebral keratan sulfate in Alzheimer's disease. *J Biol Chem* 271 (29) 16991-16994.

References

- Linsenmayer T F, Bruns R R, Mentzer A and Mayne R (1986) Type VI collagen: immunohistochemical identification as a filamentous component of the extracellular matrix of the developing avian corneal stroma. *Dev Biol* 118 (2) 425-431.
- Linsenmayer T F, Fitch J M and Birk D E (1990) Heterotypic collagen fibrils and stabilizing collagens. Controlling elements in corneal morphogenesis? *Ann N Y Acad Sci* 580 143-160.
- Linsenmayer T F, Fitch J M, Gordon M K, Cai C X, Igoe F, Marchant J K and Birk D E (1998) Development and roles of collagenous matrices in the embryonic avian cornea. *Progress in retinal and eye research* 17 (2) 231.
- Linsenmayer T F, Fitch J M and Mayne R (1984) Extracellular matrices in the developing avian eye: type V collagen in corneal and noncorneal tissues. *Invest Ophthalmol Vis Sci* 25 (1) 41-47.
- Linsenmayer T F, Fitch J M, Schmid T M, Zak N B, Gibney E, Sanderson R D and Mayne R (1983) Monoclonal antibodies against chicken type V collagen: production, specificity, and use for immunocytochemical localization in embryonic cornea and other organs. *J Cell Biol* 96 (1) 124-132.
- Linsenmayer T F, Gibney E, Igoe F, Gordon M K, Fitch J M, Fessler L I and Birk D E (1993) Type V collagen: molecular structure and fibrillar organization of the chicken alpha 1(V) NH2-terminal domain, a putative regulator of corneal fibrillogenesis. *J Cell Biol* 121 (5) 1181-1189.
- Linsenmayer T F, Smith G N and Hay E D (1977) Synthesis of two collagen types by embryonic chick corneal epithelium *in vitro*. *Proc Natl Acad Sci U S A* 74 (1) 39-43.
- Liu W, Deng C, McLaughlin C R, Fagerholm P, Lagali N S, Heyne B, Scaiano J C, Watsky M A, Kato Y, Munger R, Shinozaki N, Li F and Griffith M (2009) Collagen-phosphorylcholine interpenetrating network hydrogels as corneal substitutes. *Biomaterials* 30 (8) 1551-1559.

References

- Liu W, Merrett K, Griffith M, Fagerholm P, Dravida S, Heyne B, Scaiano J C, Watsky M A, Shinozaki N, Lagali N, Munger R and Li F (2008) Recombinant human collagen for tissue engineered corneal substitutes. *Biomaterials* 29 (9) 1147-1158.
- Liu Y and Chan-Park M B (2009) Hydrogel based on interpenetrating polymer networks of dextran and gelatin for vascular tissue engineering. *Biomaterials* 30 (2) 196-207.
- Liu Y, Gan L, Carlsson D J, Fagerholm P, Lagali N, Watsky M A, Munger R, Hodge W G, Priest D and Griffith M (2006a) A simple, cross-linked collagen tissue substitute for corneal implantation. *Invest Ophthalmol Vis Sci* 47 (5) 1869-1875.
- Liu Y, Griffith M, Watsky M A, Forrester J V, Kuffova L, Grant D, Merrett K and Carlsson D J (2006b) Properties of porcine and recombinant human collagen matrices for optically clear tissue engineering applications. *Biomacromolecules* 7 (6) 1819-1828.
- Long C J, Roth M R, Tasheva E S, Funderburgh M, Smit R, Conrad G W, and Funderburgh J L (2000) Fibroblast growth factor-2 promotes keratan sulfate proteoglycan expression by keratocytes in vitro. *Journal of Biological Chemistry* 275 (18) 13918-13923.
- Madisen L, Neubauer M, Plowman G, Rosen D, Segarini P, Dasch J, Thompson A, Ziman J, Bentz H and Purchio A F (1990) Molecular cloning of a novel bone-forming compound: osteoinductive factor. *DNA Cell Biol* 9 (5) 303-309.
- Malmström A and Aberg L (1982) Biosynthesis of dermatan sulphate. Assay and properties of the uronosyl C-5 epimerase. *Biochem J* 201 (3) 489-493.
- Marchant J K, Zhang G and Birk D E (2002) Association of type XII collagen with regions of increased stability and keratocyte density in the cornea. *Exp Eye Res* 75 (6) 683-694.
- Marchini M, Morocutti M, Ruggeri A, Koch M H, Bigi A and Roveri N (1986) Differences in the fibril structure of corneal and tendon collagen. An electron microscopy and X-ray diffraction investigation. *Connect Tissue Res* 15 (4) 269-281.
- Matsuda K, Suzuki S, Isshiki N, Yoshioka K, Okada T and Ikada Y (1990) Influence of glycosaminoglycans on the collagen sponge component of a bilayer artificial skin. *Biomaterials* 11 (5) 351-355.

References

- Matsumoto N, Horibe S, Nakamura N, Senda T, Shino K and Ochi T (1998) Effect of alignment of the transplanted graft extracellular matrix on cellular repopulation and newly synthesized collagen. *Arch Orthop Trauma Surg* 117 (4-5) 215-221.
- Maurice D (1969) Nutritional aspects of corneal grafts and prostheses. *Corneo-Plastic Surgery Proceedings of the Second International Corneo-Plastic Conference*. Pergamon Press, London, 197-207
- Maurice D M (1957) The structure and transparency of the cornea. *J Physiol* 136 (2) 263-286.
- Maurice D M (1962) Clinical physiology of the cornea. *International Ophthalmology Clinics* 2 (3) 561-572
- McCarey B E and Schmidt F H (1990) Modeling glucose distribution in the cornea. *Curr Eye Res* 9 (11) 1025-1039.
- McTigue J W (1967) The human cornea: a light and electron microscopic study of the normal cornea and its alterations in various dystrophies. *Trans Am Ophthalmol Soc* 65 591-660.
- Meek K M and Boote C (2009) The use of X-ray scattering techniques to quantify the orientation and distribution of collagen in the corneal stroma. *Prog Retin Eye Res* 28 (5) 369-392.
- Meek K M, Elliott G F and Nave C (1986) A synchrotron X-ray diffraction study of bovine cornea stained with cupromeronic blue. *Coll Relat Res* 6 (2) 203-218.
- Meek K M, Chapman J A, and Hardcastle R A (1979) The staining pattern of collagen fibrils. Improved correlation with sequence data. *Journal of Biological Chemistry* 254 (21) 10710-10714
- Meek K M, Fullwood N J, Cooke P H, Elliott G F, Maurice D M, Quantock A J, Wall R S and Worthington C R (1991) Synchrotron x-ray diffraction studies of the cornea, with implications for stromal hydration. *Biophys J* 60 (2) 467-474.
- Meek K M and Leonard D W (1993) Ultrastructure of the corneal stroma: a comparative study. *Biophys J* 64 (1) 273-280.

References

- Meek K M and Quantock A J (2001) The use of X-ray scattering techniques to determine corneal ultrastructure. *Prog Retin Eye Res* 20 (1) 95-137.
- Meek K M, Quantock A J, Boote C, Liu C Y and Kao W W (2003) An X-ray scattering investigation of corneal structure in keratocan-deficient mice. *Matrix Biol* 22 (6) 467-475.
- Meek K M, Quantock A J, Elliott G F, Ridgway A E, Tullo A B, Bron A J and Thonar E J (1989) Macular corneal dystrophy: the macromolecular structure of the stroma observed using electron microscopy and synchrotron X-ray diffraction. *Exp Eye Res* 49 (6) 941-958.
- Mendler M, Eich-Bender S G, Vaughan L, Winterhalter K H and Bruckner P (1989) Cartilage contains mixed fibrils of collagen types II, IX, and XI. *J Cell Biol* 108 (1) 191-197.
- Merrett K, Fagerholm P, McLaughlin C R, Dravida S, Lagali N, Shinozaki N, Watsky M A, Munger R, Kato Y, Li F, Marmo C J and Griffith M (2008) Tissue-engineered recombinant human collagen-based corneal substitutes for implantation: performance of type I versus type III collagen. *Invest Ophthalmol Vis Sci* 49 (9) 3887-3894.
- Merrett K, Liu W, Mitra D, Camm K D, McLaughlin C R, Liu Y, Watsky M A, Li F, Griffith M and Fogg D E (2009) Synthetic neoglycopolymer-recombinant human collagen hybrids as biomimetic cross-linking agents in corneal tissue engineering. *Biomaterials* 30 (29) 5403-5408.
- Midura R J and Hascall V C (1989) Analysis of the proteoglycans synthesized by corneal explants from embryonic chicken. II. Structural characterization of the keratan sulfate and dermatan sulfate proteoglycans from corneal stroma. *J Biol Chem* 264 (3) 1423-1430.
- Miller A and Parry D A (1973) Structure and packing of microfibrils in collagen. *J Mol Biol* 75 (2) 441-447.
- Miller A and Wray J S (1971) Molecular packing in collagen. *Nature* 230 (5294) 437-439.

References

- Minami Y, Sugihara H and Oono S (1993) Reconstruction of cornea in three-dimensional collagen gel matrix culture. *Invest Ophthalmol Vis Sci* 34 (7) 2316-2324.
- Murphy C J, Glasser A and Howland H C (1995) The anatomy of the ciliary region of the chicken eye. *Invest Ophthalmol Vis Sci* 36 (5) 889-896.
- Müller L J, Pels E, Schurmans L R and Vrensen G F (2004) A new three-dimensional model of the organization of proteoglycans and collagen fibrils in the human corneal stroma. *Exp Eye Res* 78 (3) 493-501.
- Müller L J, Pels E and Vrensen G F (2001) The specific architecture of the anterior stroma accounts for maintenance of corneal curvature. *Br J Ophthalmol* 85 (4) 437-443.
- Nagayasu A, Hosaka Y, Yamasaki A, Tsuzuki K, Ueda H, Honda T and Takehana K (2008) A preliminary study of direct application of atelocollagen into a wound lesion in the dog cornea. *Curr Eye Res* 33 (9) 727-735.
- Nakamura T, Endo K, Cooper L J, Fullwood N J, Tanifuji N, Tsuzuki M, Koizumi N, Inatomi T, Sano Y and Kinoshita S (2003) The successful culture and autologous transplantation of rabbit oral mucosal epithelial cells on amniotic membrane. *Invest Ophthalmol Vis Sci* 44 (1) 106-116.
- Nerurkar N L, Baker B M, Sen S, Wible E E, Elliott D M and Mauck R L (2009) Nanofibrous biologic laminates replicate the form and function of the annulus fibrosus. *Nat Mater* 8 (12) 986-992.
- Newsome D A, Takasugi M, Kenyon K R, Stark W F and Opelz G (1974) Human corneal cells *in vitro*: morphology and histocompatibility (HL-A) antigens of pure cell populations. *Invest Ophthalmol* 13 (1) 23-32.
- Nilsson B, Nakazawa K, Hassell J R, Newsome D A and Hascall V C (1983) Structure of oligosaccharides and the linkage region between keratan sulfate and the core protein on proteoglycans from monkey cornea. *J Biol Chem* 258 (10) 6056-6063.
- Nishida K, Yamato M, Hayashida Y, Watanabe K, Yamamoto K, Adachi E, Nagai S, Kikuchi A, Maeda N, Watanabe H, Okano T and Tano Y (2004) Corneal

References

- reconstruction with tissue-engineered cell sheets composed of autologous oral mucosal epithelium. *N Engl J Med* 351 (12) 1187-1196.
- Oh J H, Lee S Y, Kim Y H and Kim J C (2003) Comparison of Corneal Substitutes Using PLGA, Collagen, Collagen with Amniotic Membrane Homologous Cornea. *Journal of the Korean Ophthalmological Society* 44 (5) 1188-1197.
- Olde Damink L H, Dijkstra P J, van Luyn M J, van Wachem P B, Nieuwenhuis P and Feijen J (1996) Cross-linking of dermal sheep collagen using a water-soluble carbodiimide. *Biomaterials* 17 (8) 765-773.
- Olsen B (1981) Biosynthesis of collagen. *Cell Biology of the Extracellular Matrix*. ED Hay, editor. Plenum Press, New York 139-177.
- Orgel J P, Irving T C, Miller A and Wess T J (2006) Microfibrillar structure of type I collagen *in situ*. *Proc Natl Acad Sci U S A* 103 (24) 9001-9005.
- Orwin E J, Borene M L and Hubel A (2003) Biomechanical and optical characteristics of a corneal stromal equivalent. *J Biomech Eng* 125 (4) 439-444.
- Orwin E J and Hubel A (2000) *In vitro* culture characteristics of corneal epithelial, endothelial, and keratocyte cells in a native collagen matrix. *Tissue engineering* 6 (4) 307-319.
- Parfitt G J, Pinali C, Akama T O, Young R D, Nishida K, Quantock A J, and Knupp C (2011) Electron tomography reveals multiple self-association of chondroitin sulphate/dermatan sulphate proteoglycans in Chst5-null mouse corneas. *Journal of Structural Biology* 174 (3) 536-541.
- Parfitt G J, Pinali C, Young R D, Quantock A J and Knupp C (2010) Three-dimensional reconstruction of collagen-proteoglycan interactions in the mouse corneal stroma by electron tomography. *J Struct Biol* 170 (2) 392-397.
- Parry D A (1988) The molecular and fibrillar structure of collagen and its relationship to the mechanical properties of connective tissue. *Biophys Chem* 29 (1-2) 195-209.

References

- Pellegrini G, Traverso C E, Franzi A T, Zingirian M, Cancedda R and De Luca M (1997) Long-term restoration of damaged corneal surfaces with autologous cultivated corneal epithelium. *Lancet* 349 (9057) 990-993.
- Petroll W M, Vishwanath M, and Ma L (2004) Corneal fibroblasts respond rapidly to changes in local mechanical stress. *Investigative ophthalmology & visual science* 45 (10) 3466 - 3474.
- Petruska J A and Hodge AJ (1964). A Subunit Model for the Tropocollagen Macromolecule. *Proceedings of the National Academy of Sciences* 51(5): 871-876
- Pieper J S, Hafmans T, Veerkamp J H and van Kuppevelt T H (2000) Development of tailor-made collagen-glycosaminoglycan matrices: EDC/NHS cross-linking, and ultrastructural aspects. *Biomaterials* 21 (6) 581-593.
- Pins G D, Christiansen D L, Patel R and Silver F H (1997) Self-assembly of collagen fibers. Influence of fibrillar alignment and decorin on mechanical properties. *Biophys J* 73 (4) 2164-2172.
- Plaas A H, West L A, Thonar E J, Karcioğlu Z A, Smith C J, Klintworth G K and Hascall V C (2001) Altered fine structures of corneal and skeletal keratan sulfate and chondroitin sulphate/dermatan sulfate in macular corneal dystrophy. *J Biol Chem* 276 (43) 39788-39796.
- Prockop D J, Kivirikko K I, Tuderman L and Guzman N A (1979a) The biosynthesis of collagen and its disorders (first of two parts). *N Engl J Med* 301 (1) 13-23.
- Quantock A J, Kinoshita S, Capel M S and Schanzlin D J (1998) A synchrotron x-ray diffraction study of developing chick corneas. *Biophys J* 74 (2 Pt 1) 995-998.
- Quantock A J, Meek K M and Chakravarti S (2001) An x-ray diffraction investigation of corneal structure in lumican-deficient mice. *Invest Ophthalmol Vis Sci* 42 (8) 1750-1756.

References

- Quantock A J, Meek K M, Fullwood N J and Zabel R W (1993) Scheie's syndrome: the architecture of corneal collagen and distribution of corneal proteoglycans. *Can J Ophthalmol* 28 (6) 266-272.
- Quantock A J, Young R D and Akama T O (2010) Structural and biochemical aspects of keratan sulphate in the cornea. *Cell Mol Life Sci* 67 (6) 891-906.
- Rada J A, Cornuet P K and Hassell J R (1993) Regulation of corneal collagen fibrillogenesis *in vitro* by corneal proteoglycan (lumican and decorin) core proteins. *Exp Eye Res* 56 (6) 635-648.
- Radner W, Zehetmayer M, Aufreiter R and Mallinger R (1998) Interlacing and cross-angle distribution of collagen lamellae in the human cornea. *Cornea* 17 (5) 537-543.
- Rafat M, Li F, Fagerholm P, Lagali N S, Watsky M A, Munger R, Matsuura T and Griffith M (2008) PEG-stabilized carbodiimide cross-linked collagen-chitosan hydrogels for corneal tissue engineering. *Biomaterials* 29 (29) 3960-3972.
- Ramachandran G N (1967) Structure of collagen at the molecular level. *Treatise on collagen* 1 103-183.
- Ress D B, Harlow M L, Marshall R M and McMahan U J (2004) Methods for generating high-resolution structural models from electron microscope tomography data. *Structure* 12 (10) 1763-1774.
- Reynolds E S (1963) The use of lead citrate at high pH as an electron-opaque stain in electron microscopy. *The Journal of Cell Biology* 17 208-212.
- Roeder B A, Kokini K, Sturgis J E, Robinson J P and Voytik-Harbin S L (2002) Tensile mechanical properties of three-dimensional type I collagen extracellular matrices with varied microstructure. *J Biomech Eng* 124 (2) 214-222.
- Rosenberg L C, Choi H U, Tang L H, Johnson T L, Pal S, Webber C, Reiner A and Poole A R (1985) Isolation of dermatan sulfate proteoglycans from mature bovine articular cartilages. *J Biol Chem* 260 (10) 6304-6313.

References

- Ross M H, Reith E J and Romrell L J (1989) *Histology: A Text and Atlas 2nd Edition*. Williams & Wilkins, Baltimore, MD.
- Roughley P J and Lee E R (1994) Cartilage proteoglycans: structure and potential functions. *Microsc Res Tech* 28 (5) 385-397.
- Roughley P J, Rodriguez E and Lee E R (1995) The interactions of 'non-aggregating' proteoglycans. *Osteoarthritis Cartilage* 3 (4) 239-248.
- Ruberti J, Kowalski G and Burkey D (2007) Nanoloom for controlling polymer assembly. World Intellectual Property Organisation. WO Patent WO/2007/038,601.
- Ruberti J W and Zieske J D (2008) Prelude to corneal tissue engineering - gaining control of collagen organization. *Prog Retin Eye Res* 27 (5) 549-577.
- Ruggiero F, Burillon C and Garrone R (1996) Human corneal fibrillogenesis. Collagen V structural analysis and fibrillar assembly by stromal fibroblasts in culture. *Invest Ophthalmol Vis Sci* 37 (9) 1749-1760.
- Sayers Z, Koch M H, Whitburn S B, Meek K M, Elliott G F and Harmsen A (1982) Synchrotron x-ray diffraction study of corneal stroma. *J Mol Biol* 160 (4) 593-607.
- Schaeffel F and Howland H C (1987) Corneal accommodation in chick and pigeon. *J Comp Physiol A* 160 (3) 375-384.
- Schneider A I, Maier-Reif K and Graeve T (1999) Constructing an *in vitro* cornea from cultures of the three specific corneal cell types. *In Vitro Cell Dev Biol Anim* 35 (9) 515-526.
- Scott J E (1972) Histochemistry of Alcian blue. 3. The molecular biological basis of staining by Alcian blue 8GX and analogous phthalocyanins. *Histochemie* 32 (3) 191-212.
- Scott J E (1988) Proteoglycan-fibrillar collagen interactions. *Biochem J* 252 (2) 313-323.
- Scott J E (1992) Morphometry of cupromeronic blue-stained proteoglycan molecules in animal corneas, versus that of purified proteoglycans stained *in vitro*, implies that tertiary structures contribute to corneal ultrastructure. *J Anat* 180 (Pt 1) 155-164.

References

- Scott J E (1996) Proteodermatan and proteokeratan sulfate (decorin, lumican/fibromodulin) proteins are horseshoe shaped. Implications for their interactions with collagen. *Biochemistry* 35 (27) 8795-8799.
- Scott J E (2001) Structure and function in extracellular matrices depend on interactions between anionic glycosaminoglycans. *Pathol Biol (Paris)* 49 (4) 284-289.
- Scott J E and Bosworth T R (1990) A comparative biochemical and ultrastructural study of proteoglycan-collagen interactions in corneal stroma. Functional and metabolic implications. *Biochem J* 270 (2) 491-497.
- Scott J E and Haigh M (1985) 'Small'-proteoglycan:collagen interactions: keratan sulphate proteoglycan associates with rabbit corneal collagen fibrils at the 'a' and 'c' bands. *Biosci Rep* 5 (9) 765-774.
- Scott J E and Haigh M (1988) Identification of specific binding sites for keratan sulphate proteoglycans and chondroitin-dermatan sulphate proteoglycans on collagen fibrils in cornea by the use of cupromeronic blue in 'critical-electrolyte-concentration' techniques. *Biochem J* 253 (2) 607-610.
- Scott J E, Orford C R and Hughes E W (1981) Proteoglycan-collagen arrangements in developing rat tail tendon. An electron microscopical and biochemical investigation. *Biochem J* 195 (3) 573-581.
- Scott P G, McEwan P A, Dodd C M, Bergmann E M, Bishop P N and Bella J (2004) Crystal structure of the dimeric protein core of decorin, the archetypal small leucine-rich repeat proteoglycan. *Proc Natl Acad Sci U S A* 101 (44) 15633-15638.
- Shimmura S, Doillon C J, Griffith M, Nakamura M, Gagnon E, Usui A, Shinozaki N and Tsubota K (2003) Collagen-poly(N-isopropylacrylamide)-based membranes for corneal stroma scaffolds. *Cornea* 22 (7 Suppl) S81-88.
- Siegler V and Quantock A J (2002) Two-stage compaction of the secondary avian cornea during development. *Exp Eye Res* 74 (3) 427-431.
- Smith J W (1968) Molecular pattern in native collagen. *Nature* 219 (5150) 157-158.

References

- Smith J W (1970) The transparency of the corneal stroma. *Vision Res* 10 (1) 109-110.
- Stegman S J, Chu S, Bensch K and Armstrong R (1987) A light and electron microscopic evaluation of Zyderm collagen and Zyplast implants in aging human facial skin. A pilot study. *Arch Dermatol* 123 (12) 1644-1649.
- Stoesser T R, Church R L and Brown S I (1978) Partial characterization of human collagen and procollagen secreted by human corneal stromal fibroblasts in cell culture. *Invest Ophthalmol Vis Sci* 17 (3) 264-271.
- Stopak D, Wessells N K and Harris A K (1985) Morphogenetic rearrangement of injected collagen in developing chicken limb buds. *Proc Natl Acad Sci U S A* 82 (9) 2804-2808.
- Svoboda K K, Nishimura I, Sugrue S P, Ninomiya Y and Olsen B R (1988) Embryonic chicken cornea and cartilage synthesize type IX collagen molecules with different amino-terminal domains. *Proc Natl Acad Sci U S A* 85 (20) 7496-7500.
- Sweeney D F, Xie R Z, O'Leary D J, Vannas A, Odell R, Schindhelm K, Cheng H Y, Steele J G and Holden B A (1998) Nutritional requirements of the corneal epithelium and anterior stroma: clinical findings. *Invest Ophthalmol Vis Sci* 39 (2) 284-291.
- Säämänen A M, Tammi M, Kiviranta I, Jurvelin J and Helminen H J (1989) Levels of chondroitin-6-sulfate and nonaggregating proteoglycans at articular cartilage contact sites in the knees of young dogs subjected to moderate running exercise. *Arthritis Rheum* 32 (10) 1282-1292.
- Söderhäll C, Marenholz I, Kerscher T, Rüschenhoff F, Esparza-Gordillo J, Worm M, Gruber C, Mayr G, Albrecht M, Rohde K, Schulz H, Wahn U, Hubner N and Lee Y A (2007) Variants in a novel epidermal collagen gene (COL29A1) are associated with atopic dermatitis. *PLoS Biol* 5 (9) e242.
- Takahashi T, Cho H I, Kublin C L and Cintron C (1993) Keratan sulfate and dermatan sulfate proteoglycans associate with type VI collagen in fetal rabbit cornea. *J Histochem Cytochem* 41 (10) 1447-1457.

References

- Takezawa T, Ozaki K, Nitani A, Takabayashi C and Shimo-Oka T (2004) Collagen vitrigel: a novel scaffold that can facilitate a three-dimensional culture for reconstructing organoids. *Cell Transplant* 13 (4) 463-473.
- Tanaka Y, Baba K, Duncan T J, Kubota A, Asahi T, Quantock A J, Yamato M, Okano T and Nishida K (2011a) Transparent, tough collagen laminates prepared by oriented flow casting, multi-cyclic vitrification and chemical cross-linking. *Biomaterials* 32 (13) 3358-3366.
- Tanaka Y, Kubota A, Matsusaki M, Duncan T, Hatakeyama Y, Fukuyama K, Quantock A J, Yamato M, Akashi M and Nishida K (2011b) Anisotropic mechanical properties of collagen hydrogels induced by uniaxial-flow for ocular applications. *J Biomater Sci Polym Ed* 22 (11) 1427-1442.
- Tasheva E S, Koester A, Paulsen A Q, Garrett A S, Boyle D L, Davidson H J, Song M, Fox N and Conrad G W (2002) Mimecan/osteoglycin-deficient mice have collagen fibril abnormalities. *Mol Vis* 8 407-415.
- Tegtmeyer S, Papantoniou I and Müller-Goymann C C (2001) Reconstruction of an *in vitro* cornea and its use for drug permeation studies from different formulations containing pilocarpine hydrochloride. *Eur J Pharm Biopharm* 51 (2) 119-125.
- Terry M A (2000) The evolution of lamellar grafting techniques over twenty-five years. *Cornea* 19 (5) 611-616.
- Thompson R W, Price M O, Bowers P J and Price F W (2003) Long-term graft survival after penetrating keratoplasty. *Ophthalmology* 110 (7) 1396-1402.
- Tisdale A S, Spurr-Michaud S J, Rodrigues M, Hackett J, Krachmer J and Gipson I K (1988) Development of the anchoring structures of the epithelium in rabbit and human fetal corneas. *Invest Ophthalmol Vis Sci* 29 (5) 727-736.
- Toole B P and Trelstad R L (1971) Hyaluronate production and removal during corneal development in the chick. *Dev Biol* 26 (1) 28-35.

References

- Torbet J, Malbouyres M, Builles N, Justin V, Roulet M, Damour O, Oldberg A, Ruggiero F and Hulmes D J (2007) Orthogonal scaffold of magnetically aligned collagen lamellae for corneal stroma reconstruction. *Biomaterials* 28 (29) 4268-4276.
- Torii T, Fukuta M and Habuchi O (2000) Sulfation of sialyl N-acetyllactosamine oligosaccharides and fetuin oligosaccharides by keratan sulfate Gal-6-sulfotransferase. *Glycobiology* 10 (2) 203-211.
- Trelstad R L (1982) Multistep assembly of type I collagen fibrils. *Cell* 28 (2) 197-198.
- Trelstad R L, Birk D E and Silver F H (1982) Collagen fibrillogenesis in tissues, in a solution and from modeling: a synthesis. *J Invest Dermatol* 79 Suppl 1 109s-112s.
- Trelstad R L and Coulombre A J (1971) Morphogenesis of the collagenous stroma in the chick cornea. *J Cell Biol* 50 (3) 840-858.
- Trelstad R L and Hayashi K (1979) Tendon collagen fibrillogenesis: intracellular subassemblies and cell surface changes associated with fibril growth. *Dev Biol* 71 (2) 228-242.
- Trelstad R L, Hayashi K and Gross J (1976) Collagen fibrillogenesis: intermediate aggregates and suprafibrillar order. *Proc Natl Acad Sci USA* 73 (11) 4027-4031.
- Trelstad R L, Hayashi K and Toole B P (1974) Epithelial collagens and glycosaminoglycans in the embryonic cornea. Macromolecular order and morphogenesis in the basement membrane. *J Cell Biol* 62 (3) 815-830.
- Trelstad R L and Silver F H (1981) *Matrix assembly*. In *Cell Biology of the Extracellular Matrix*, E. D. Hay, editor. Plenum Press. New York.
- Troilo D and Wallman J (1987) Changes in corneal curvature during accommodation in chicks. *Vision Res* 27 (2) 241-247.
- Tucker R P (1991) The distribution of J1/tenascin and its transcript during the development of the avian cornea. *Differentiation* 48 (2) 59-66.

References

- Vaughan L, Mendler M, Huber S, Bruckner P, Winterhalter K H, Irwin M I and Mayne R (1988) D-periodic distribution of collagen type IX along cartilage fibrils. *J Cell Biol* 106 (3) 991-997.
- von Helmholtz H (1962) *Helmholtz's treatise on physiological optics*. Dover Publications.
- Vrana N E, Builles N, Justin V, Bednarz J, Pellegrini G, Ferrari B, Damour O, Hulmes D J and Hasirci V (2008) Development of a reconstructed cornea from collagen-chondroitin sulfate foams and human cell cultures. *Invest Ophthalmol Vis Sci* 49 (12) 5325-5331.
- Wallace D, McPherson J, Ellingsworth L, Cooperman L, Armstrong R and Piez K (1988) Injectable collagen for tissue augmentation. *Collagen* 3 117-144.
- Watson P G and Young R D (2004) Scleral structure, organisation and disease. A review. *Exp Eye Res* 78 (3) 609-623.
- Weber I T, Harrison R W and Iozzo R V (1996) Model structure of decorin and implications for collagen fibrillogenesis. *J Biol Chem* 271 (50) 31767-31770.
- Wenstrup R J, Langland G T, Willing M C, D'Souza V N and Cole W G (1996) A splice-junction mutation in the region of COL5A1 that codes for the carboxyl propeptide of pro alpha 1(V) chains results in the gravis form of the Ehlers-Danlos syndrome (type I). *Hum Mol Genet* 5 (11) 1733-1736.
- Wess T J, Hammersley A P, Wess L and Miller A (1998) A consensus model for molecular packing of type I collagen. *J Struct Biol* 122 (1-2) 92-100.
- Wessel H, Anderson S, Fite D, Halvas E, Hempel J and SundarRaj N (1997) Type XII collagen contributes to diversities in human corneal and limbal extracellular matrices. *Invest Ophthalmol Vis Sci* 38 (11) 2408-2422.
- Whitcher J P, Srinivasan M and Upadhyay M P (2001) Corneal blindness: a global perspective. *Bull World Health Organ* 79 (3) 214-221.

References

- White J, Werkmeister J A, Ramshaw J A and Birk D E (1997) Organization of fibrillar collagen in the human and bovine cornea: collagen types V and III. *Connect Tissue Res* 36 (3) 165-174.
- Wilson D L, Martin R, Hong S, Cronin-Golomb M, Mirkin C A and Kaplan D L (2001) Surface organization and nanopatterning of collagen by dip-pen nanolithography. *Proc Natl Acad Sci U S A* 98 (24) 13660-13664.
- Wollensak J and Buddecke E (1990) Biochemical studies on human corneal proteoglycans--a comparison of normal and keratoconic eyes. *Graefes Arch Clin Exp Ophthalmol* 228 (6) 517-523.
- Worthington C and Inouye H (1985) X-ray diffraction study of the cornea. *International Journal of Biological Macromolecule* 7 (1) 2-8.
- Yamaguchi N, Mayne R and Ninomiya Y (1991) The alpha 1 (VIII) collagen gene is homologous to the alpha 1 (X) collagen gene and contains a large exon encoding the entire triple helical and carboxyl-terminal non-triple helical domains of the alpha 1 (VIII) polypeptide. *J Biol Chem* 266 (7) 4508-4513.
- Young B B, Zhang G, Koch M and Birk D E (2002) The roles of types XII and XIV collagen in fibrillogenesis and matrix assembly in the developing cornea. *J Cell Biochem* 87 (2) 208-220.
- Young R D (1985) The ultrastructural organization of proteoglycans and collagen in human and rabbit scleral matrix. *J Cell Sci* 74 95-104.
- Young R D, Gealy E C, Liles M, Caterson B, Ralphs J R and Quantock A J (2007) Keratan sulfate glycosaminoglycan and the association with collagen fibrils in rudimentary lamellae in the developing avian cornea. *Invest Ophthalmol Vis Sci* 48 (7) 3083-3088.
- Young R D, Tudor D, Hayes A J, Kerr B, Hayashida Y, Nishida K, Meek K M, Caterson B and Quantock A J (2005) Atypical composition and ultrastructure of proteoglycans in the mouse corneal stroma. *Invest Ophthalmol Vis Sci* 46 (6) 1973-1978.

References

- Zeng Y, Yang J, Huang K, Lee Z and Lee X (2001) A comparison of biomechanical properties between human and porcine cornea. *J Biomech* 34 (4) 533-537.
- Zhang G, Chen S, Goldoni S, Calder B W, Simpson H C, Owens R T, McQuillan D J, Young M F, Iozzo R V and Birk D E (2009) Genetic evidence for the coordinated regulation of collagen fibrillogenesis in the cornea by decorin and biglycan. *J Biol Chem* 284 (13) 8888-8897.
- Zhang G, Simpson H and Birk D (2006) Decorin/biglycan regulation of corneal collagen fibrillogenesis. *Matrix Biology* 25 S40-S40.
- Zhong S, Teo W E, Zhu X, Beuerman R, Ramakrishna S, and Yung L Y L (2005) Formation of collagen-glycosaminoglycan blended nanofibrous scaffolds and their biological properties. *Biomacromolecules* 6 (6) 2998-3004.
- Zhong S, Teo W E, Zhu X, Beuerman R W, Ramakrishna S and Yung L Y (2006) An aligned nanofibrous collagen scaffold by electrospinning and its effects on *in vitro* fibroblast culture. *J Biomed Mater Res A* 79 (3) 456-463.
- Zieske J D, Mason V S, Wasson M E, Meunier S F, Nolte C J M, Fukai N, Olsen B R et al. (1994) Basement membrane assembly and differentiation of cultured corneal cells: importance of culture environment and endothelial cell interaction. *Experimental cell research* 214 (2) 621-633.

APPENDICES

Asn	Asparagine
CO ₂	Carbon Dioxide
COO ⁻	Carboxylate ion
Cu ⁻	Copper ion
DSEAK	Descemet's stripping endothelial keratoplasty
EDC	1-ethyl-3-(3 dimethyl aminopropyl) carbodiimide
FACIT	Fibril associated collagens with interrupted triple helices
Gly	Glycine
HCl	Hydrochloric Acid
K ⁺	Potassium ion
kDa	Kilodalton
MCD-I	Macular corneal dystrophy type I
MgCl ₂	Magnesium Chloride
ml	Millilitre
mm	Millimetre
mM	Millimole
M	Moles
Na ⁺	Sodium ion
NaOH	Sodium hydroxide
NH ₂	Ammonia
NHS	N-hydroxysuccimide
nm	Nanometre
PBS	Phosphate buffered saline
PEG	Poly ethylene glycol
PO ₄ ⁻	Phosphate ion
Ser	Serine
SLRP	Small leucine-rich proteoglycans
SO ₄ ⁻	Sulphate ion
Thr	Threonine
WO ₄ ²⁻	Tungsten oxide ion
μL	Microlitre
μm	Micrometer

Appendices

Chemicals

Supplier

Acid freeze-dried type I porcine atelocollagen	Nippon Meat Packers/CosmoBio Co. Ltd
Tarivid (ofloxacin) ophthalmic ointment	Santen, Japan
Levofloxacin ophthalmic ointment	Santen, Japan
Araldite Monomer CY212	TAAB/Agar Scientific
BDMA Accelerator	TAAB/Agar Scientific
Chloroform	TAAB/Fischer
Colloidal gold (10nm)	BB International
Cuprolinic blue	BDH
DDSA Hardener	TAAB/Agar Scientific
DPX mounting fluid	TAAB
EDC	Wako pure chemicals, Japan/Fischer
Eosin	TAAB
Ethanol	TAAB/Sigma-Aldrich
Ethylene dichloride	Sigma-Aldrich
2.5% Glutaraldehyde	TAAB/Agar Scientific
Haematoxylin	TAAB
Ketamine hydrochloride	Sankyo, Tokyo, Japan
Lead nitrate	TAAB/Agar Scientific
Magnesium chloride	TAAB
NHS	Thermo science, USA/Acros Organics
1% Osmium tetroxide	TAAB
Paraformaldehyde	Sigma
Phosphotungstic acid	TAAB
Polyetherimide granules	Goodfellow
Propylene oxide	TAAB/Agar Scientific
Sodium acetate	TAAB
Sodium cacodylate	TAAB
Sodium citrate	TAAB/Agar Scientific
Sodium tungstate	TAAB
Uranyl acetate	TAAB/BDH
Xylazine	Bayer, Munich, Germany
Xylene	TAAB

Appendices

Equipment	Supplier
Biorevo BZ-9000 Fluorescent Microscope	Keyence, Japan
Coated microscope slides	TAAB
Diamond knife	Diatome
EM UC6 Microtome	Leica
EMKMR2 glass cutter	Leica
EZ Test series Universal Testing Instrument	SHIMADZU, Japan
Glass for knives	Leica
2218 Historange microtome	LKB bromma
H7600 Transmission electron microscope	Hitachi
JEM1010 Transmission electron microscope	Jeol
Kodak MegaPlus 1.4/digital CCD camera	Gatan
Leur-lock syringes	Terumo
Mesh grids	TAAB
ORIOUS SC1000 CCD camera	Gatan
Slot grids (2mm x 1mm)	TAAB
Ultracut Microtome	Reichert-Jung
UV/vis-spectrophotometer	SHIMAZU, Japan
T-shaped stopcock valves	Terumo/The West Group

8.1. Appendix 1

Proteoglycan dimension measurements in the developing avian corneal stroma.

Proteoglycan length and width measurements were calculated using a known pixel size of 0.33nm and Fiji software. 10nm gold fiducial markers were used for calibration. Measurements were taken from a transverse section micrograph, and were restricted to those proteoglycans whose whole length was contained within the section.

Developmental Day 12			
Length (pixels)	Width (pixels)	Length (nm)	Width (nm)
49.396	12.806	16.30068	4.22598
107.87	14.56	35.5971	4.8048
176.59	19.142	58.2747	6.31686
68.118	15.232	22.47894	5.02656
65.054	19.799	21.46782	6.53367
157.277	18.088	51.90141	5.96904
117.047	14.56	38.62551	4.8048
151.605	20.591	50.02965	6.79503
123.369	21.633	40.71177	7.13889
109.636	17.205	36.17988	5.67765
129.8	21.633	42.834	7.13889
64.498	16.492	21.28434	5.44236
49.193	21.26	16.23369	7.0158
107.517	20.881	35.48061	6.89073
109.836	21.633	36.24588	7.13889
212.038	24.083	69.97254	7.94739
142.338	16.492	46.97154	5.44236
82.098	16.125	27.09234	5.32125
60.729	15.232	20.04057	5.02656
89.889	14	29.66337	4.62
86.371	14.56	28.50243	4.8048
74.243	22.361	24.50019	7.37913
65.115	14.422	21.48795	4.75926
63.246	18.868	20.87118	6.22644
84.853	22	28.00149	7.26
154.402	21.541	50.95266	7.10853
142.239	19.698	46.93887	6.50034
128.577	16.492	42.43041	5.44236
42	14.3	13.86	4.719
120.416	25.06	39.73728	8.2698
76.368	14.142	25.20144	4.66686
77.279	22	25.50207	7.26
115.815	18.439	38.21895	6.08487
50.636	14.56	16.70988	4.8048
146.055	17	48.19815	5.61

Appendices

Developmental Day 14			
Length (pixels)	Width (pixels)	Length (nm)	Width (nm)
137.605	19.698	45.40965	6.50034
84.095	20	27.75135	6.6
100.319	20	33.10527	6.6
104.938	17.088	34.62954	5.63904
84.38	13.416	27.8454	4.42728
86.833	21.633	28.65489	7.13889
171.593	26	56.62569	8.58
111.212	20.591	36.69996	6.79503
70	20.396	23.1	6.73068
120.416	20.396	39.73728	6.73068
77.897	20	25.70601	6.6
90.355	19.799	29.81715	6.53367
121.606	25.06	40.12998	8.2698
60.465	15.62	19.95345	5.1546
141.676	23.324	46.75308	7.69692
103.73	23.409	34.2309	7.72497
108.849	26.833	35.92017	8.85489
83.187	19.698	27.45171	6.50034
144.014	28.636	47.52462	9.44988
83.522	14.142	27.56226	4.66686
83.952	18.974	27.70416	6.26142
107.464	24.739	35.46312	8.16387
186.507	33.541	61.54731	11.06853
101.823	19.799	33.60159	6.53367
211.849	22.361	69.91017	7.37913
36.878	16.125	12.16974	5.32125
51.884	11.662	17.12172	3.84846
52.345	16.971	17.27385	5.60043
58.31	18	19.2423	5.94
104.48	26.683	34.4784	8.80539
145.121	20.396	47.88993	6.73068
119.867	26.077	39.55611	8.60541
101.863	18.439	33.61479	6.08487
130.43	19.698	43.0419	6.50034
79.624	14.56	26.27592	4.8048

Appendices

Developmental Day 16			
Length (pixels)	Width (pixels)	Length (nm)	Width (nm)
169.706	18.439	56.00298	6.08487
168.012	30.067	55.44396	9.92211
149.345	26.306	49.28385	8.68098
113.278	16.971	37.38174	5.60043
82.873	16.125	27.34809	5.32125
71.218	17.889	23.50194	5.90337
108.812	18.974	35.90796	6.26142
115.447	16.125	38.09751	5.32125
120.88	21.26	39.8904	7.0158
102.956	17.889	33.97548	5.90337
75.71	16.125	24.9843	5.32125
188.997	23.409	62.36901	7.72497
77.795	21.633	25.67235	7.13889
116	18.439	38.28	6.08487
176.433	20.881	58.22289	6.89073
66.483	18.439	21.93939	6.08487
129.321	25.06	42.67593	8.2698
141.484	21.541	46.68972	7.10853
125.3	16	41.349	5.28
109.636	20	36.17988	6.6
114.63	20.591	37.8279	6.79503
131.045	18	43.24485	5.94
182.242	32.802	60.13986	10.82466
123.968	24.739	40.90944	8.16387
65.054	19.799	21.46782	6.53367
133.062	22.361	43.91046	7.37913
181.511	18.868	59.89863	6.22644
129.273	19.71	42.66009	6.5043
217.34	23.808	71.7222	7.85664
98.162	21.414	32.39346	7.06662
78.355	18.372	25.85715	6.06276
119.706	18.439	39.50298	6.08487
76.026	21.26	25.08858	7.0158
169.158	30.284	55.82214	9.99372
214.568	32.807	70.80744	10.82631

8.2. Appendix 2

Publications

Duncan T, Tanaka Y, Shi D, Kubota A, Quantock A J, Nishida K (2010) Flow manipulated, cross-linked collagen gels for use as corneal equivalents. *Biomaterials* 31 (34) 8996-9005.

Tanaka Y, Baba K, Duncan T J, Kubota A, Asahi T, Quantock A J, Yamato M, Okano T and Nishida K (2011a) Transparent, tough collagen laminates prepared by oriented flow casting, multi-cyclic vitrification and chemical cross-linking. *Biomaterials* 32 (13) 3358-3366.

Tanaka Y, Kubota A, Matsusaki M, Duncan T, Hatakeyama Y, Fukuyama K, Quantock A J, Yamato M, Akashi M and Nishida K (2011b) Anisotropic mechanical properties of collagen hydrogels induced by uniaxial-flow for ocular applications. *J Biomater Sci Polym Ed* 22 (11) 1427-1442.